

**AUTOMATED DERIVATIZATION AND IDENTIFICATION OF  
CONTROLLED SUBSTANCES VIA TOTAL VAPORIZATION SOLID  
PHASE MICROEXTRACTION (TV-SPME) AND GAS  
CHROMATOGRAPHY-MASS SPECTROMETRY (GC-MS)**

by

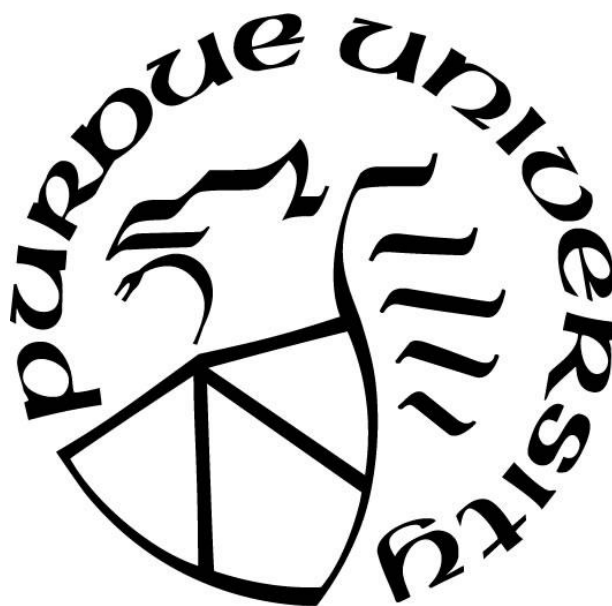
**Logan D. Hickey**

**A Thesis**

*Submitted to the Faculty of Purdue University*

*In Partial Fulfillment of the Requirements for the degree of*

**Master of Science**



Department of Forensic & Investigative Sciences

Indianapolis, Indiana

May 2018

**THE PURDUE UNIVERSITY GRADUATE SCHOOL**  
**STATEMENT OF COMMITTEE APPROVAL**

Dr. John Goodpaster, Chair

Forensic and Investigative Sciences Program

Dr. Nicholas Manicke

Forensic and Investigative Sciences Program

Dr. Rajesh Sardar

Department of Chemistry & Chemical Biology

**Approved by:**

Dr. John Goodpaster

Head of the Graduate Program

*For my family, by blood or otherwise, who have always supported me and reminded me that I  
could do anything I set my mind to.*

## **ACKNOWLEDGMENTS**

I would like to thank my advisor, Dr. John Goodpaster, for guiding me on this journey, for sharing his expertise, for encouraging me to pursue opportunities, and for not making me sleep in the laboratory. I also want to thank my fellow students Zackery Roberson, Ashur Rael, Courtney Cruse, Jackie Ruchti, and Kymeri Davis for their help and friendship along the way. Lastly, I would like to thank Jordan Ash for mentoring me in the laboratory, for being a great friend, and of course for his research, which laid the foundation for my own and is the topic of chapter 1 of this thesis.

This research was made possible by the National Institute of Justice (Award No. 2015-DN-BX-K058) and the Forensic Sciences Foundation Jan S. Bashinski Criminalistics Graduate Thesis Grant. The opinions, findings, and conclusions expressed here are those of the author and do not necessarily reflect those of the aforementioned organizations.

## TABLE OF CONTENTS

LIST OF TABLES .....	vi
LIST OF FIGURES .....	vii
ABSTRACT .....	xi
CHAPTER 1. TRADITIONAL DERIVATIZATION AND LIQUID INJECTION	
ANALYSIS .....	1
Introduction .....	1
Experimental .....	7
Results and Discussion .....	8
Conclusions .....	25
CHAPTER 2. DEVELOPMENT OF TV-SPME ON-FIBER DERIVATIZATION OF CONTROLLED SUBSTANCES .....	
Introduction .....	28
Experimental .....	32
Results .....	34
Conclusion .....	51
CHAPTER 3. REALISTIC SAMPLES AND SOLID DRUG DERIVATIZATION .....	
Introduction .....	55
Experimental .....	58
Results .....	61
Conclusion .....	67
CHAPTER 4. FUTURE WORK .....	
Toxicology .....	69
Beverage Samples .....	72
Method Improvement .....	72
REFERENCES .....	76

## LIST OF TABLES

Table 1. References in which the zwitterions and primary amines presented in this work were successfully detected by GC-MS “as is” or using a derivatization agent of the category indicated. Reactions that were completed and will be discussed in this paper are also indicated. ....	6
Table 2. Comparing asymmetry factors for underivatized drugs and their derivative(s) .....	25
Table 3. Comparing separation efficiency (number of theoretical plates) for underivatized .....	25
Table 4. Comparing sensitivity (peak area) for underivatized drugs and their derivative(s) .....	25
Table 5. A summary of the results of this work. + indicates the formation of a single chromatographic peak which could be unambiguously identified. – indicates no relevant peak was formed. 0 indicates multiple peaks were formed. ....	25
Table 6. Comparing asymmetry factors for underivatized drugs and their derivatives .....	51
Table 7. Comparing separation efficiency (number of theoretical plates) for underivatized drugs and their derivatives.....	51
Table 8. Comparing sensitivity (peak area) for underivatized drugs and their derivative.....	51
Table 9. Summary of results for liquid injection and TV-SPME methods. + indicates the formation of a single chromatographic peak which could be unambiguously identified. 0 indicates that multiple peaks formed, and – indicates that no peak formed.....	53

## LIST OF FIGURES

Figure 1. Chemical structures of the drugs analyzed in this work.....	2
Figure 2. A generalized reaction between TFSA and a primary amine .....	3
Figure 3. A generalized reaction with BSTFA where X is a nitrogen or an oxygen atom .....	4
Figure 4. A generalized reaction between DMF-DMA and a carboxylic acid .....	4
Figure 5. A generalized reaction between DMF-DMA and a primary amine .....	5
Figure 6. A generalized representation of chloroformate derivatization .....	5
Figure 7. TIC of A: 0.5 mg/mL clorazepate derivatized with BSTFA + 1% TMCS, B: 0.5 mg/mL clorazepate in methanol.....	10
Figure 8. Structure and mass spectrum for clorazepate TMS. MW = 386 .....	10
Figure 9. TIC of A: 0.5 mg/mL vigabatrin derivatized with BSTFA + 1% TMCS, B: 0.5 mg/mL vigabatrin in methanol.....	11
Figure 10. TIC of A: 0.5 mg/mL vigabatrin derivatized with DMF-DMA, B: 0.5 mg/mL vigabatrin in methanol.....	12
Figure 11. Structure and mass spectrum for vigabatrin TMS. MW = 201 .....	12
Figure 12. Structure and mass spectrum for vigabatrin DMAM. MW = 198.....	13
Figure 13. TIC of A: 0.5 mg/mL amphetamine derivatized with TFSA and B: 0.5mg/mL amphetamine in methanol. As = asymmetry factor. N = number of theoretical plates. ....	15
Figure 14. TIC of A: 0.5 mg/mL amphetamine derivatized with DMF-DMA and B: 0.5 mg/mL amphetamine in methanol. As = asymmetry factor. N = number of theoretical plates.....	15
Figure 15. Structure and mass spectrum for amphetamine TFA. MW = 231.....	16
Figure 16. Structure and mass spectrum of amphetamine DMAM. MW = 190.....	16
Figure 17. TIC of A: 0.5 mg/mL 2C-I derivatized with TFSA and B: 0.5 mg/mL 2C-I in methanol. As = asymmetry factor. N = number of theoretical plates. ....	17
Figure 18. TIC of A: 0.5 mg/mL 2C-I derivatized with DMF-DMA and B: 0.5 mg/mL 2C-I in methanol. As = asymmetry factor. N = number of theoretical plates. ....	18
Figure 19. Structure and mass spectrum for 2C-I TFA. MW = 403.....	18
Figure 20. Structure and mass spectrum of 2C-I DMAM. MW = 362.....	19

Figure 21. TIC of A: 0.5 mg/mL gabapentin derivatized with TFAA and B: 0.5 mg/mL gabapentin in methanol. As = asymmetry factor. N = number of theoretical plates. ..	20
Figure 22. TIC of A: 0.5 mg/mL gabapentin derivatized with DMF-DMA and B: 0.5 mg/mL gabapentin in methanol. As = asymmetry factor. N = number of theoretical plates.....	21
Figure 23. Structure and mass spectrum for gabapentin TFA. MW = 267.....	21
Figure 24. Structure and mass spectrum for gabapentin DMAM. MW = 240 .....	22
Figure 25. TIC of A: 0.5 mg/mL lorazepam derivatized with BSTFA + 1% TMCS and B: 0.5 mg/mL lorazepam in methanol. As = asymmetry factor. N = number of theoretical plates.....	23
Figure 26. Structure and mass spectrum for lorazepam TMS. MW = 464 .....	24
Figure 27. Depiction of the On-Fiber Total Vaporization Solid-Phase Microextraction process.....	29
Figure 28. Structures, molecular weights, and octanol:water partition coefficient (LogPow) of the drugs analyzed in this work. ....	30
Figure 29. Structures, molecular weights, and octanol:water partition coefficient (LogPow) of the zwitterionic drugs analyzed in this work. ....	31
Figure 30. Graph of peak area vs extraction temperature for underivatized phenethylamines. Peak area was calculated using the extracted ion profile (EIP) for the ion indicated. ....	35
Figure 31. Graph of peak area vs extraction temperature for underivatized designer drugs. Peak area was calculated using the extracted ion profile (EIP) for the ion indicated. ....	35
Figure 32. Graph of peak area vs extraction temperature for underivatized zwitterions. Peak area was calculated using the extracted ion profile (EIP) for the ion indicated.....	36
Figure 33. Graph of experimentally determined optimum extraction temperature vs known boiling point for underivatized drugs.....	36
Figure 34. TIC of A: 24 µg of amphetamine in 18 µL of acetonitrile derivatized with TFAA, B: 24 µg of amphetamine in 24 µL of methanol. As = asymmetry factor, N = number of theoretical plates. ....	37



Figure 35. TIC of A: 24 µg of methamphetamine in 18 µL of acetonitrile derivatized with TFAA, B: 24 µg of methamphetamine in 24 µL of methanol. As = asymmetry factor, N = number of theoretical plates. ....	38
Figure 36. Structure and mass spectrum for methamphetamine TFA. MW = 245.....	38
Figure 37. TIC for 24 µg of ephedrine in 24 µL of methanol.....	39
Figure 38. TIC of A: 24 µg of 2C-I in 18 µL of acetonitrile derivatized with TFAA, B: 24 µg of 2C-I in 24 µL of methanol. As = asymmetry factor, N = number of theoretical plates. ....	40
Figure 39. TIC of A: 24 µg of 25I-NBOMe in 18 µL of acetonitrile derivatized with TFAA, B: 24 µg of 25I-NBOMe in 24 µL of methanol. As = asymmetry factor, N = number of theoretical plates. ....	41
Figure 40. Fragmentation diagram and mass spectrum, underivatized 25I-NBOMe. MW = 427.....	42
Figure 41. Fragmentation diagram and mass spectrum of 25I-NBOMe TFA. MW = 523 .....	42
Figure 42. TIC of A: 24 µg of 25I-NBOH in 18 µL of acetonitrile derivatized with TFAA, B: 24 µg of 25I-NBOH in 24 µL of methanol. As = asymmetry factor, N = number of theoretical plates. ....	43
Figure 43. Fragmentation diagram and mass spectrum of underivatized 25I-NBOH. MW = 413.....	44
Figure 44. Fragmentation diagram and mass spectrum for 25I-NBOH TFA. MW = 509 .....	44
Figure 45. TIC of A: 24 µg of psilocin in 18 µL of acetonitrile derivatized with BSTFA + 1% TMCS, B: 24 µg of psilocin in 24 µL of methanol. As = asymmetry factor, N = number of theoretical plates.....	45
Figure 46. Fragmentation diagram and mass spectrum for psilocin TMS. MW = 276 .....	46
Figure 47. TIC of A: 14.4 µg of GHB in 18 µL of acetonitrile derivatized with BSTFA + 1% TMCS, B: 14.4 µg of GHB in 24 µL of methanol. ....	47
Figure 48. Structure and mass spectrum of GHB di-TMS. MW = 248.....	47
Figure 49. TIC of 14.4 µg of gabapentin in 24 µL of methanol. ....	48
Figure 50. TIC of 24 µg of lorazepam in 24 µL of methanol. ....	49
Figure 51. TIC of 24 µg of pregabalin in 24 µL of methanol.....	50

Figure 52. The synthetic pathway from ephedrine to methamphetamine via the Emde method <sup>35</sup> .....	56
Figure 53. The synthetic pathway from ephedrine to methamphetamine via the Nagai method <sup>38</sup> .....	56
Figure 54. The synthetic pathway from ephedrine to methamphetamine via the “Nazi/Birch” method <sup>39</sup> .....	56
Figure 55. The conversion of GHB to GBL via dehydration ( $\Delta H_o = 4.5 \pm 0.2$ kJ/mol) <sup>44</sup> .....	57
Figure 56. “street meth” chromatogram showing the methamphetamine derivative and caffeine (left) and zoomed in to show the ephedrine derivative (right). .....	62
Figure 57. Plot of the GHB signal (measured by the area under the curve for EIC m/z 233) vs the time spent by the SPME fiber in headspace of the derivatization vial. ....	63
Figure 58. Stacked chromatograms for Coke® spiked with 8 mg/mL GHB, analyzed without derivatization (B) and with on-fiber derivatization using BSTFA + 1% TMCS (A) ..	64
Figure 59. Stacked chromatograms for rum spiked with 0.8 mg/mL GHB, analyzed without derivatization (B) and with on-fiber derivatization using BSTFA + 1% TMCS (A) ..	64
Figure 60. Stacked chromatograms for rum spiked with 8 mg/mL GHB, analyzed without derivatization (B) and with on-fiber derivatization using BSTFA + 1% TMCS (A) ..	65
Figure 61. Chromatograms for A: methamphetamine TFA and B: methamphetamine underivatized .....	66
Figure 62. Chromatograms for A: GHB di-TMS and B: GHB underivatized .....	66
Figure 63. Chromatograms of A: ephedrine TFA and B: ephedrine underivatized .....	67
Figure 64. Chromatograms of A: gabapentin DMAM and B: gabapentin underivatized .....	67
Figure 65. TIC of human hair derivatized with BSTFA + 1% TMCS (Data courtesy of Kymeri Davis) .....	71
Figure 66. EIC for m/z 233 of human hair derivatized with BSTFA + 1% TMCS (Data courtesy of Kymeri Davis) .....	71

## ABSTRACT

Author: Hickey, Logan D. MS

Institution: Purdue University

Degree Received: May 2018

Title: Automated Derivatization and Identification of Controlled Substances via Total Vaporization Solid Phase Microextraction (TV-SPME) and Gas Chromatography-Mass Spectrometry (GC-MS)

Major Professor: John Goodpaster

Gas chromatography-mass spectrometry (GC-MS) is one of the most widely used instrumental techniques for chemical analyses in forensic science laboratories around the world due to its versatility and robustness. The most common type of chemical evidence submitted to forensic science laboratories is seized drug evidence, the analysis of which is largely dominated by GC-MS. Despite this, some drugs are difficult or impossible to analyze by GC-MS under normal circumstances. For these drugs, derivatization can be employed to make them more suitable for GC-MS.

In Chapter 1, the derivatization of primary amino and zwitterionic drugs with three different derivatization agents, trifluoroacetic anhydride (TFAA); N,O-bis(trimethylsilyl)trifluoroacetamide + 1% trimethylchlorosilane (BSTFA + 1% TMCS); and dimethylformamide dimethylacetal (DMF-DMA), is discussed. The chromatographic performance was quantified for comparison between the derivatives and their parent drugs. Peak symmetry was compared using the asymmetry factor ( $A_s$ ), separation efficiency was measured by the number of theoretical plates ( $N$ ), and sensitivity was compared by measuring the peak areas.

In Chapter 2, derivatization techniques were adapted for an automated on-fiber derivatization procedure using a technique called total vaporization solid phase microextraction (TV-SPME). TV-SPME is a variation of SPME in which a small volume of sample solution is

used which can be totally vaporized, removing the need to consider the equilibrium between analytes in the solution and analytes in the headspace. By allowing derivatization agent to adsorb to the SPME fiber prior to introduction to the sample vial, the entire derivatization process can take place on the fiber or in the headspace surrounding it. The use of a robotic sampler made the derivatization procedure completely automated.

In Chapter 3, this on-fiber derivatization technique was tested on standards of 14 controlled substances as well as on realistic samples including simulated “street meth”, gamma-hydroxybutyric acid (GHB) in mixed drinks, and hallucinogenic mushrooms, and was also tested on several controlled substances as solid powders.

Future work in this area is discussed in Chapter 4, including adapting the method to toxicological analyses both in biological fluids and in hair. Some of the expected difficulties in doing so are discussed, including the endogenous nature of GHB in the human body. The presence of natural GHB in beverages is also discussed, which highlights the need for a quantitative addition to the method. Additional method improvements are also discussed, including proposed solutions for complete derivatization of more of the analytes, and for decreasing analysis time.

## **CHAPTER 1. TRADITIONAL DERIVATIZATION AND LIQUID INJECTION ANALYSIS**

### **Introduction**

A wide variety of controlled substances are submitted to forensic laboratories, making up a significant portion of all samples analyzed. However, some of these controlled substances are difficult to analyze by the typical means employed in forensic science laboratories. For example, Gas Chromatography-Mass Spectrometry (GC-MS) is a “workhorse” technique for drug chemistry units. However, not all drugs are amenable to GC-MS. For a substance to be analyzed by GC-MS, it must be volatile (i.e., exhibit a vapor pressure of at least one torr at the temperature of the GC inlet) and thermally stable (to at least 200 degrees Celsius). Additionally, some analytes exhibit poor chromatography due to non-ideal interactions with the stationary phase of the column. For example, zwitterions (which have at least one positively and one negatively charged functional group) and basic molecules such as amines are notorious for poor performance in gas chromatography.

This chapter will discuss a portion of the work completed by Jordan Ash<sup>1</sup>, specifically the analysis and derivatization of several zwitterionic anti-epileptic drugs as well as primary amines, the structures of which are shown in Figure 1.

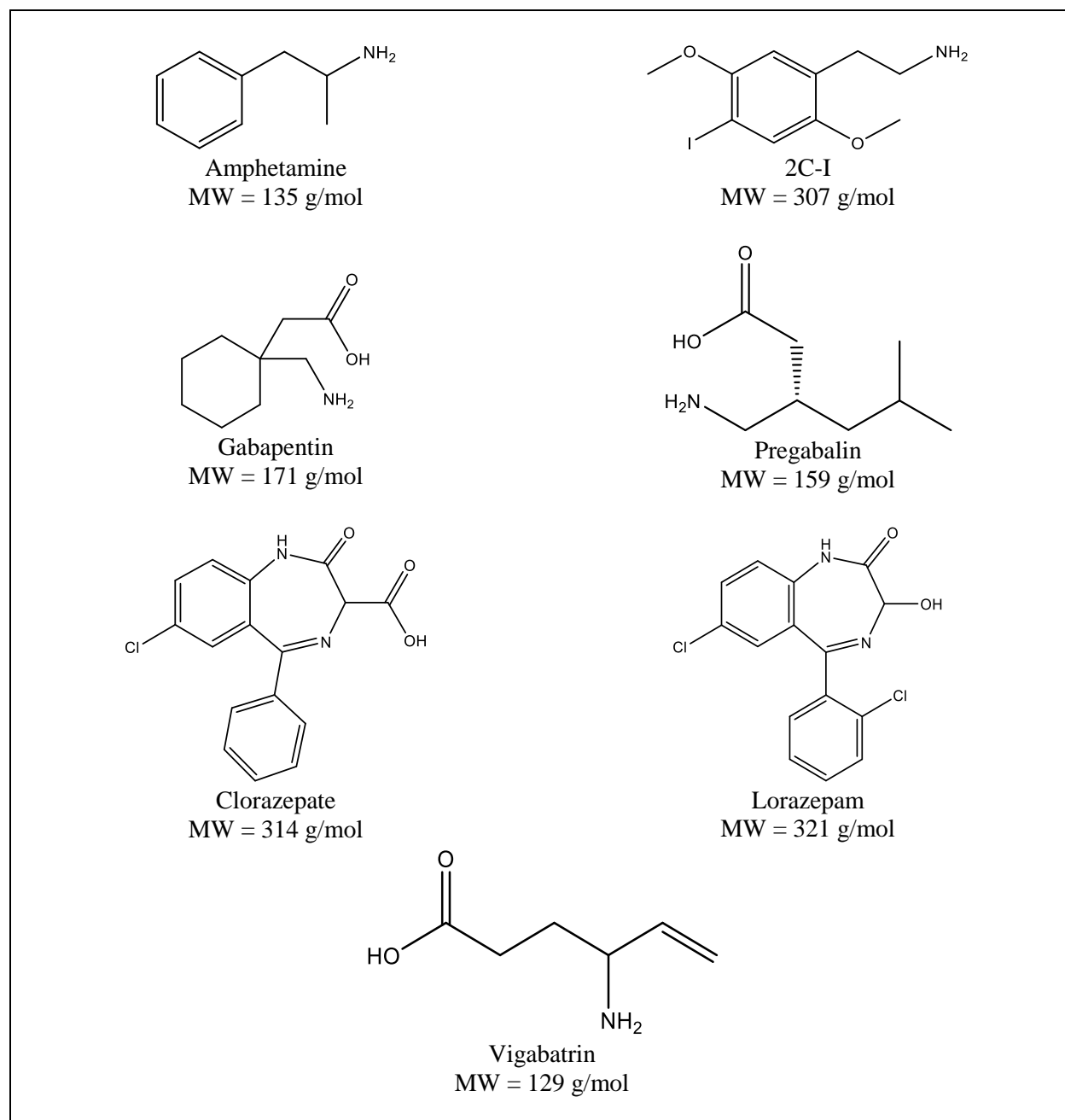


**Figure 1.** Chemical structures of the drugs analyzed in this work

A common way to increase the volatility, thermal stability, and chromatographic performance of an analyte is via derivatization<sup>2</sup>. The process of derivatization replaces a labile hydrogen on the analyte molecule with a new functional group that increases the stability of the molecule. Derivatives are most commonly formed via acylation, silylation and alkylation reactions. As shown in Figure 2, amine and hydroxylamine compounds can be derivatized via acylation, which is the replacement of a labile hydrogen with an acyl group<sup>3-4</sup>. Trifluoroacetic anhydride (TFAA) is a common acylation agent<sup>3, 5</sup>. In this reaction, the amine hydrogen is removed and replaced with a trifluoroacetyl group.

TFAA

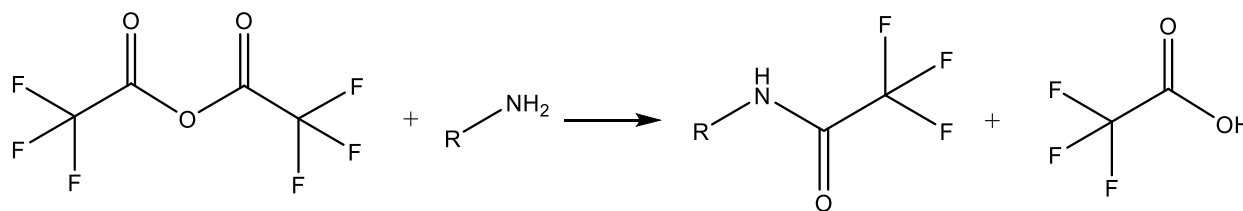


**Figure 2.** A generalized reaction between TFAA and a primary amine

As shown in Figure 3, carboxylic and phosphonic acids can be derivatized by silylation, which is the replacement of a labile hydrogen with a trimethylsilyl group<sup>4, 6</sup>. N,O-bis(trimethylsilyl)trifluoroacetamide (BSTFA) with trimethylchlorosilane (TMCS) is a commonly used silylating agent. Other silylation agents are available which attach larger silyl groups. For example, methyl-N-t-butyldimethylsilyltrifluoroacetamide (MTBSTFA) replaces labile hydrogens with t-butyldimethylsilyl groups. While MTBSTFA derivatives require more time to form, they are more stable<sup>7</sup>.

BSTFA

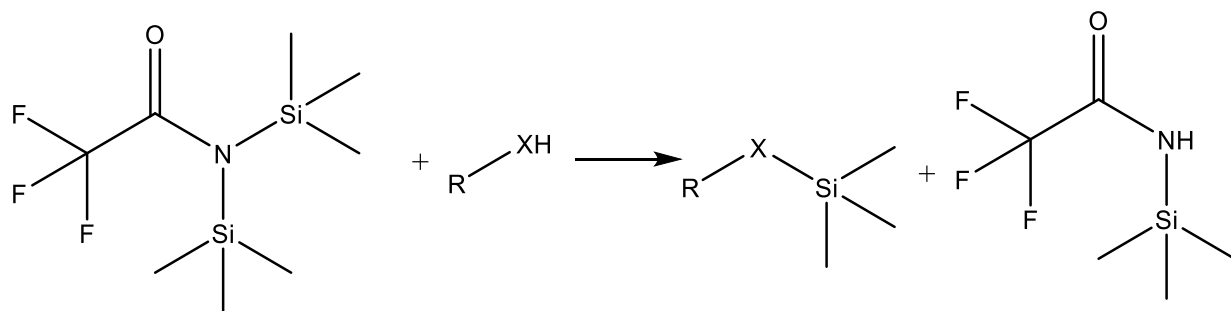


**Figure 3.** A generalized reaction with BSTFA where X is a nitrogen or an oxygen atom

As shown in Figure 4, alkylation is the replacement of a labile hydrogen with an alkyl group<sup>4</sup>. Alkylation can be achieved through base- or acid-catalyzed transesterification using reagents such as KOH/methanol or H<sub>2</sub>SO<sub>4</sub>/methanol. N,N-dimethylformamide dimethyl acetal (DMF-DMA) is an alkylation reagent that does not require catalysis and is compatible with most organic solvents. DMF-DMA has been used for the alkylation of fatty acids<sup>8</sup>, as well as the derivatization of amino acids<sup>9-10</sup> and heterocyclic amines<sup>11</sup>. As shown in Figure 5, primary amines undergo Schiff base condensation, meaning that they lose 2 hydrogens, which are replaced with a dimethylaminomethylene (DMAM) group. A carbon-nitrogen double bond was thus formed, resulting in an imine<sup>9-11</sup>. In the case of amino acids, the carboxyl moiety is methylated as well, to form a methyl ester<sup>9-10</sup>. Though well known for those applications, the use of DMF-DMA for the derivatization of drugs of abuse has not been previously reported.

DMF-DMA

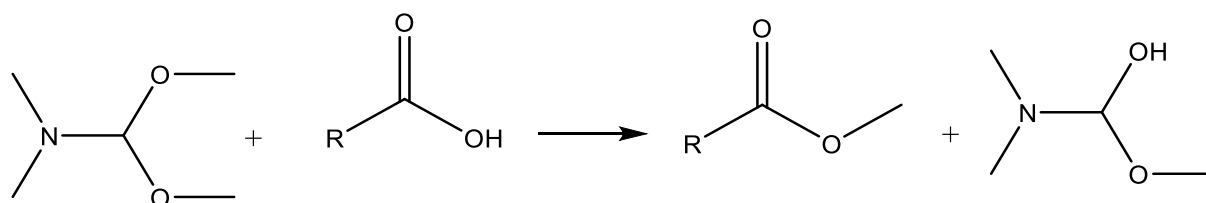


**Figure 4.** A generalized reaction between DMF-DMA and a carboxylic acid



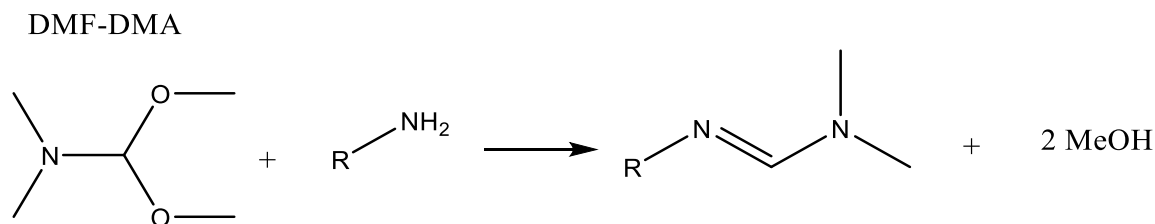


**Figure 5.** A generalized reaction between DMF-DMA and a primary amine

As shown in Figure 6, chloroformates can be used to derivatize zwitterions. Although these reagents will not be discussed in this paper, ethyl chloroformate derivatives have been formed from pregabalin as a solid, in urine, and in pharmaceuticals<sup>12-13</sup>. Hexyl chloroformate derivatives have been formed from gabapentin, vigabatrin, and pregabalin in serum<sup>14</sup>.

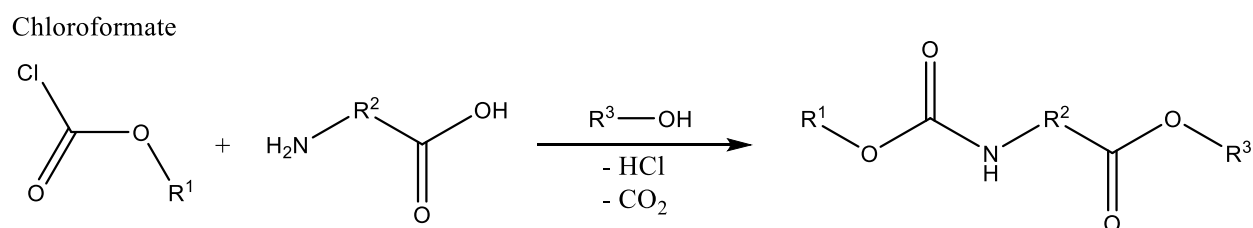


**Figure 6.** A generalized representation of chloroformate derivatization

Spectrophotometric, spectrofluorometric, and liquid chromatographic methods have been reported for the identification of gabapentin, vigabatrin, and pregabalin<sup>15</sup>. Successful GC-MS analysis without derivatization has been reported for 2C-I in rat urine<sup>16</sup>, gabapentin in human serum<sup>17</sup>, and amphetamine<sup>18</sup> and lorazepam<sup>19</sup> in human urine. Amphetamine has been analyzed in hair<sup>20</sup> and urine<sup>3, 21</sup> using TFAA derivatization. N- N-methyl-bis(trifluoroacetamide) (MBTFA) has been used for the analysis of pure amphetamine samples<sup>5</sup>. 2C-I has been analyzed in rat urine using TFAA derivatization<sup>16</sup>. Gabapentin has been analyzed following derivatization with N-tert-butyltrimethylsilyl-N-methyltrifluoroacetamide (MTBSTFA) in blood plasma and serum<sup>22</sup>. Lorazepam has been analyzed in urine utilizing both MTBSTFA derivatization<sup>23</sup> and a dual derivatization procedure with MTBSTFA and TFAA<sup>24</sup>.

Despite these previous efforts, the reactions between several drugs and derivatization agents have not been explored. For example, the use of DMF-DMA with these drugs has not been previously reported. A summary of previous work in this area as well as those reactions that are reported here for the first time appears in Table 1.

**Table 1.** References in which the zwitterions and primary amines presented in this work were successfully detected by GC-MS “as is” or using a derivatization agent of the category indicated. Reactions that were completed and will be discussed in this paper are also indicated.

Drug	Underivatized	Acylation	Silylation	Alkylation
Amphetamine	n <sup>18</sup>	a <sup>3, 20-21</sup> , d <sup>5</sup>	b <sup>[This Work]</sup>	c <sup>[This Work]</sup>
2C-I	n <sup>16</sup>	a <sup>16</sup>	b <sup>[This Work]</sup>	c <sup>[This Work]</sup>
Gabapentin	n <sup>17</sup>	a <sup>[This Work]</sup>	e <sup>22</sup>	c <sup>[This Work]</sup>
Lorazepam	n <sup>19</sup>	f <sup>24</sup>	e <sup>23</sup> f <sup>24</sup>	c <sup>[This Work]</sup>
Vigabatrin	n <sup>[This Work]</sup>	a <sup>[This Work]</sup>	b <sup>[This Work]</sup>	c <sup>[This Work]</sup>
Pregabalin	n <sup>[This Work]</sup>	a <sup>[This Work]</sup>	b <sup>[This Work]</sup>	c <sup>[This Work]</sup>
Clorazepate	n <sup>[This Work]</sup>	a <sup>[This Work]</sup>	b <sup>[This Work]</sup>	c <sup>[This Work]</sup>

a = Trifluoroacetic anhydride (TFAA)

b = N,O-bis(trimethylsilyl)trifluoroacetamide (BSTFA)

c = Dimethylformamide-dimethylacetal (DMF-DMA)

d = N-Methyl-bis(trifluoroacetamide) (MBTFA)

e = N-tert-Butyldimethylsilyl-N-methyltrifluoroacetamide (MTBSTFA)

f = Dual derivatization with TFAA and MTBSTFA

n = none

## Experimental

### *Materials*

Gabapentin, vigabatrin, and 2C-I HCl were purchased from Cayman Chemical (Ann Arbor, Michigan). Lorazepam, pregabalin, amphetamine, dimethylformamide dimethyl acetal (DMF-DMA) and trifluoroacetic anhydride (TFAA) were purchased from Sigma-Aldrich (St. Louis, Missouri). Clorazepate dipotassium was purchased from Grace Chemical (Columbia, Maryland). HPLC grade methanol, Optima acetonitrile, and N,O-bis(trimethylsilyl)trifluoroacetamide with 1% trimethylchlorosilane (BSTFA + 1% TMCS) were purchased from Thermo Fisher Scientific (Waltham, Massachusetts).

### *Sample Preparation*

The drug standards were dissolved in methanol at a concentration of 0.5 mg/mL. When samples were analyzed without derivatization, the solution in methanol was directly injected into the GC. Whenever derivatization was employed, additional sample preparation steps had to be taken. A volume of one milliliter of the methanolic drug solution was transferred to a GC autosampler vial. The methanol was then evaporated using a blow-down apparatus. Two hundred microliters of derivatization agent were then added to the vial and allowed to react at 60°C until the solid had completely dissolved. Eight hundred microliters of acetonitrile were then added to bring the total volume back up to one milliliter before injection into the GC.

### *GC-MS Parameters*

An Agilent 6890N GC coupled to an Agilent 5975 inert Mass Selective Detector with an attached Gerstel PAL RTC Multi-Purpose Sampler (MPS) was used for all experiments. The GC

column was an Agilent Technologies DB-5MS column with a length of 30 m, a 0.250 mm inner diameter, and a 0.25  $\mu\text{m}$  film thickness. An injection volume of one microliter was used.

The inlet temperature was set to 250°C and operated in split mode with a 15:1 ratio for amphetamine and in splitless mode for all other analytes. The initial oven temperature of 90°C was held for one minute, then the temperature was ramped at 15°C/min to 280°C where it was held for one minute. A speed optimized flow of 2.5 mL/min hydrogen was maintained. The mass transfer line was held at 280°C. The source was kept at 230°C and the quadrupoles were kept at 150°C. A scan range of  $m/z$  40-  $m/z$  550 was used.

## Results and Discussion

### *Assessing Chromatographic Performance*

Comparisons of chromatographic performance between underivatized drugs and their derivatives were desired for those drugs which were detected without derivatization. Peak symmetry, separation efficiency, and sensitivity were compared. Asymmetry factor ( $A_s$ ) is calculated using equation 1, where  $b$  is the distance from the center of the peak to the tail edge of the peak at 10% peak height and  $a$  is the distance from the center of the peak to the front edge of the peak at 10% peak height. The closer  $A_s$  is to 1.0, the more symmetrical the peak. Conversely, values of  $A_s$  less than one indicate fronting while values greater than one indicate tailing. Percent improvement in symmetry was calculated using equation 2, where  $A_s^0$  is the asymmetry factor of the underivatized drug and  $A_s^1$  is the asymmetry factor of the derivatized drug.

$$A_s = b/a \quad (1)$$

$$\frac{|A_s^0 - 1| - |A_s^1 - 1|}{|A_s^0 - 1|} * 100\% \quad (2)$$

Separation efficiency was evaluated using the number of theoretical plates ( $N$ ). The calculation for  $N$  is presented in equation 3, below, where  $t_r$  is the retention time and  $W$  is the peak width. Percent increase in separation efficiency was calculated using equation 4, where  $N^0$  is the

number of theoretical plates for the underivatized drug and  $N^1$  is the number of theoretical plates for the derivatized drug.

$$N = 16 \left( \frac{t_r}{W} \right)^2 \quad (3)$$

$$\frac{N^1 - N^o}{N^o} * 100\% \quad (4)$$

Sensitivity was evaluated using peak areas, which were calculated by the auto-integration feature of the data analysis software. Percent increase in sensitivity was calculated using equation 5, where  $A^o$  is the area under the curve for the underivatized drug and  $A^1$  is the area under the curve for the derivatized drug.

$$\frac{A^1 - A^o}{A^o} * 100\% \quad (5)$$

### *Clorazepate*

Clorazepate was not detected in underivatized form. Analysis was also unsuccessful using TFMA derivatization due to the formation of multiple peaks which did not include the target derivative.

BSTFA derivatization, however, produced a single chromatographic peak which was identified as the clorazepate-TMS derivative (see Figure 7). The derivative was not in the NIST library, but its structure was elucidated by its fragmentation pattern (see Figure 8). The amine group of clorazepate was preferentially silylated. Decarboxylation resulted in the  $m/z$  45 and  $m/z$  341 ions. The latter ion exhibited an isotopic pattern confirming that one Cl atom was present. Cleavage of the TMS group resulted in the  $m/z$  73 ion. Derivatization with DMF-DMA was unsuccessful for clorazepate as multiple peaks were formed, none of which was attributed to the expected derivative.

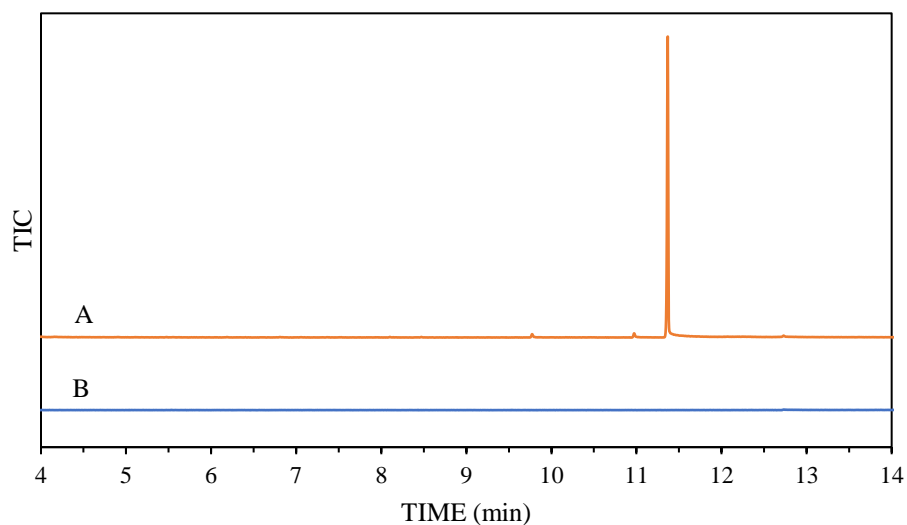


**Figure 7.** TIC of A: 0.5 mg/mL clorazepate derivatized with BSTFA + 1% TMCS, B: 0.5 mg/mL clorazepate in methanol.

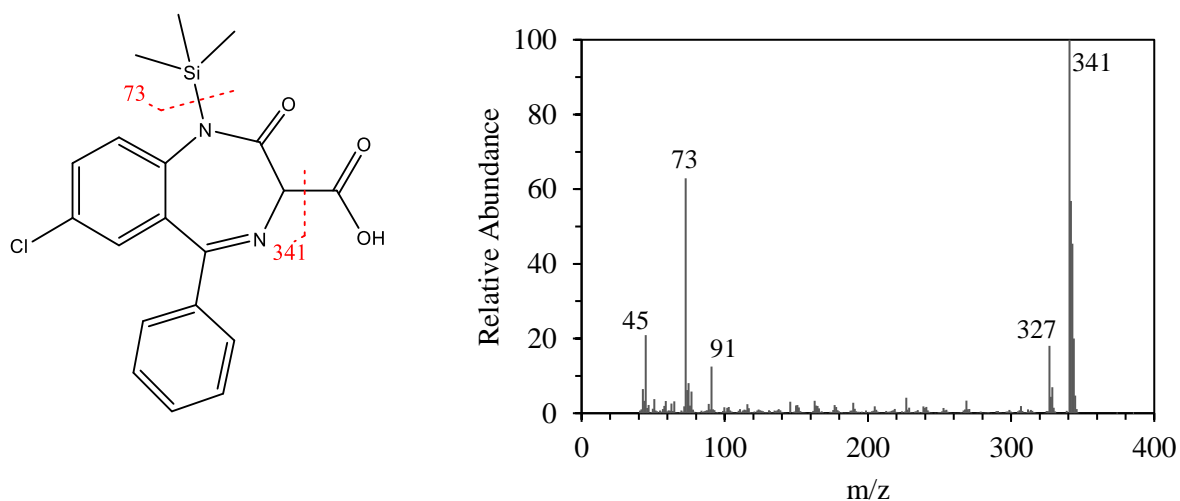


**Figure 8.** Structure and mass spectrum for clorazepate TMS. MW = 386

### *Vigabatrin*

Vigabatrin was not detectable in the underivatized form and derivatization of vigabatrin with TFAA produced no results.

When silylated with BSTFA, a single chromatographic peak was produced (see Figure 9). This derivative was not in the NIST library, but its structure was elucidated by the fragmentation pattern (see Figure 11). Loss of a methyl group produced an  $[M-15]^+$  ion at  $m/z$  186. From the  $m/z$  186 fragment, a loss of 17 was observed in the form of ammonia following hydrogen rearrangement<sup>25</sup>. The base peak of  $m/z$  56 was formed by alpha cleavage at the nitrogen.

Derivatization with DMF-DMA produced a single chromatographic peak (see Figure 10). Vigabatrin underwent the same derivatization process with DMF-DMA as gabapentin. This derivative was not in the NIST library, but its structure was elucidated by the fragmentation pattern (see Figure 12). The molecular ion of  $m/z$  198 was seen. The ion at  $m/z$  167 was a result of the loss of the methoxy group, the base peak of  $m/z$  111 was formed via alpha cleavage at the original nitrogen, and the  $m/z$  154 ion was produced by alpha cleavage in the other direction losing the dimethylamine.

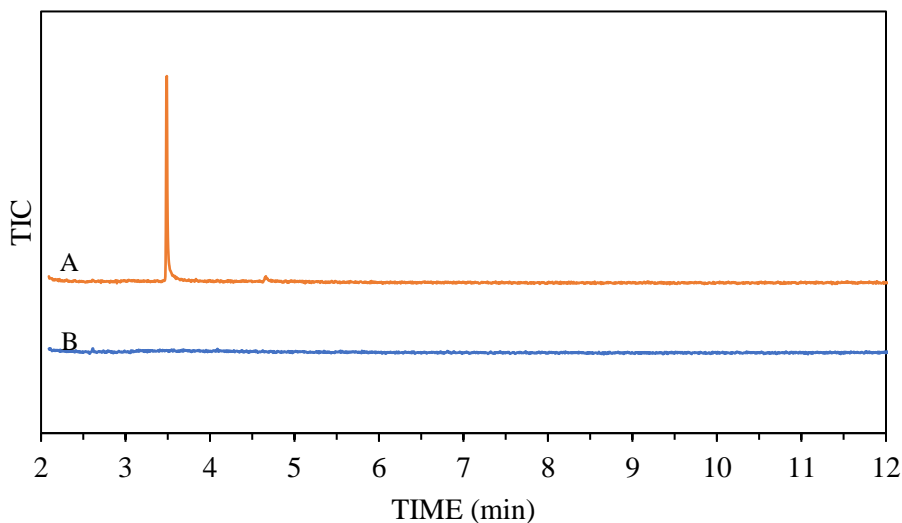


**Figure 9.** TIC of A: 0.5 mg/mL vigabatrin derivatized with BSTFA + 1% TMCS, B: 0.5 mg/mL vigabatrin in methanol.

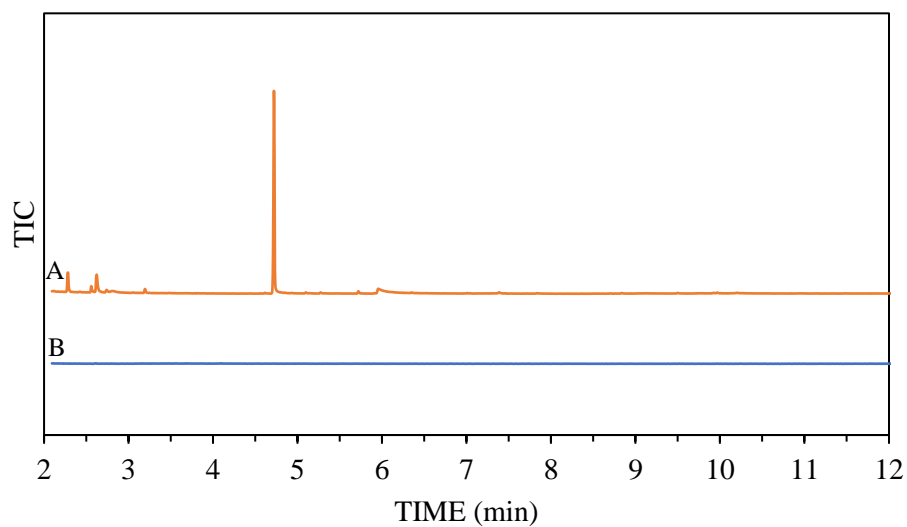


**Figure 10.** TIC of A: 0.5 mg/mL vigabatrin derivatized with DMF-DMA, B: 0.5 mg/mL vigabatrin in methanol.

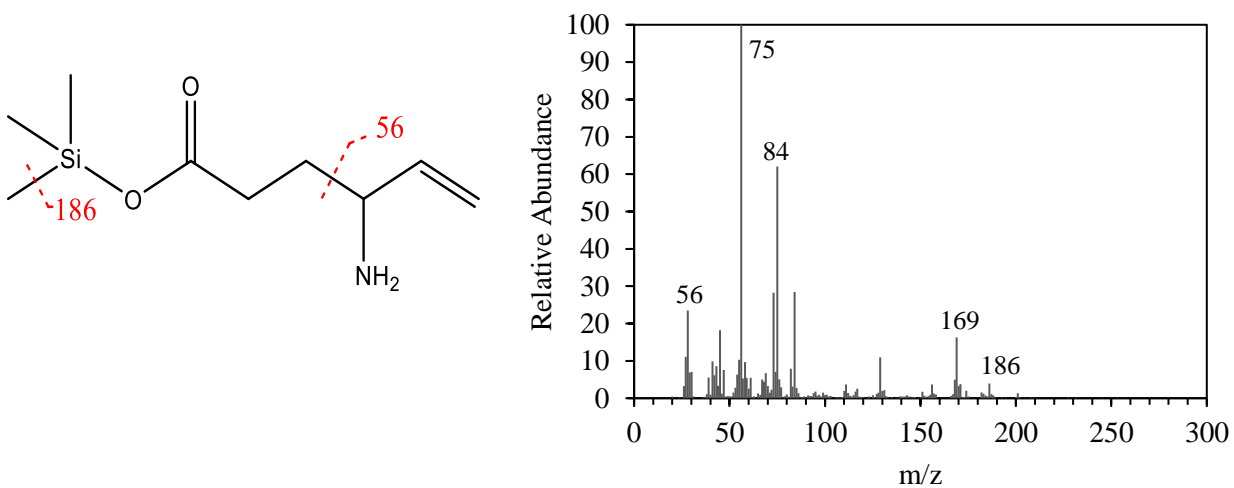


**Figure 11.** Structure and mass spectrum for vigabatrin TMS. MW = 201



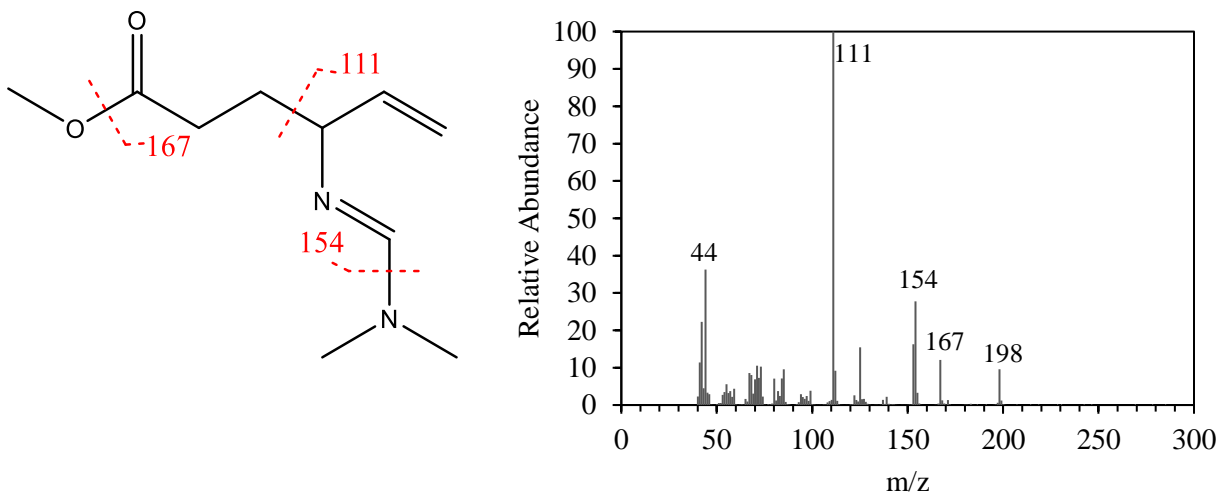


**Figure 12.** Structure and mass spectrum for vigabatrin DMAM. MW = 198

### *Pregabalin*

The results for pregabalin were generally negative. The parent compound was not detected in the underivatized form. Derivatization using TFAA produced several chromatographic peaks, none of which were the expected derivative. The derivatization of pregabalin with BSTFA produced several peaks, including mono-, di-, and tri-TMS derivatives of pregabalin. Due to peaks for multiple products from one drug and a peak for underivatized pregabalin, the derivatization with BSTFA was considered unsuccessful. Derivatization with DMF-DMA also proved unsuccessful, with the target derivative detected but accompanied by multiple unidentified peaks.

### *Amphetamine*

As expected, amphetamine could be identified without derivatization. It produced a single chromatographic peak with a mass spectrum that could be identified with a NIST mass spectral library search.

Derivatization of amphetamine with TFAA produced a much larger, narrower, and more symmetric chromatographic peak compared to a solution of underivatized amphetamine at the

same concentration (see Figure 13). The TFA derivative of amphetamine was not in the NIST library, but the mass spectrum was easily identified by the fragmentation pattern (see Figure 15). The  $m/z$  118 fragment resulted from McLafferty rearrangement with charge migration<sup>25</sup>. Alpha cleavage resulted in  $m/z$  91 (tropylium) and a  $m/z$  140 peak for the amine side chain.

The reaction of amphetamine with BSTFA was not complete. The target compound (amphetamine-TMS) was formed and identified, but the underivatized form of the drug was still present in the sample. Several attempts were made to force the reaction to completion (e.g., increase in reagent concentration, increase in temperature for the reaction, increase in the amount of time allocated for the reaction to reach completion), but none were successful.

Lastly, the reaction of amphetamine with DMF-DMA resulted in a product that has not been previously reported (see Figure 14). Amphetamine followed the same derivatization mechanism as heterocyclic amines with DMF-DMA (see Figure 16)<sup>11</sup>. There was no molecular ion seen in the mass spectrum, but alpha cleavage at the nitrogen originally present in amphetamine resulted in a fragment at  $m/z$  91 (tropylium) and  $m/z$  99, the base peak. The peak at  $m/z$  44 was formed from alpha cleavage from that same nitrogen but cleaved after the carbon in the DMAM.

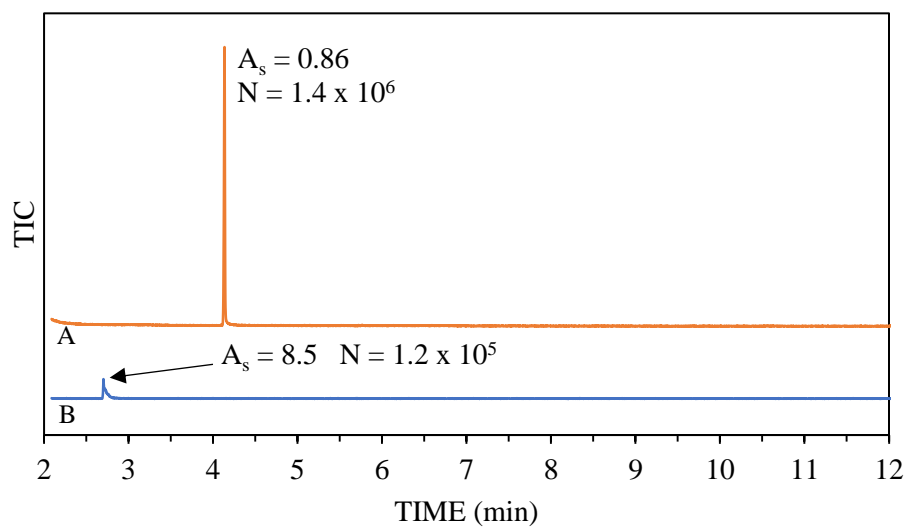


**Figure 13.** TIC of A: 0.5 mg/mL amphetamine derivatized with TFPA and B: 0.5mg/mL amphetamine in methanol.  $A_s$  = asymmetry factor.  $N$  = number of theoretical plates.

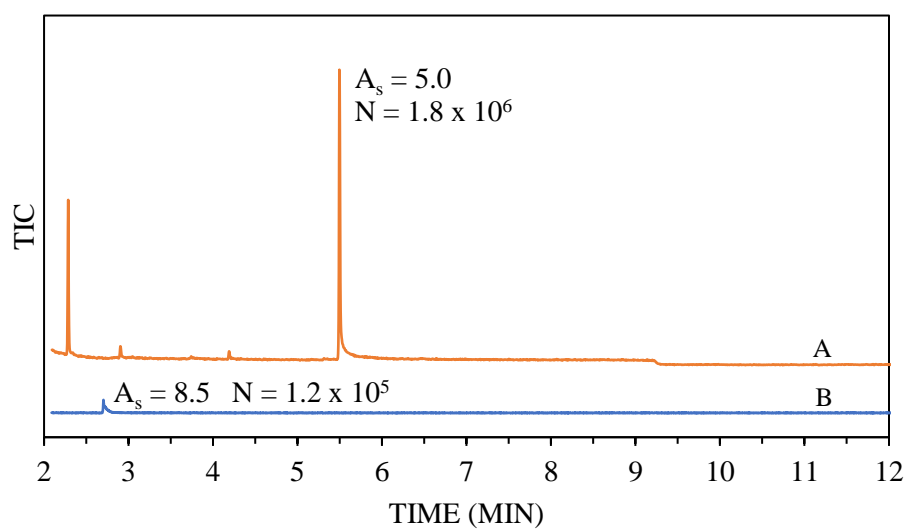


**Figure 14.** TIC of A: 0.5 mg/mL amphetamine derivatized with DMF-DMA and B: 0.5 mg/mL amphetamine in methanol.  $A_s$  = asymmetry factor.  $N$  = number of theoretical plates.

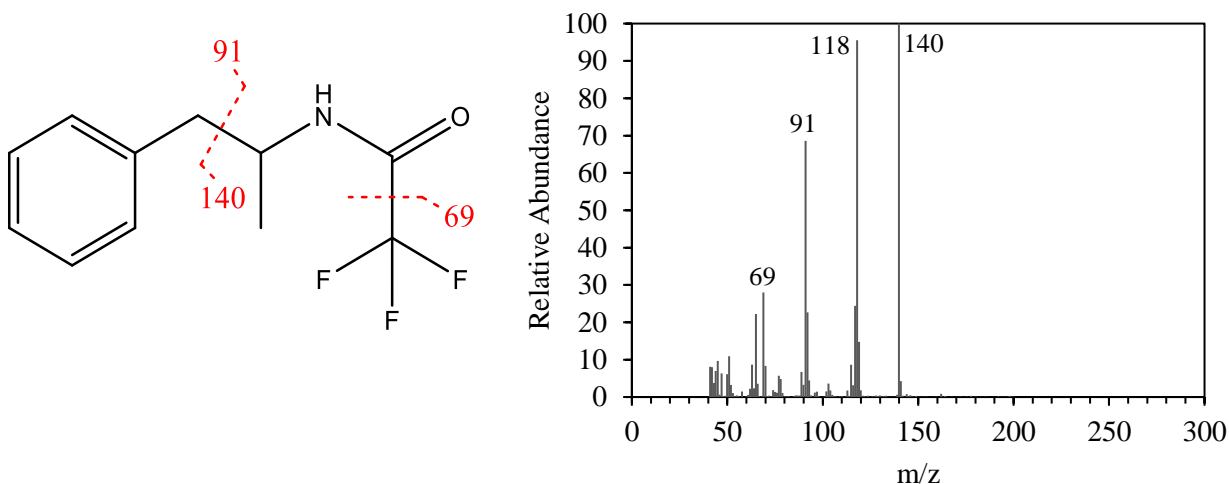


**Figure 15.** Structure and mass spectrum for amphetamine TFA. MW = 231

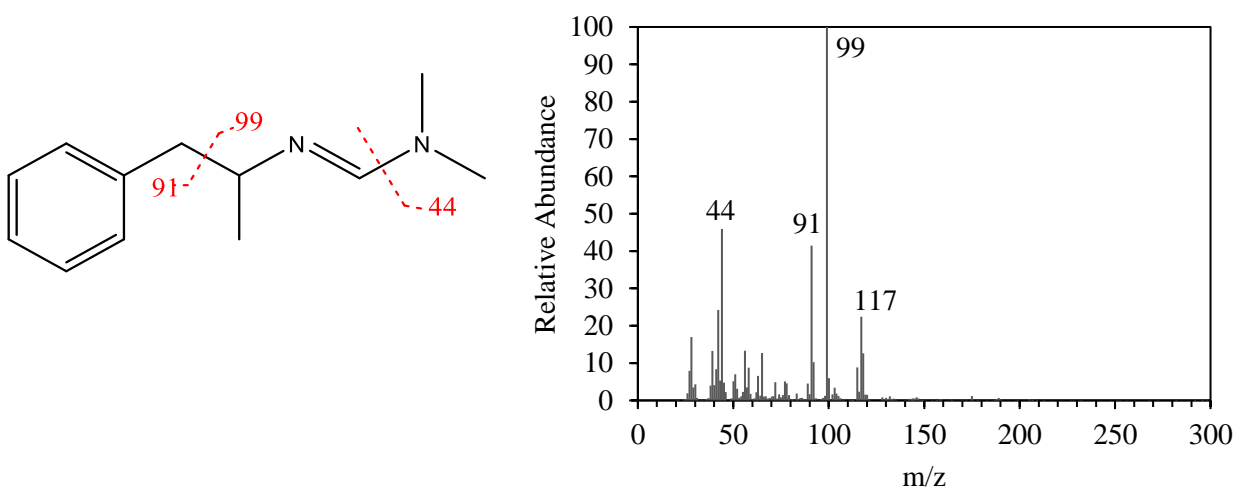


**Figure 16.** Structure and mass spectrum of amphetamine DMAM. MW = 190

### 2C-I

Like amphetamine, 2C-I was detected without derivatization, producing a single chromatographic peak with a mass spectrum that was identified with a NIST mass spectral library search.

The reaction of TFAA with 2C-I also resulted in a taller and narrower peak than that produced by underivatized 2C-I (see Figure 17). The 2C-I TFA derivative was not in the NIST

library, but the structure was elucidated by its fragmentation pattern (see Figure 19). After derivatization with TFAA, 2C-I had a molecular ion at  $m/z$  403. The ion at  $m/z$  290 was the result of McLafferty rearrangement with charge migration<sup>25</sup>. The molecular ion underwent alpha cleavage at the nitrogen, which produced a fragment at  $m/z$  277 and a fragment at  $m/z$  126. The fragment at  $m/z$  247 was a result of cleavage of two methyl groups from the  $m/z$  277 fragment.

Derivatization with BSTFA yielded both a 2C-I derivative with one TMS group on the primary nitrogen and a derivative with two TMS groups on the primary nitrogen. Due to the formation of two derivatives from one analyte, this reaction was determined to be unsatisfactory.

Derivatization of 2C-I with DMF-DMA was, as with amphetamine, a new approach that produced a novel product (see Figure 18). Just like amphetamine, the labile hydrogens on the primary amine in 2C-I were replaced with a DMAM group (see Figure 20). The same alpha cleavage paths resulted in the base peak of  $m/z$  85 and the characteristic  $m/z$  44. There was no molecular ion seen in 2C-I, however there was a small ion at  $m/z$  331. This fragment was a result of the molecular ion losing 31 mass units (methoxy) from the aromatic ring.

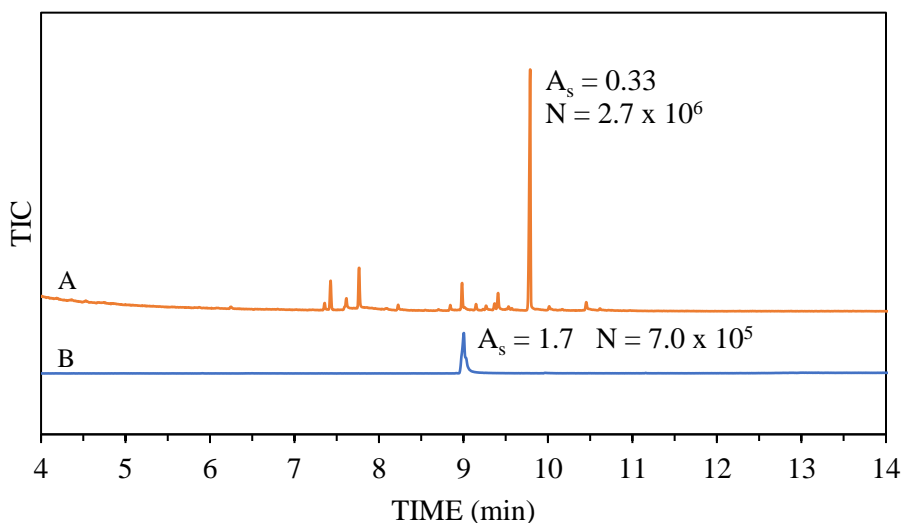


**Figure 17.** TIC of A: 0.5 mg/mL 2C-I derivatized with TFAA and B: 0.5 mg/mL 2C-I in methanol.  $A_s$  = asymmetry factor.  $N$  = number of theoretical plates.

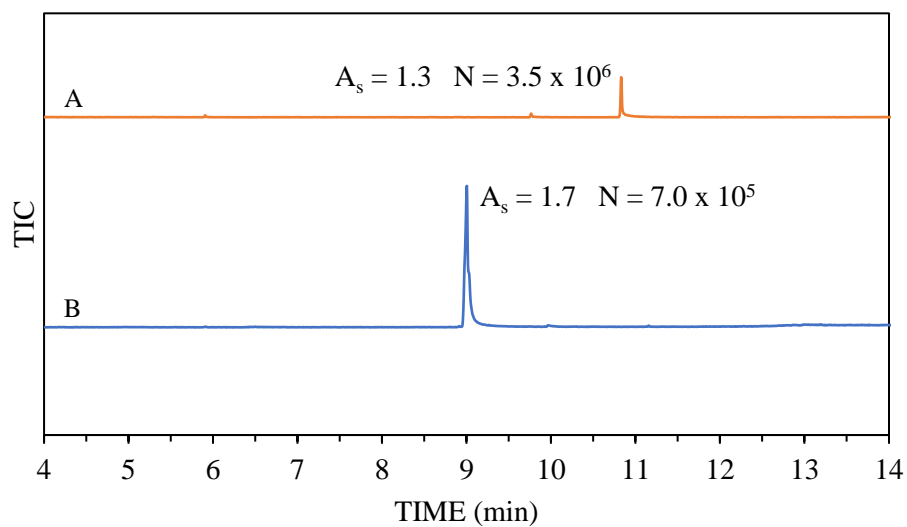


**Figure 18.** TIC of A: 0.5 mg/mL 2C-I derivatized with DMF-DMA and B: 0.5 mg/mL 2C-I in methanol.  $A_s$  = asymmetry factor.  $N$  = number of theoretical plates.

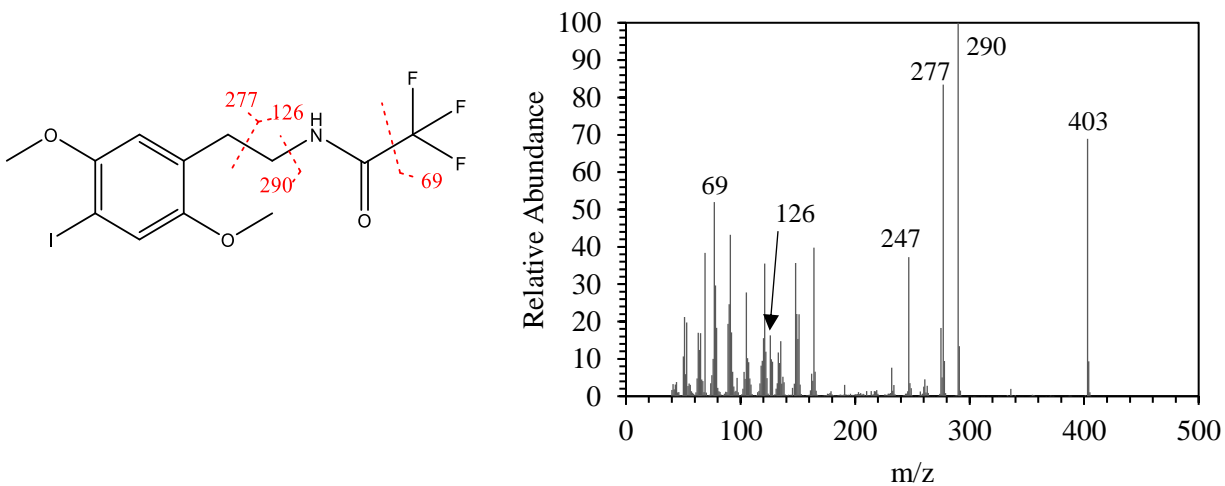


**Figure 19.** Structure and mass spectrum for 2C-I TFA. MW = 403

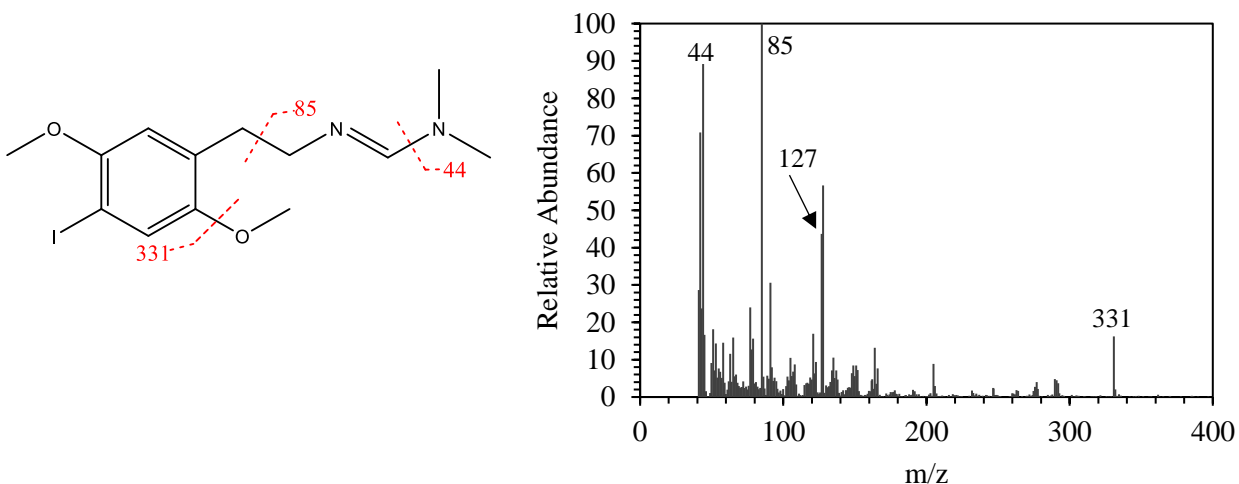


**Figure 20.** Structure and mass spectrum of 2C-I DMAM. MW = 362

### *Gabapentin*

Although potentially problematic for GC-MS analysis, underivatized gabapentin produced a single chromatographic peak with a mass spectrum that was identified with a NIST mass spectral library search. After ionization, gabapentin underwent a loss of water resulting in an ion at  $m/z$  154. The remaining structure cyclized via hydrogen rearrangement prior to the cleavage of the cycloalkane. The low mass ions seen in the mass spectrum were characteristic of the fragmentation of cycloalkanes.

Derivatization with TFAA produced a single chromatographic peak (Figure 21). This derivative was not in the NIST library, but its mass spectrum was identified by analyzing the fragmentation pattern (see Figure 23). One of the hydrogens on the amine nitrogen was replaced by a trifluoroacetyl group. The molecular ion was not seen on the mass spectrum. Instead, an  $M-18$  ( $m/z$  249) peak was seen arising from the loss of water. The  $m/z$  180 base peak was formed by the further loss of  $CF_3$ .

Derivatization of gabapentin with BSTFA was not successful. No target derivative was formed. Derivatization of gabapentin by DMF-DMA produced a single chromatographic peak (see Figure 22). This derivative was not in the NIST library, but its mass spectrum was identified by analyzing the fragmentation pattern (see Figure 24). Gabapentin contains both a primary amine and a carboxylic acid, so its derivatization was directly analogous to that of primary amino acids<sup>9</sup>. The amine underwent the same process as that in amphetamine and 2C-I, and the carboxylic acid was methylated in one step, resulting in an N,N-dimethylaminomethylene methyl ester<sup>9</sup>. The molecular ion ( $m/z$  240) was seen in very small abundance in the mass spectrum. A fragment was seen at  $m/z$  209 which was the result of the molecular ion losing 31 mass units in the form of a methoxy radical. The base peak of  $m/z$  85 resulted from alpha cleavage at the original nitrogen. Loss of the dimethylamino group resulted in an  $m/z$  44 and an  $m/z$  196 fragment.

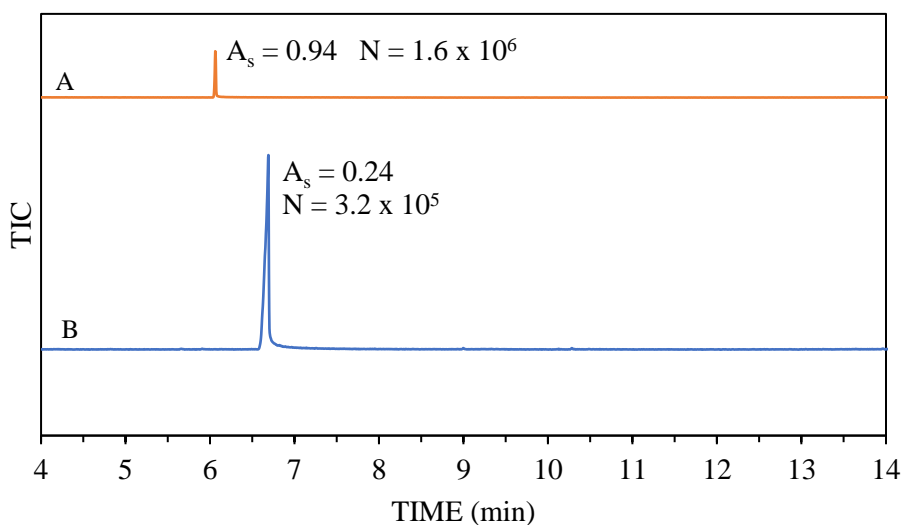


**Figure 21.** TIC of A: 0.5 mg/mL gabapentin derivatized with TFMA and B: 0.5 mg/mL gabapentin in methanol.  $A_s$  = asymmetry factor.  $N$  = number of theoretical plates.



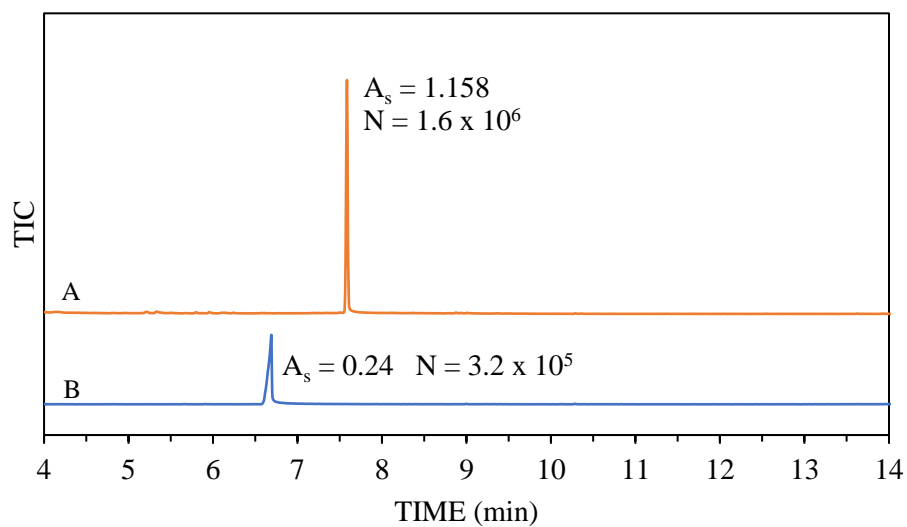


**Figure 22.** TIC of A: 0.5 mg/mL gabapentin derivatized with DMF-DMA and B: 0.5 mg/mL gabapentin in methanol.  $A_s$  = asymmetry factor.  $N$  = number of theoretical plates.

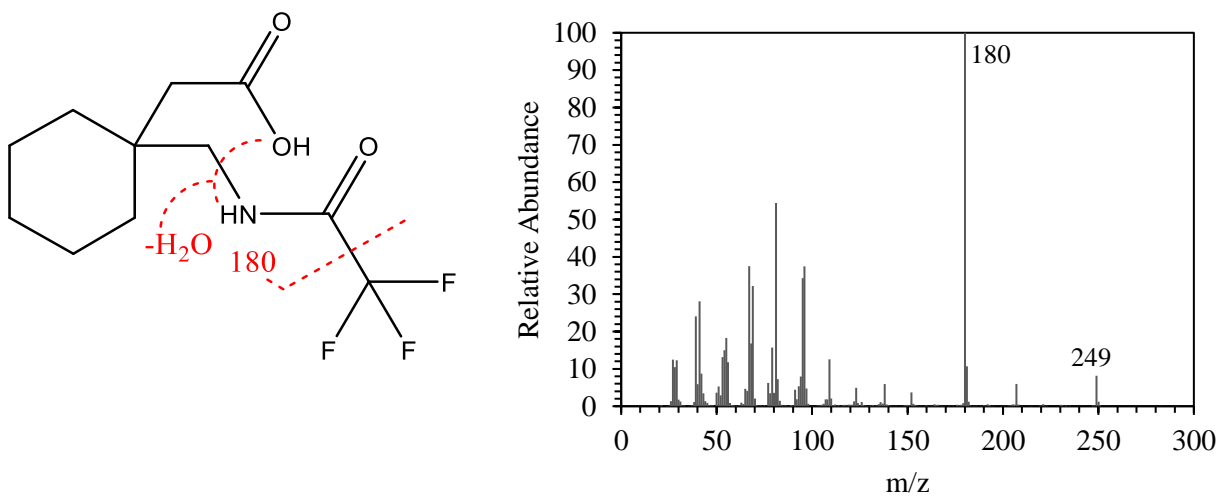


**Figure 23.** Structure and mass spectrum for gabapentin TFA. MW = 267

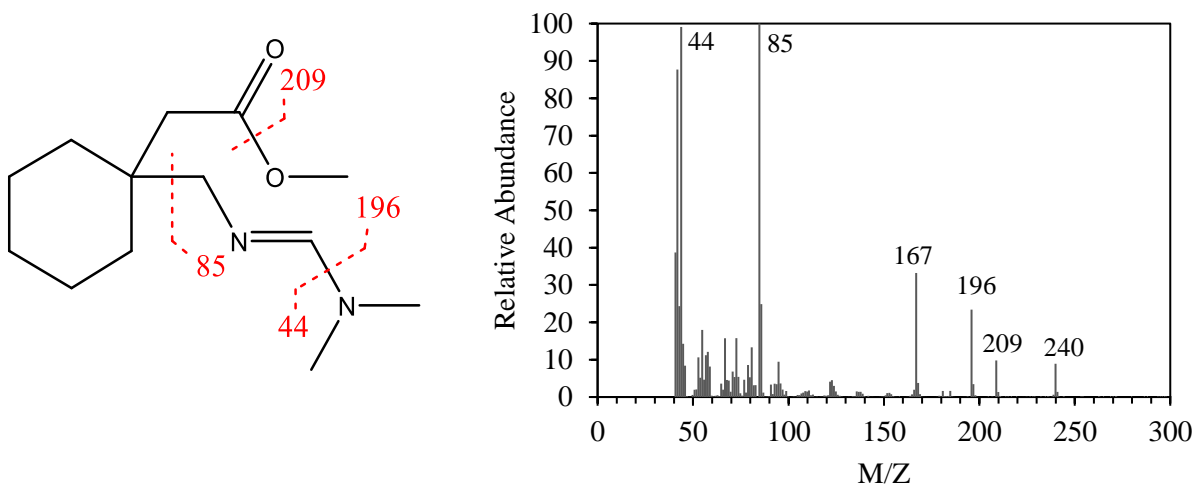


**Figure 24.** Structure and mass spectrum for gabapentin DMAM. MW = 240

### *Lorazepam*

Despite some concerns about the analysis of lorazepam by GC/MS, it produced a single chromatographic peak that was identified with a NIST library search. The mass spectrum of lorazepam had a low mass ion series that was indicative of aromatic compounds (e.g.,  $m/z$  50, 51, 63, 64, 74, 75, and 76)<sup>25</sup>. This most likely arose from fragmentation of the aromatic ring following the alpha cleavage from the nitrogen. A fragment of  $m/z$  302 corresponded to a loss of 20 amu from the molecular ion. The isotopic signature of chlorine was used to determine the number of chlorines in each ion<sup>25</sup>. Because  $^{37}\text{Cl}$  is present at about one third the abundance of  $^{35}\text{Cl}$  in nature, an ion two mass units heavier than the target ion with one third the abundance of the target ion indicates the presence of one chlorine in the target fragment while an ion two mass units heavier than the target ion with two thirds the abundance indicates the presence of two chlorines. Given this, it was determined that the loss of one chlorine radical from the  $m/z$  302 fragment resulted in a fragment of  $m/z$  267, the loss of 28 from the  $m/z$  302 fragment resulted in a fragment at  $m/z$  274,

and the loss of both a chlorine and an additional 28 mass units from the  $m/z$  302 fragment resulted in the base peak at  $m/z$  239.

Derivatization with TFSA was unsuccessful as no derivative was detected. Derivatization with BSTFA produced a single chromatographic peak with a mass spectrum that was identified as the di-TMS derivative of lorazepam by a NIST library search. The base peak at  $m/z$  429 results from the loss of a chlorine radical.

DMF-DMA derivatization was unsuccessful with lorazepam due to the formation of multiple peaks which could not be attributed to the target derivative.

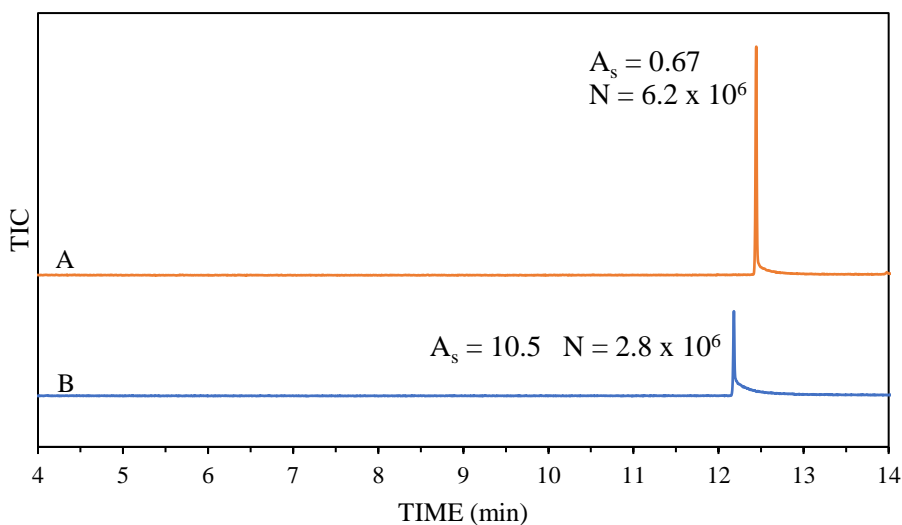


**Figure 25.** TIC of A: 0.5 mg/mL lorazepam derivatized with BSTFA + 1% TMCS and B: 0.5 mg/mL lorazepam in methanol.  $A_s$  = asymmetry factor.  $N$  = number of theoretical plates

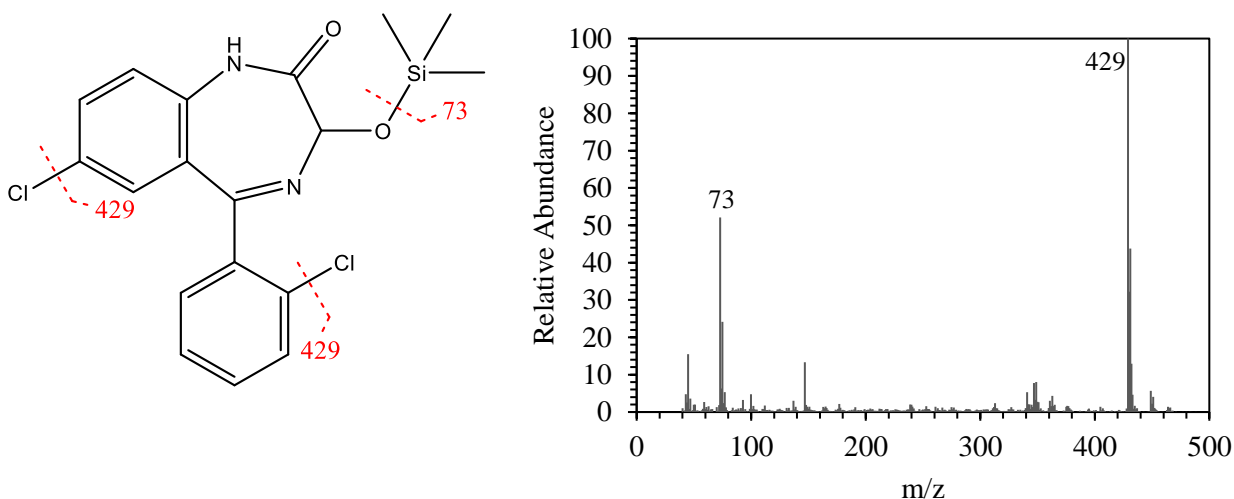


**Figure 26.** Structure and mass spectrum for lorazepam TMS. MW = 464

As shown in Tables 2 – 4, chromatographic performance was greatly improved through derivatization. For example, the peak asymmetry for amphetamine improved by 47% with the DMAM derivative and 98% with the TFA derivative. In addition, separation efficiency increased by 1,355% for the DMAM derivative and 1,047% for the TFA derivative. Sensitivity increased by 1,220% for the DMAM derivative and 533% for the TFA derivative. The peak asymmetry for 2C-I improved by 55% with the DMAM derivative and 9% with the TFA derivative. Separation efficiency for 2C-I increased by 406% for the DMAM derivative and 279% for the TFA derivative. The sensitivity decreased by 86% for the DMAM derivative and increased by 118% for the TFA derivative. The peak asymmetry for gabapentin improved by 79% with the DMAM derivative and 92% with the TFA derivative. Separation efficiency was also increased by 393% for the DMAM derivative and 403% for the TFA derivative. Sensitivity for gabapentin was increased by 63% for the DMAM derivative and decreased by 91% for the TFA derivative. The peak asymmetry for lorazepam improved by 96% with the TMS derivative. Separation efficiency was increased by 119%, and sensitivity was increased by 64%.

**Table 2.** Comparing asymmetry factors for underivatized drugs and their derivative(s)

Drug	Underivatized	TFA	TMS	DMAM
Amphetamine	8.5	0.86	-	5.0
2C-I	1.7	0.33	-	1.3
Gabapentin	0.24	0.94	-	1.2
Lorazepam	10.5	-	0.67	-

**Table 3.** Comparing separation efficiency (number of theoretical plates) for underivatized drugs and their derivative(s)

Drug	Underivatized (/10 <sup>6</sup> )	TFA (/10 <sup>6</sup> )	TMS (/10 <sup>6</sup> )	DMAM (/10 <sup>6</sup> )
Amphetamine	0.12	1.4	-	1.8
2C-I	0.7	2.7	-	3.5
Gabapentin	0.32	1.6	-	1.6
Lorazepam	2.8	-	6.2	-

**Table 4.** Comparing sensitivity (peak area) for underivatized drugs and their derivative(s)

Drug	Underivatized (/10 <sup>7</sup> )	TFA (/10 <sup>7</sup> )	TMS (/10 <sup>7</sup> )	DMAM (/10 <sup>7</sup> )
Amphetamine	1.1	6.8	-	14
2C-I	42	91	-	5.7
Gabapentin	68	6.0	-	110
Lorazepam	7.2	-	12	-

## Conclusions

Basic and zwitterionic drugs can be amongst the most difficult to analyze via GC/MS due to their thermal instability and non-ideal behavior resulting in broad, asymmetric peaks. A summary of the drugs and derivatizations discussed in this paper appears in Table 5.

**Table 5.** A summary of the results of this work. + indicates the formation of a single chromatographic peak which could be unambiguously identified. – indicates no relevant peak was formed. 0 indicates multiple peaks were formed.

Drug	Underivatized	TFAA	BSTFA	DMF-DMA
Amphetamine	+	+	0	+
2C-I	+	+	0	+
Gabapentin	+	+	-	+
Lorazepam	+	-	+	-
Vigabatrin	-	-	+	+
Pregabalin	-	-	0	0
Clorazepate	-	-	+	-

Amphetamine, 2C-I, gabapentin, and lorazepam were successfully analyzed by GC/MS without modification. However, the number of theoretical plates achieved was dramatically increased by derivatization and peak symmetry was greatly improved. Direct GC/MS analysis of vigabatrin, pregabalin and clorazepate yielded negative results, as no peaks were formed.

Among the drugs of interest, amphetamine and 2C-I were readily derivatized with TFAA. The derivatives produced more intense and narrower chromatographic peaks than their underivatized forms. Gabapentin was also successfully derivatized with TFAA, but the resulting chromatographic peak was smaller in magnitude than that of the underivatized drug. Lorazepam, vigabatrin, pregabalin, and clorazepate were not successfully derivatized by TFAA – lorazepam and vigabatrin produced no chromatographic peaks, while pregabalin and clorazepate both produced multiple peaks, none of which were the target derivatives.

Derivatization with BSTFA + 1% TMCS produced single chromatographic peaks for lorazepam, vigabatrin, and clorazepate. The derivatization was incomplete for amphetamine and wholly unsuccessful for gabapentin, producing no derivative. BSTFA derivatization yielded multiple derivatives with one, two, or even three TMS groups for 2C-I and pregabalin.

As previously discussed, methyl-N-t-butyldimethylsilyltrifluoroacetamide (MTBSTFA) and other silylation reagents that replace active hydrogens with larger t-butyldimethylsilyl rather than trimethylsilyl groups generally take longer to form, but are more stable. Additionally, the t-butyldimethylsilyl group is more sterically hindering than the trimethylsilyl group, so t-butyldimethylsilyl reagents will likely form only one derivative with primary amines. It is therefore possible that reactions with BSTFA that were unsuitable due to multiple products or for which no derivative was detected here may produce useful results when reacted with larger silylation reagents such as MTBSTFA.

Lastly, DMF-DMA proved an effective new method for the derivatization of the primary amines amphetamine, 2C-I, gabapentin, and vigabatrin. The primary amine hydrogens in amphetamine and 2C-I were replaced with a DMAM group. Gabapentin and vigabatrin, containing both a primary amine and a carboxyl group, underwent the addition of a methyl group and a DMAM group. Derivatization with DMF-DMA did not yield favorable results for lorazepam, pregabalin, or clorazepate. As previously discussed, the derivative for pregabalin was formed, but there were several other peaks present in the chromatogram that could not be identified. The chromatograms for both lorazepam and clorazepate showed multiple peaks, none of which could be attributed to the target derivatives.

## CHAPTER 2. DEVELOPMENT OF TV-SPME ON-FIBER DERIVATIZATION OF CONTROLLED SUBSTANCES

### Introduction

Derivatization has long been used to improve the characteristics of controlled substances that are not sufficiently volatile and/or thermally unstable during GC-MS analysis. By derivatizing these compounds, the chromatographic performance is significantly improved<sup>2</sup>. Chapter 1 demonstrated the effectiveness of traditional liquid derivatization techniques coupled with liquid injection GC-MS methods for several controlled substances.

Derivatization offers many benefits, but traditional solution phase techniques are work intensive and time consuming. However, derivatization can be adapted to a sampling technique developed by our laboratory called Total Vaporization Solid-Phase Microextraction (TV-SPME) to simplify and automate the process. Solid-Phase Microextraction (SPME) is a technique in which the analytes are pre-concentrated onto a fiber coated in absorptive or adsorptive material. TV-SPME is a novel technique in which a small aliquot of solution is placed in a vial and heated until the sample completely vaporizes<sup>26-27</sup>. A SPME fiber is then introduced and the sample is adsorbed onto the fiber coating. TV-SPME is analogous to immersion SPME in that both are two-phase systems unlike headspace SPME, which is a three-phase system.

The maximum volume for total vaporization of a given solvent can be easily calculated given the solvent vapor pressure, molecular weight, vial volume and temperature<sup>26</sup>. For example, the calculated maximum volume of methanol for total vaporization in a 20-mL vial at 60°C is 24  $\mu\text{L}$ .

The use of TV-SPME for sampling can streamline the process of derivatization by allowing it to be done simultaneously with the extraction step in a process called on-fiber derivatization.



On-fiber derivatization has been used before in conjunction with headspace or immersion SPME<sup>3, 28-31</sup>. It would be desirable, however, to bring the advantages offered by TV-SPME to bear for on-fiber derivatization. In on-fiber derivatization with TV-SPME, a SPME fiber is exposed to the headspace of a vial containing a small amount of liquid derivatization agent. The fiber is then moved to the heated headspace of a vial containing the sample. The reaction between the analyte and the derivatization agent then takes place directly on the SPME fiber or in the headspace surrounding the fiber. After sufficient time for reaction and adsorption, the fiber is moved to the inlet of the GC for desorption. The use of a robotic autosampler can make this a fully automated process wherein the only sample prep necessary is to dissolve the sample in a suitable solvent and place an aliquot into the vial.

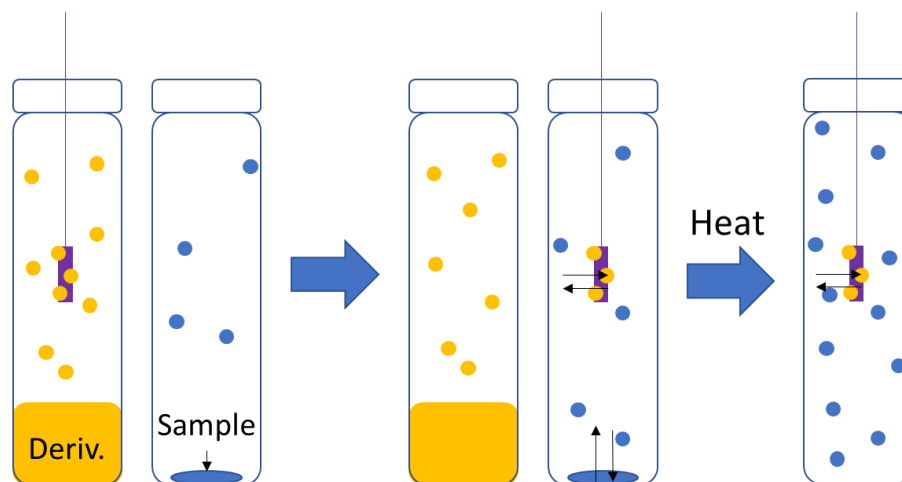


**Figure 27.** Depiction of the On-Fiber Total Vaporization Solid-Phase Microextraction process.

The controlled substances chosen for this project were a combination of drugs commonly encountered in forensic laboratories and drugs that are difficult or impossible to analyze “as is” by traditional GC-MS methods. The structures and molecular weights of the chosen drugs are displayed in figures 28 and 29, below.

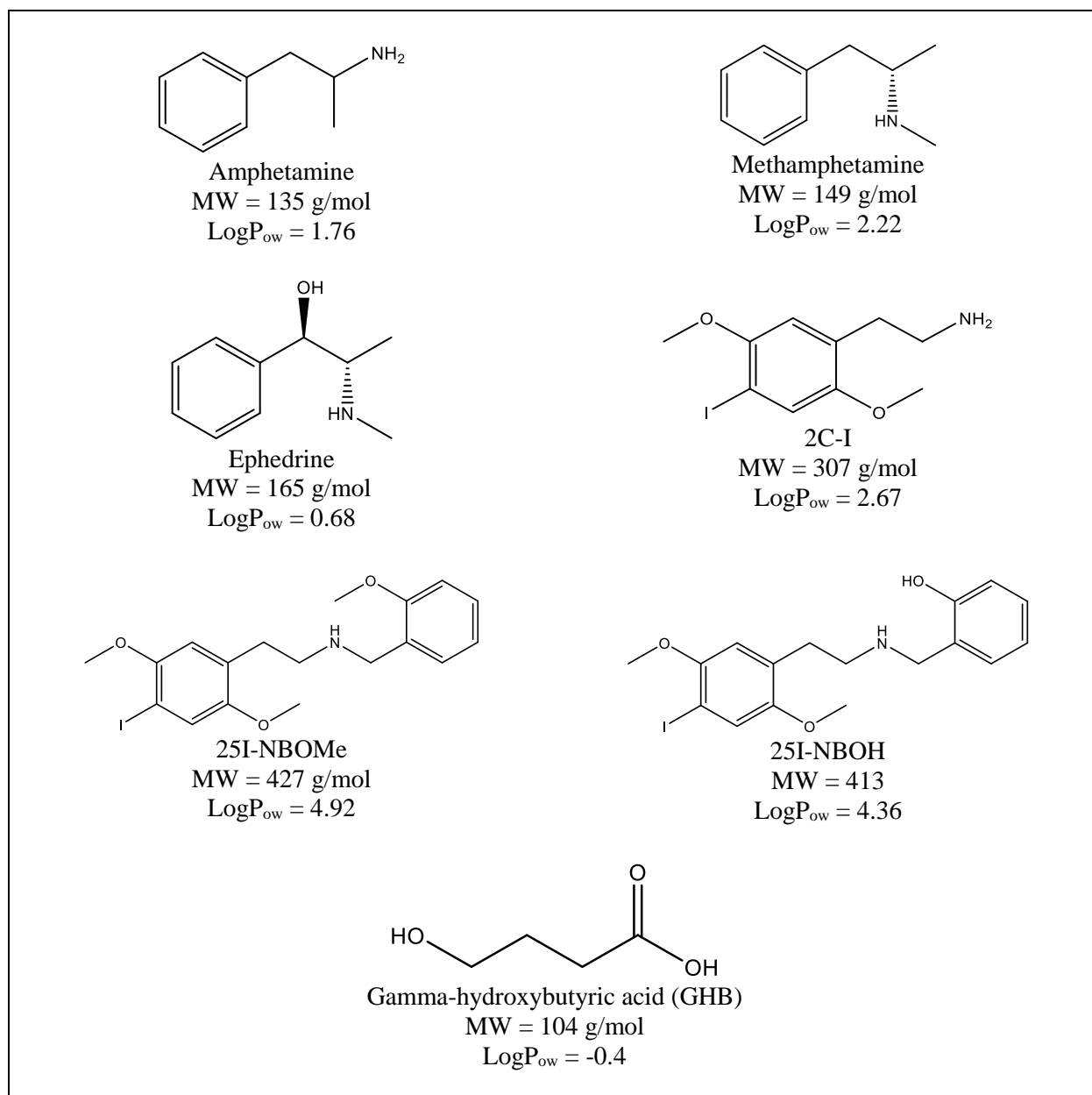


**Figure 28.** Structures, molecular weights, and octanol:water partition coefficient (LogPow) of the drugs analyzed in this work.

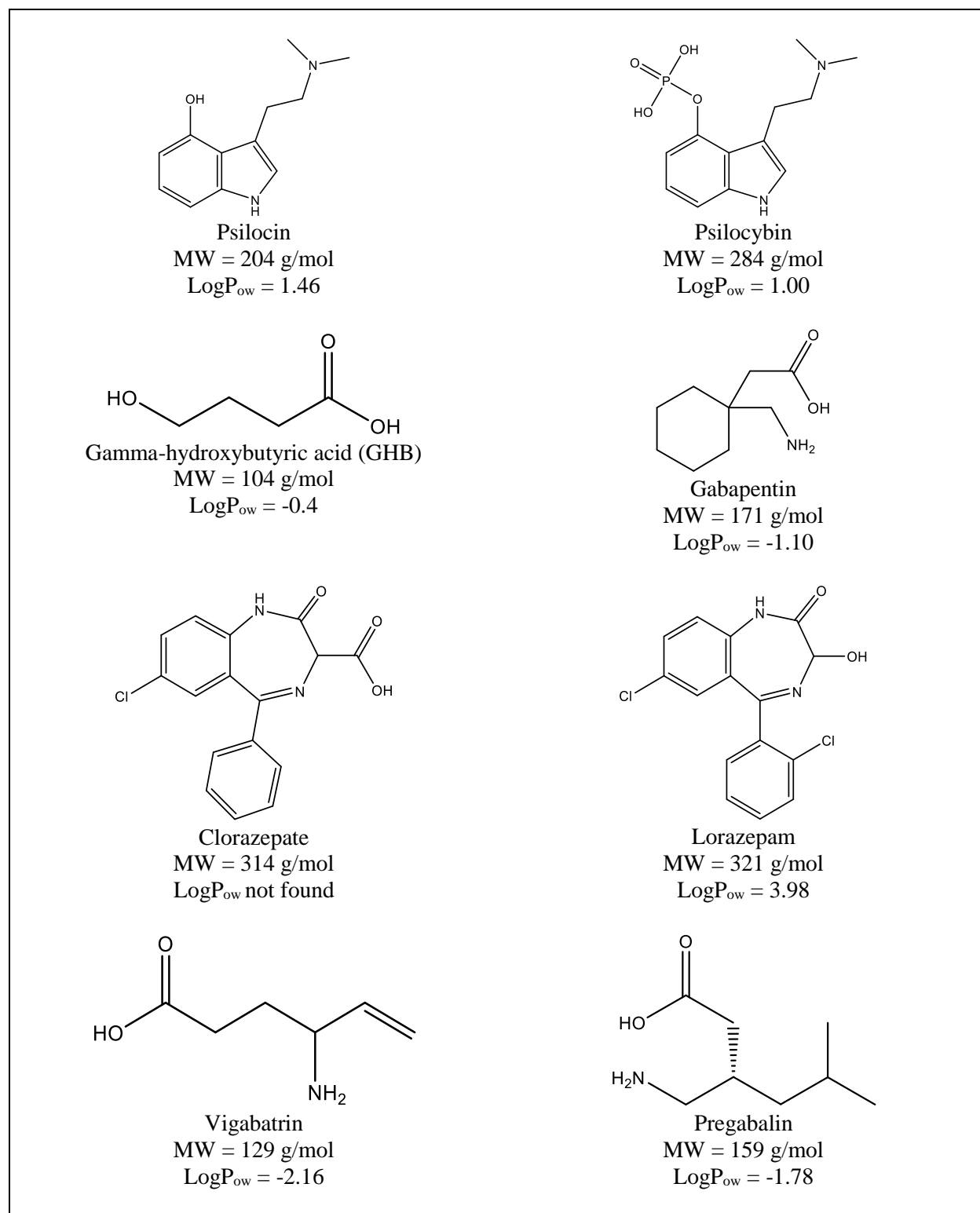


**Figure 29.** Structures, molecular weights, and octanol:water partition coefficient (LogPow) of the zwitterionic drugs analyzed in this work.

## Experimental

### *Materials*

Amphetamine sulfate, methamphetamine HCl, ephedrine HCl, lorazepam, pregabalin, and dimethylformamide dimethyl acetal (DMF-DMA) were purchased from Sigma-Aldrich (St. Louis, Missouri). Psilocybin, psilocin, 4-iodo-2,5-dimethoxy- $\beta$ -phenethylamine (2C-I) hydrochloride, 4-iodo-2,5-dimethoxy-N-(2-methoxybenzyl) phenethylamine (25I-NBOMe) hydrochloride, 2-[[2-(4-iodo-2,5 dimethoxyphenyl) ethylamino] methyl] phenol (25I-NBOH) hydrochloride, gamma-hydroxybutyric acid (GHB), gabapentin, and vigabatrin were purchased from Cayman Chemical (Ann Arbor, Michigan). Clorazepate dipotassium was purchased from Grace Chemical (Columbia, Maryland). HPLC grade methanol, Optima acetonitrile, stabilized HPLC grade methylene chloride, trifluoroacetic anhydride (TFAA), and N,O-bis(trimethylsilyl)trifluoroacetamide with 1% trimethylchlorosilane (BSTFA + 1% TMCS) were purchased from Thermo Fisher Scientific (Waltham, Massachusetts). Polydimethyl siloxane solid phase microextraction fibers, 100  $\mu$ m film thickness, were purchased from Supelco (Bellefonte, Pennsylvania).

### *Sampling Method*

Standard solutions of all drugs were prepared in methanol at a concentration of 1 mg/mL, except for GHB, gabapentin, and vigabatrin, which were at a concentration of 0.6 mg/mL. For underivatized drugs, 24  $\mu$ L of each drug solution in methanol was dispensed into a 20-mL headspace vial for analysis. The SPME fiber was exposed to the contents of the vial, which was heated with agitation to 30, 60, 90, 120, 150, 180, or 200°C, for 15 minutes before moving to the inlet of the GC for desorption at 250°C.

For derivatization, 24  $\mu\text{L}$  of drug solution in methanol were dispensed into a 20-mL headspace vial and the solvent was evaporated. 18  $\mu\text{L}$  of acetonitrile were then added to the vial. A new vial containing fresh derivatization agent (TFAA, BSTFA +1% TMCS, or DMF-DMA) was prepared at the beginning of each day. The derivatization agent used for each drug was determined by previous work done with liquid-phase derivatization in our laboratory. Amine and hydroxylamine drugs were designated for derivatization with TFAA. Psilocin and psilocybin were designated for derivatization with both TFAA and BSTFA + 1% TMCS. GHB was designated for derivatization with BSTFA + 1% TMCS. The zwitterionic drugs were designated for derivatization with both BSTFA + 1% TMCS and DMF-DMA. The SPME fiber was exposed to the headspace of the derivatization vial for five minutes, then exposed to the drug vial, which was heated with agitation at the optimum temperature found for the underivatized drug, for 10 minutes before moving to the inlet of the GC for desorption at 250°C. The fiber was cleaned by heating it in the second inlet of the GC at 250°C for 10 minutes after each derivatization run.

#### *GC-MS Parameters*

An Agilent 6890N GC coupled to an Agilent 5975 inert Mass Selective Detector with an attached Gerstel PAL RTC MultiPurpose Sampler (MPS) was used for all experiments. The GC column was an Agilent Technologies DB-5MS column with a length of 30 m, a 0.250 mm inner diameter, and a 0.25  $\mu\text{m}$  film thickness. Straight inlet liners of 1.2 mm inner diameter from SGE Analytical Science were used. This type of inlet liner was chosen because the vapor volume introduced in derivatization runs was too great for 0.75 mm inner diameter SPME-specific inlet liners, resulting in split peaks and “echo” effects for derivatives and derivatization agents.

The inlet temperature was set to 250°C and operated in split mode with a 15:1 split ratio. The initial oven temperature of 60°C was held for one minute, then the temperature was ramped at

15°C/min to 280°C where it was held for three minutes. A constant flow of 2.5 mL/min of hydrogen was maintained. The source was kept at 230°C and the quadrupoles were kept at 150°C. A scan range of  $m/z$  40-  $m/z$  550 was used, with a solvent delay of 2 minutes.

## Results

### *Extraction Temperature Study*

Each drug was analyzed “as is” with extraction temperatures ranging from 30°C to 200°C to determine the optimum temperature. Figures 30-32 illustrate the effect of extraction temperature on analyte signal for those drugs that were detected in the underivatized form by TV-SPME. The optimum extraction temperature was then chosen as the starting extraction temperature for on-fiber derivatization. When the boiling point of each analyte is plotted against its experimentally determined optimum extraction temperature, a trend is revealed. The coefficient of determination ( $R^2$ ) describes how well the regression line represents the data. For this data set  $R^2 = 0.6892$ , indicating that the predicting power of the regression line is rather low. The correlation coefficient ( $r$ ) is a measure of how closely the two variables, in this case boiling point and optimum extraction temperature, are correlated. For this data set  $r = 0.8302$ , indicating that there is a modest but significant correlation between an analyte’s boiling point and its optimum extraction temperature. Taken together, the correlation coefficient and coefficient of determination tell us that boiling point and optimum extraction temperature are correlated, but that not all of the variation in optimum extraction temperature can be explained by boiling point alone. The plot of optimum extraction temperature vs. boiling point is shown in Figure 33.

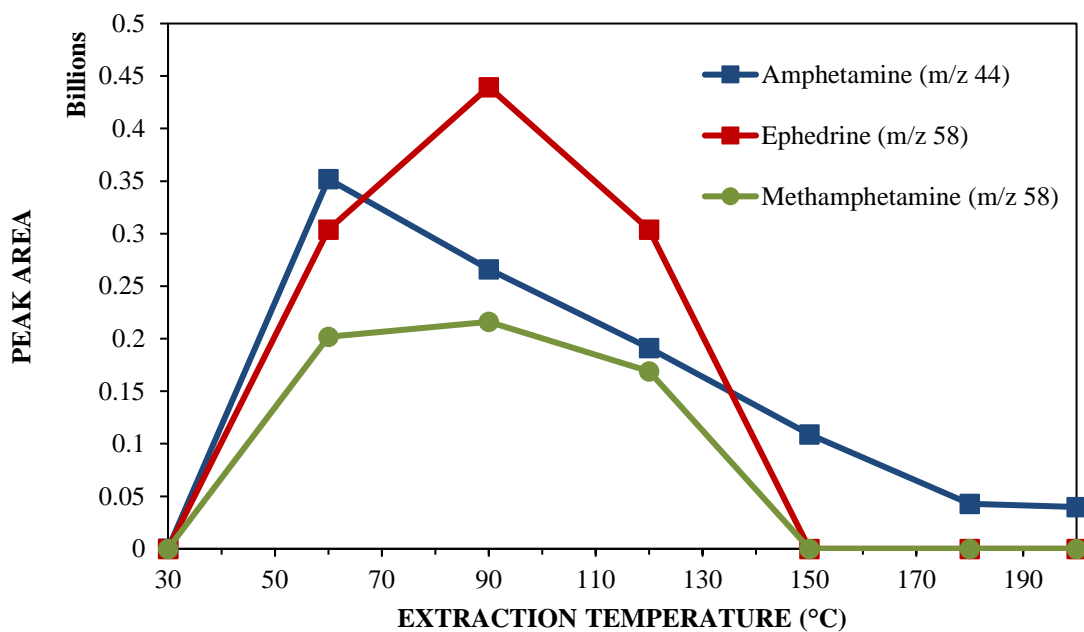


**Figure 30.** Graph of peak area vs extraction temperature for underivatized phenethylamines. Peak area was calculated using the extracted ion profile (EIP) for the ion indicated.

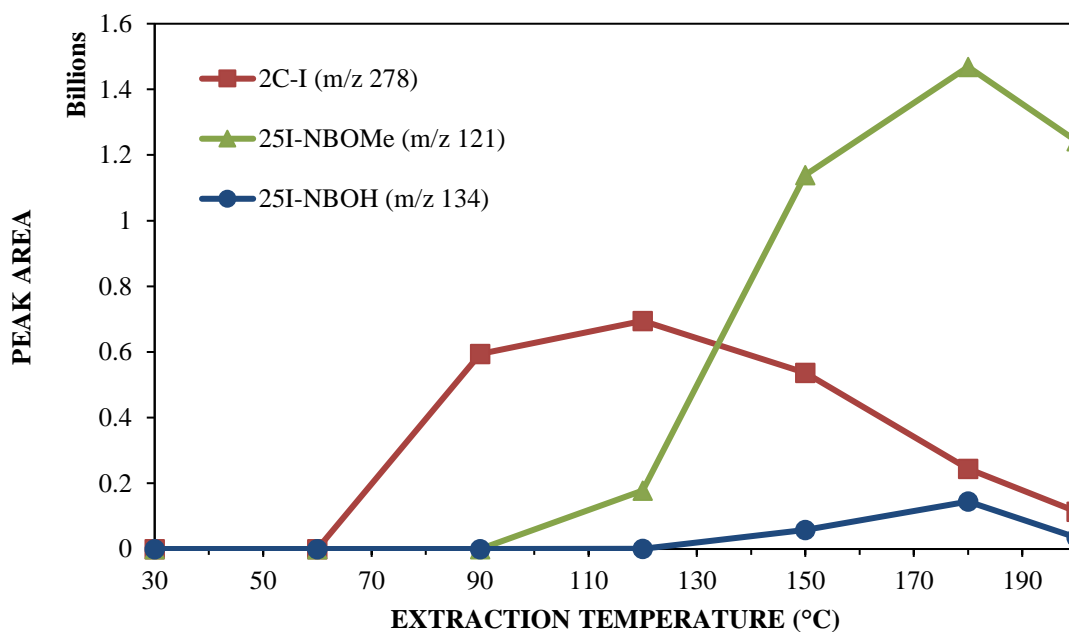


**Figure 31.** Graph of peak area vs extraction temperature for underivatized designer drugs. Peak area was calculated using the extracted ion profile (EIP) for the ion indicated.

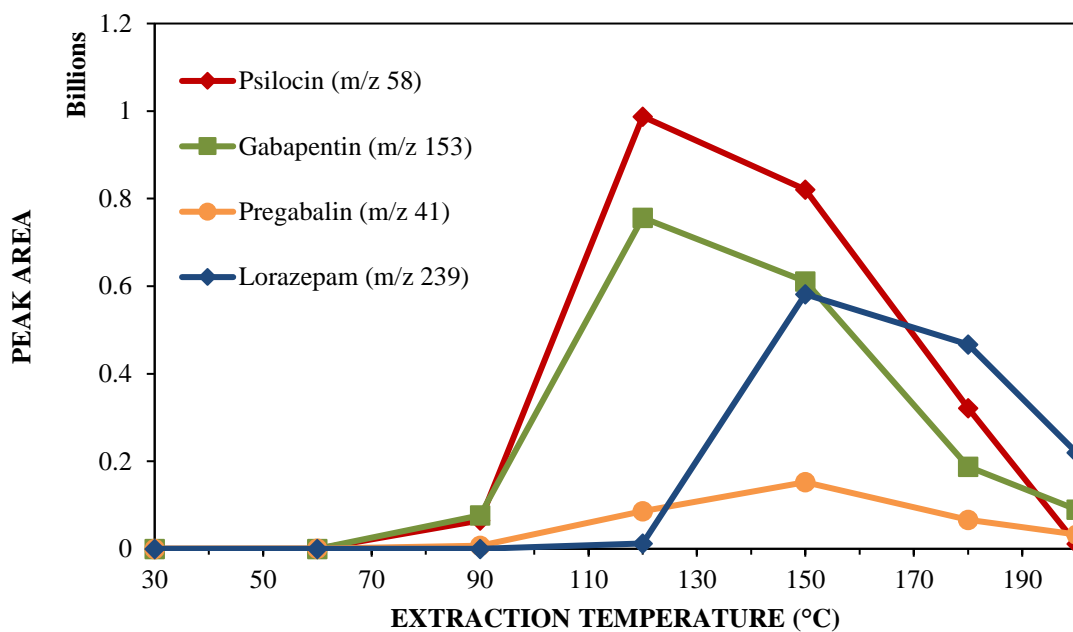


**Figure 32.** Graph of peak area vs extraction temperature for underivatized zwitterions. Peak area was calculated using the extracted ion profile (EIP) for the ion indicated.

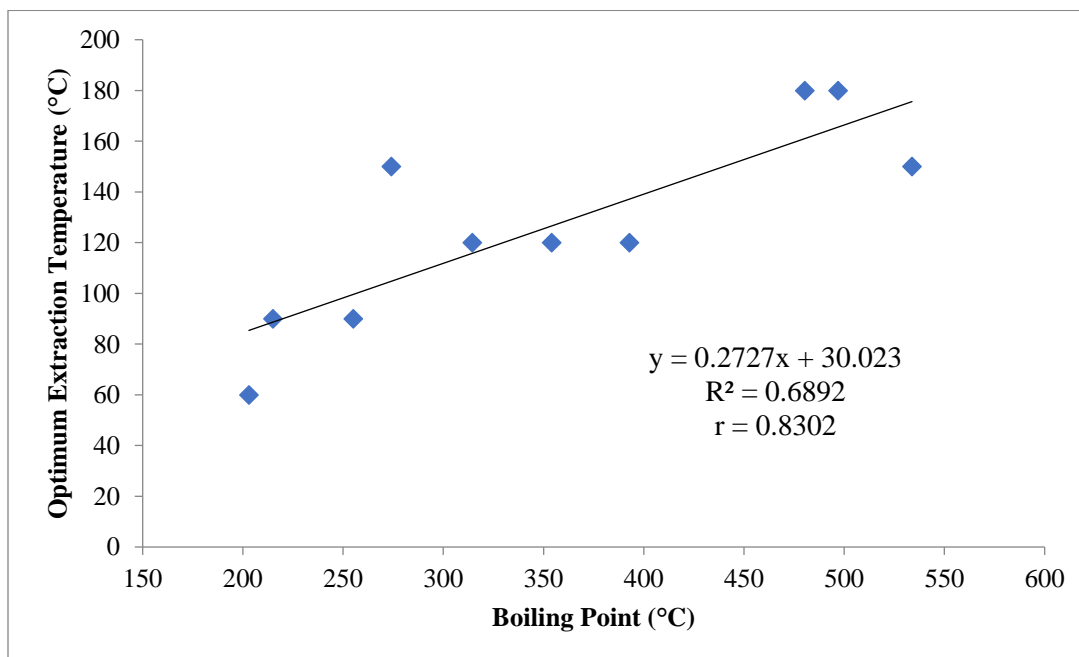


**Figure 33.** Graph of experimentally determined optimum extraction temperature vs known boiling point for underivatized drugs.



### Amphetamine

Amphetamine was detected in the underivatized form, with 60°C being the optimum extraction temperature. It produced a single chromatographic peak which could be identified with a NIST mass spectral library search. A single chromatographic peak which corresponded to the amphetamine TFA derivative was produced when amphetamine was derivatized with TFSA on-fiber. This peak was slightly overloaded, causing some mild fronting. The derivative was not found in the NIST mass spectral library, but was identified by its fragmentation pattern, the interpretation of which was discussed in chapter 1. See equations 1-5 in chapter 1 for the calculation of asymmetry factor, number of theoretical plates, sensitivity, and their respective percent improvements.

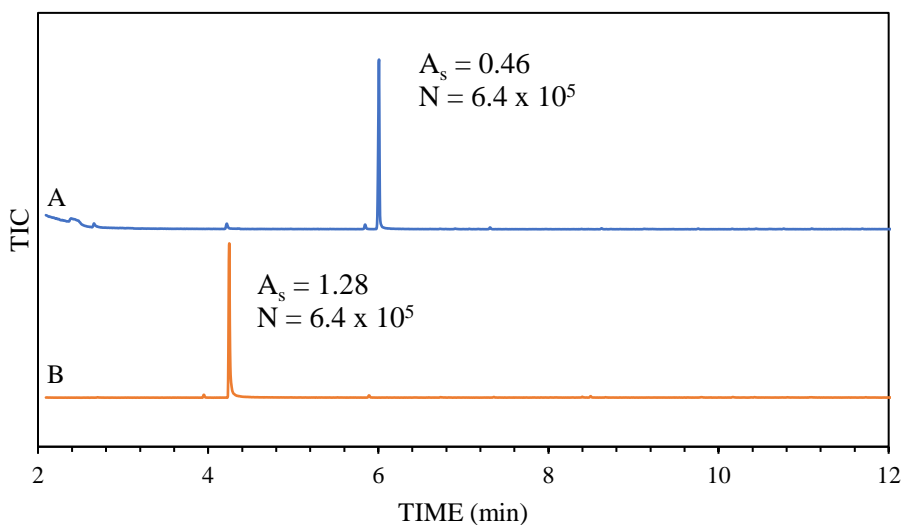


**Figure 34.** TIC of A: 24  $\mu$ g of amphetamine in 18  $\mu$ L of acetonitrile derivatized with TFSA, B: 24  $\mu$ g of amphetamine in 24  $\mu$ L of methanol.  $A_s$  = asymmetry factor,  $N$  = number of theoretical plates.

### Methamphetamine

Methamphetamine was detected in the underivatized form but exhibited exceedingly poor chromatographic behavior and many extraneous chromatographic peaks. It was identified by a NIST mass spectral library search. On-fiber derivatization with TFAA produced a single chromatographic peak which was identified with a NIST mass spectral library search as well.

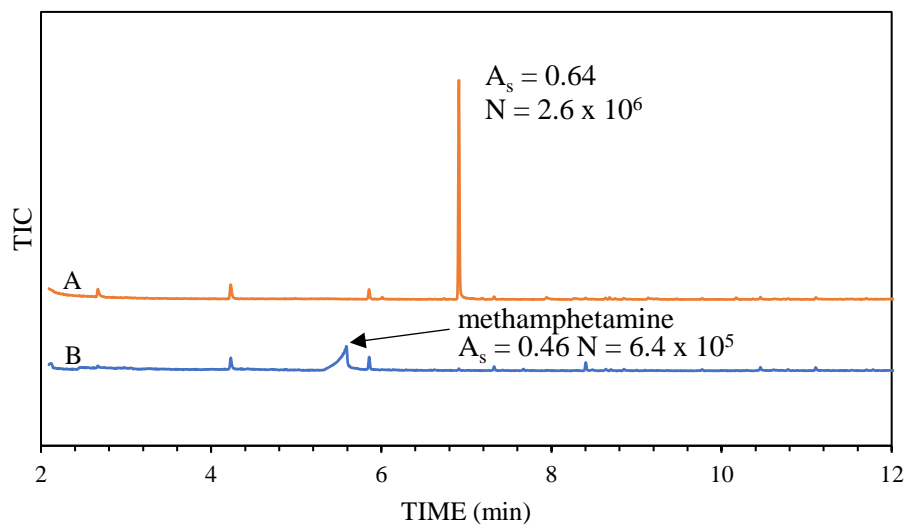


**Figure 35.** TIC of A: 24  $\mu\text{g}$  of methamphetamine in 18  $\mu\text{L}$  of acetonitrile derivatized with TFAA, B: 24  $\mu\text{g}$  of methamphetamine in 24  $\mu\text{L}$  of methanol.  $A_s$  = asymmetry factor,  $N$  = number of theoretical plates.

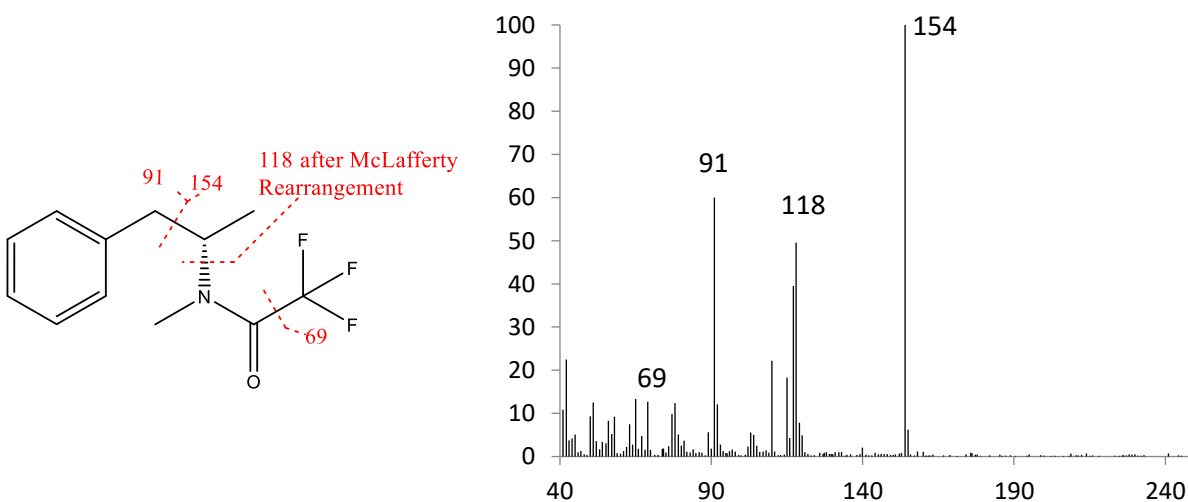


**Figure 36.** Structure and mass spectrum for methamphetamine TFA. MW = 245

*Ephedrine*

Ephedrine was detected in the underivatized form, with an optimum extraction temperature of 90°C. A single chromatographic peak was produced, aside from low-abundance background siloxanes, which was identified with a NIST mass spectral library search. However, derivatization on-fiber with TFAA was unsuccessful. Though the derivative was formed, the signal was much lower than that of the drug when underivatized and many siloxanes were present in the chromatogram at greater abundance than the derivative. The ephedrine TFA derivative was identified by liquid injection using traditional solution-phase derivatization in previous work in our laboratory<sup>1</sup>, as well as by others<sup>32-34</sup>. Furthermore, as will be discussed in chapter 3, successful identification of the ephedrine TFA derivative, with excellent signal, was achieved using solid ephedrine powder with a much greater sample mass (1 mg). It is possible that the problem stems from the fact that ephedrine is the most hydrophilic of the phenethylamines analyzed ( $\text{LogP}_{\text{o/w}} = 0.68$ ), but there are too many variables to know exactly why this is happening without further experimentation.

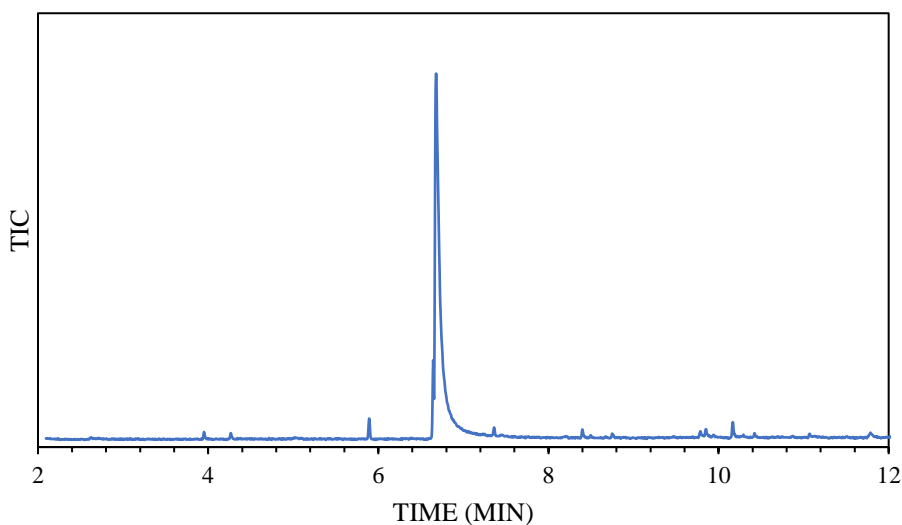


**Figure 37.** TIC for 24 µg of ephedrine in 24 µL of methanol.

*2C-I*

2C-I was detected in the underivatized form, with an optimum extraction temperature of 120°C. It produced a single chromatographic peak which could not be identified with a NIST mass spectral library search, but was identified by its fragmentation pattern, as has been previously reported<sup>16</sup>. A single chromatographic peak for 2C-I TFA was produced when 2C-I was derivatized with TFAA on-fiber. This derivative was not found in the NIST mass spectral library, but was identified by its fragmentation pattern, the interpretation of which was discussed in chapter 1.

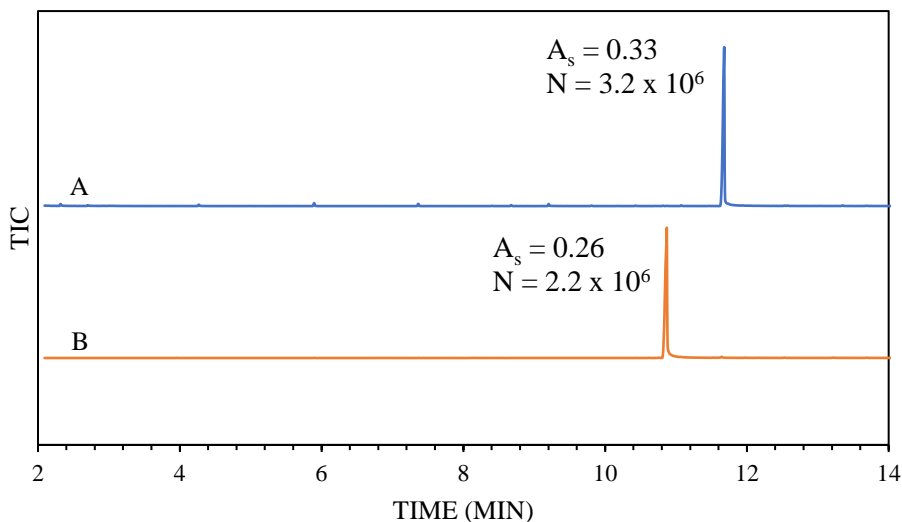


**Figure 38.** TIC of A: 24  $\mu\text{g}$  of 2C-I in 18  $\mu\text{L}$  of acetonitrile derivatized with TFAA, B: 24  $\mu\text{g}$  of 2C-I in 24  $\mu\text{L}$  of methanol.  $A_s$  = asymmetry factor,  $N$  = number of theoretical plates.

*25I-NBOMe*

This drug was detected without derivatization, with an optimum extraction temperature of 180°C. A single chromatographic peak was produced, which could not be found in the NIST mass spectral library, but which could be identified by its fragmentation pattern. Initial alpha cleavage at the nitrogen produced a fragment with  $m/z$  150. Another fragment with  $m/z$  150 could have

formed with the loss of iodine from the larger fragment after alpha cleavage. A further loss of  $\text{CNH}_3$  radical from this fragment yields an ion with  $m/z$  121, the base peak<sup>25</sup>

A single chromatographic peak for the 25I-NBOMe TFA derivative was produced by on-fiber derivatization with TFAA. The derivative was not found in the NIST mass spectral library but could be identified by its fragmentation pattern. The derivative had a molecular ion at  $m/z$  523. Alpha cleavage at the nitrogen resulted in a fragment with  $m/z$  277. The side chain fragment then cleaved at the nitrogen, resulting in a fragment which consisted of an aromatic ring with a methoxy and a methylene group,  $m/z$  121.

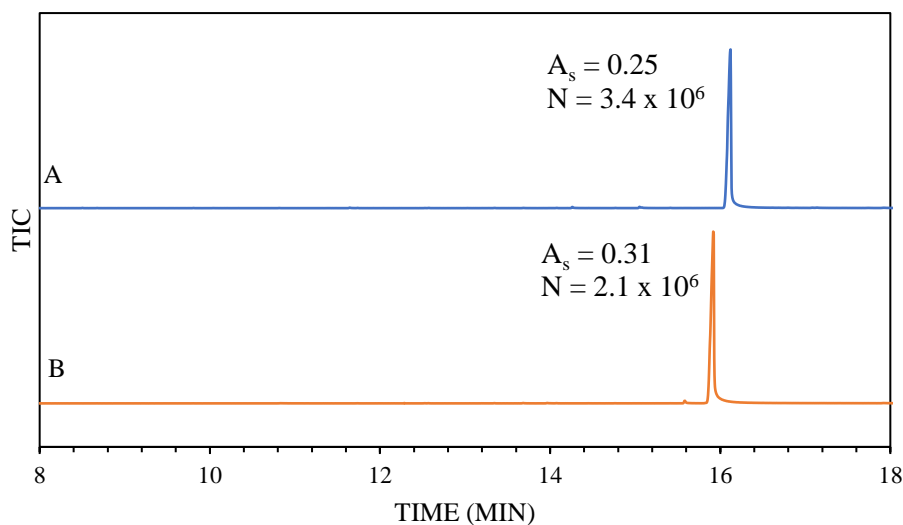


**Figure 39.** TIC of A: 24  $\mu\text{g}$  of 25I-NBOMe in 18  $\mu\text{L}$  of acetonitrile derivatized with TFAA, B: 24  $\mu\text{g}$  of 25I-NBOMe in 24  $\mu\text{L}$  of methanol.  $A_s$  = asymmetry factor,  $N$  = number of theoretical plates.

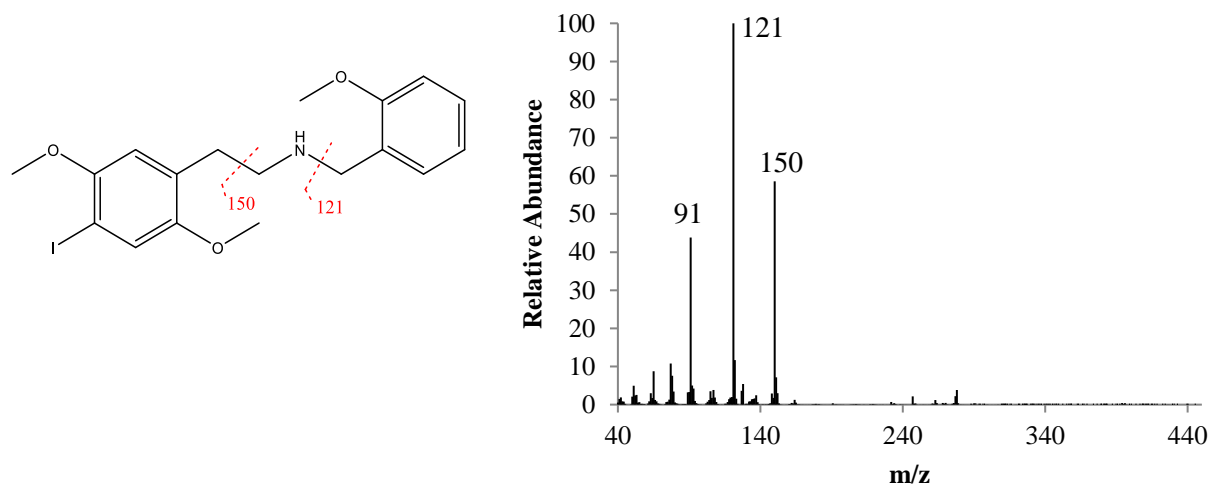


**Figure 40.** Fragmentation diagram and mass spectrum, underivatized 25I-NBOMe. MW = 427

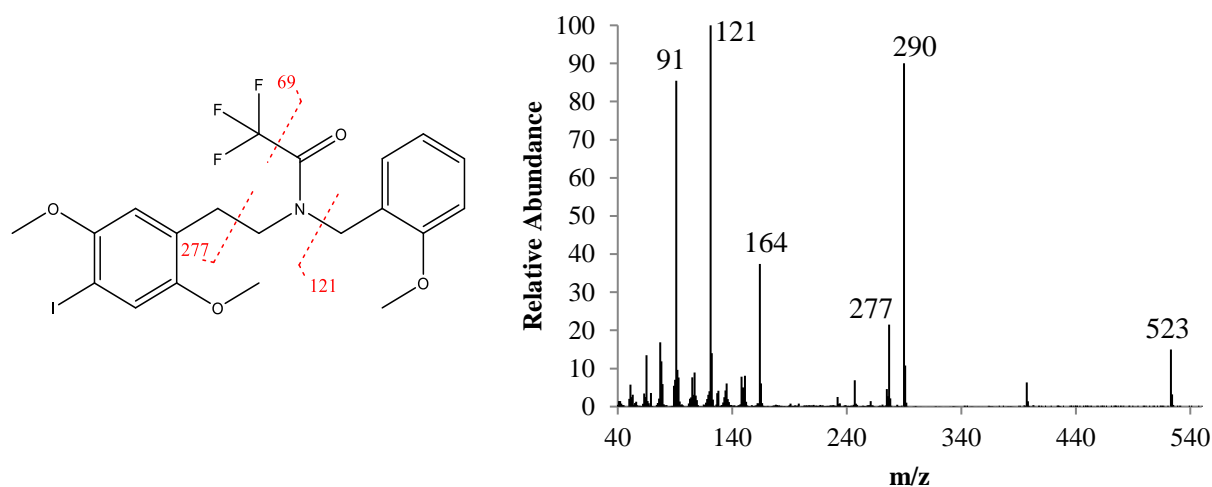


**Figure 41.** Fragmentation diagram and mass spectrum of 25I-NBOMe TFA. MW = 523

### 25I-NBOH

25I-NBOH was detected without derivatization at an extraction temperature of 180°C. The target compound was only present as a poorly shaped peak with low abundance. The chromatogram was dominated by the peak for 2C-I, which 25I-NBOH is known to convert to in the heated GC inlet. The detection of 25I-NBOH by GC-MS has not been reported. The mass spectrum was not present in the NIST library, but it could be identified by its fragmentation pattern.

Upon ionization, 25I-NBOH lost the two labile hydrogens from the amine and hydroxyl groups. Subsequent alpha cleavage on the side of the nitrogen closest to the iodine resulted in a fragment with  $m/z$  277 and another with  $m/z$  134.

The chromatographic peak for the 25I-NBOH derivative was not the only peak produced by on-fiber derivatization of 25I-NBOH with TFAA. A peak for 2C-I was present as well as several unidentified peaks, but 25I-NBOH TFA was the most prominent peak in the chromatogram. The derivative was not found in the NIST mass spectral library but could be identified by its fragmentation pattern. The derivative had a molecular ion of  $m/z$  509. The hydrogen of the hydroxyl group could be lost, which was necessary to produce the  $m/z$  107 peak. Alpha cleavage at the nitrogen produced a fragment with  $m/z$  277. McLafferty rearrangement with charge migration<sup>25</sup> resulted in the fragment with  $m/z$  290.

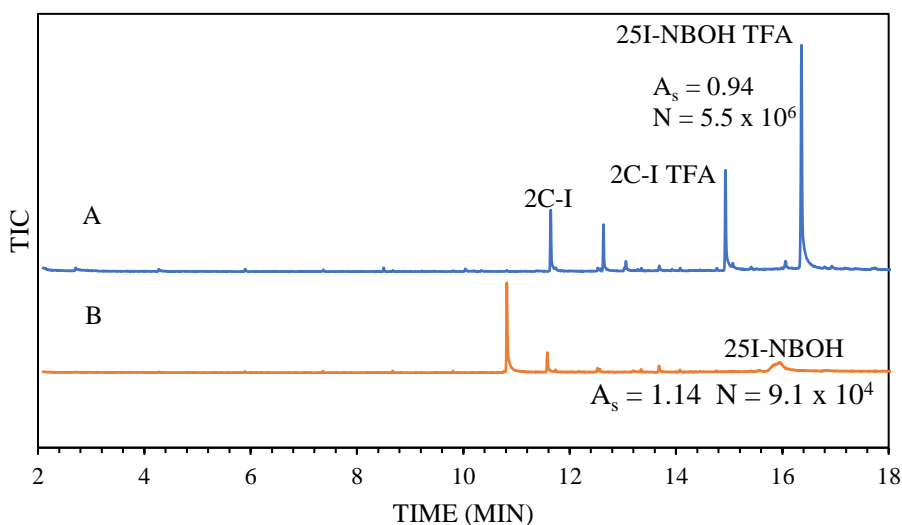


**Figure 42.** TIC of A: 24  $\mu\text{g}$  of 25I-NBOH in 18  $\mu\text{L}$  of acetonitrile derivatized with TFAA, B: 24  $\mu\text{g}$  of 25I-NBOH in 24  $\mu\text{L}$  of methanol.  $A_s$  = asymmetry factor,  $N$  = number of theoretical plates.

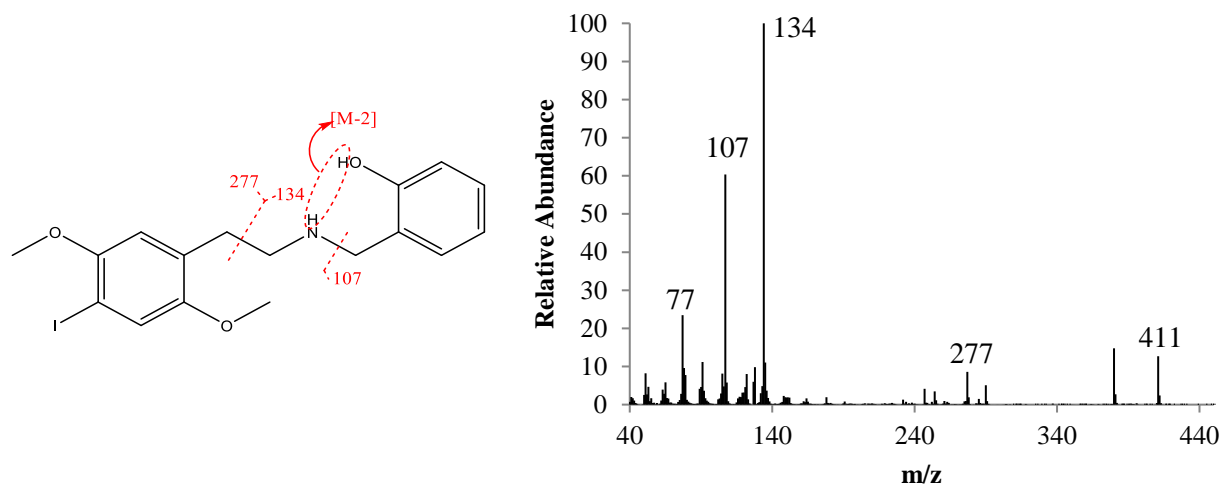


**Figure 43.** Fragmentation diagram and mass spectrum of underivatized 25I-NBOH. MW = 413

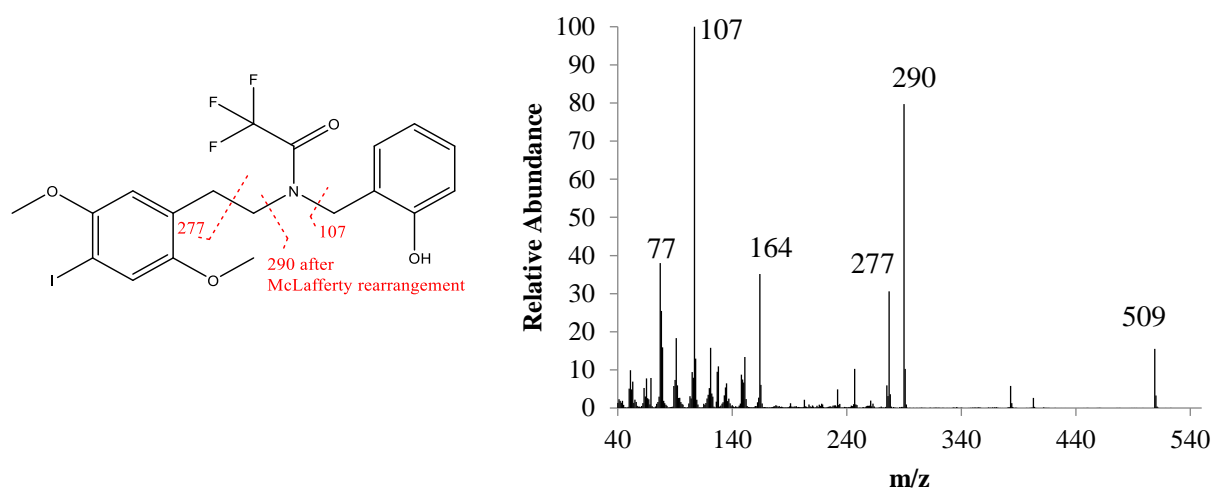


**Figure 44.** Fragmentation diagram and mass spectrum for 25I-NBOH TFA. MW = 509

### *Psilocin*

Psilocin was detected in the underivatized form, with 90°C being the optimum extraction temperature. It produced a single chromatographic peak which could be identified with a NIST mass spectral library search. However, derivatization with TFAA was unsuccessful. BSTFA + 1% TMCS derivatization was successful with psilocin, though incomplete. There remained a small chromatographic peak for underivatized psilocin, but the psilocin TMS peak dominated the



chromatogram. It is suspected that this derivatization could be brought to completion by exposing the fiber to the derivatization agent for a longer time or by increasing the extraction time. The mass spectrum for the derivative was not in the NIST library, but it was identified using its fragmentation pattern. The molecular ion is present at  $m/z$  276. Alpha cleavage at the nitrogen resulted in fragments at  $m/z$  218 and  $m/z$  58. The TMS group, which is present in all TMS derivatives, is the fragment at  $m/z$  73.

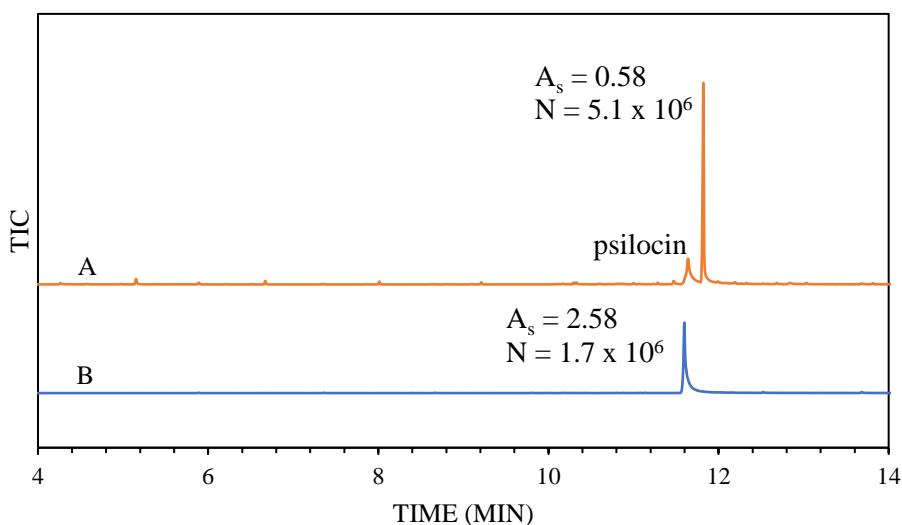


**Figure 45.** TIC of A: 24  $\mu\text{g}$  of psilocin in 18  $\mu\text{L}$  of acetonitrile derivatized with BSTFA + 1% TMCS, B: 24  $\mu\text{g}$  of psilocin in 24  $\mu\text{L}$  of methanol.  $A_s$  = asymmetry factor,  $N$  = number of theoretical plates.

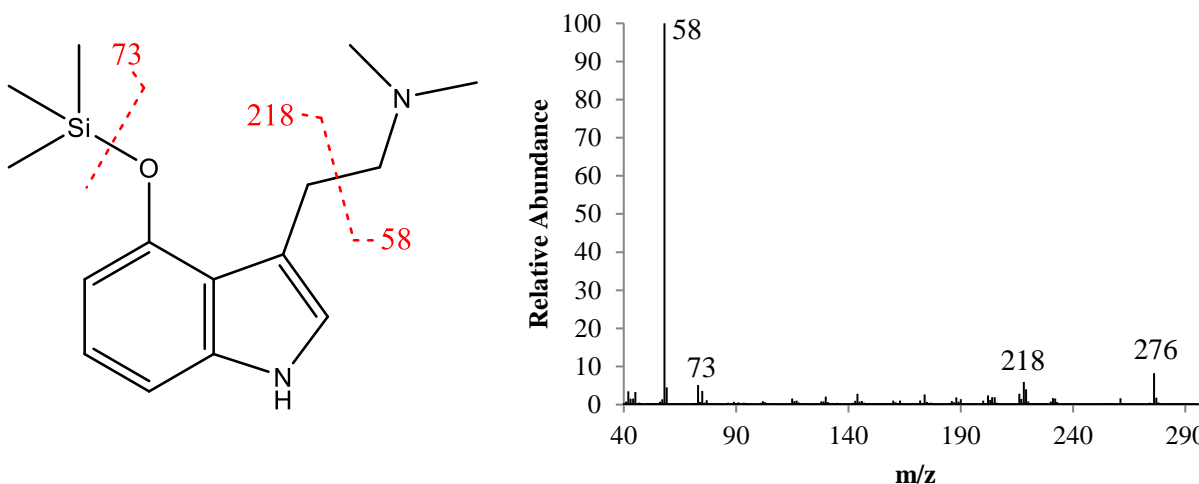


**Figure 46.** Fragmentation diagram and mass spectrum for psilocin TMS. MW = 276

### *Psilocybin*

Psilocybin was not detected by TV-SPME either with or without derivatization. No peaks were formed that could be identified as either psilocybin or one of its derivatives.

### *GHB*

Gamma-hydroxybutyric acid could not be detected without derivatization due to its low volatility and poor thermal stability. Derivatization with BSTFA + 1% TMCS resulted in a single peak for GHB di-TMS. Derivatization replaced both hydroxyl hydrogens with TMS groups. This derivative was identified by a NIST mass spectral library search. As is common with TMS derivatives, the molecular ion was not present. An  $[M-15]^+$  fragment, formed by the loss of a methyl from the TMS group, was present at  $m/z$  233 and can be used as an ion indicative of GHB di-TMS. Cleavage of the carbon chain formed an  $m/z$  117 fragment. The fragment  $m/z$  73, which corresponds to a single TMS group, is very common in TMS derivatives. Among derivatives with multiple TMS ether groups close together,  $m/z$  147 is also a very common fragment as it

corresponds to a TMS group bonded to an oxygen which is bonded to a dimethylsilyl group<sup>28</sup>. This forms the base peak in the mass spectrum of GHB di-TMS.

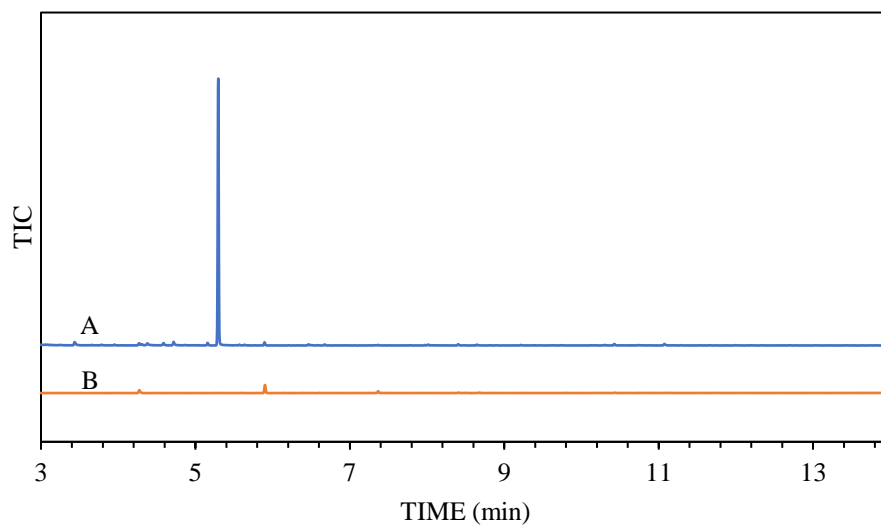


**Figure 47.** TIC of A: 14.4  $\mu\text{g}$  of GHB in 18  $\mu\text{L}$  of acetonitrile derivatized with BSTFA + 1% TMCS, B: 14.4  $\mu\text{g}$  of GHB in 24  $\mu\text{L}$  of methanol.

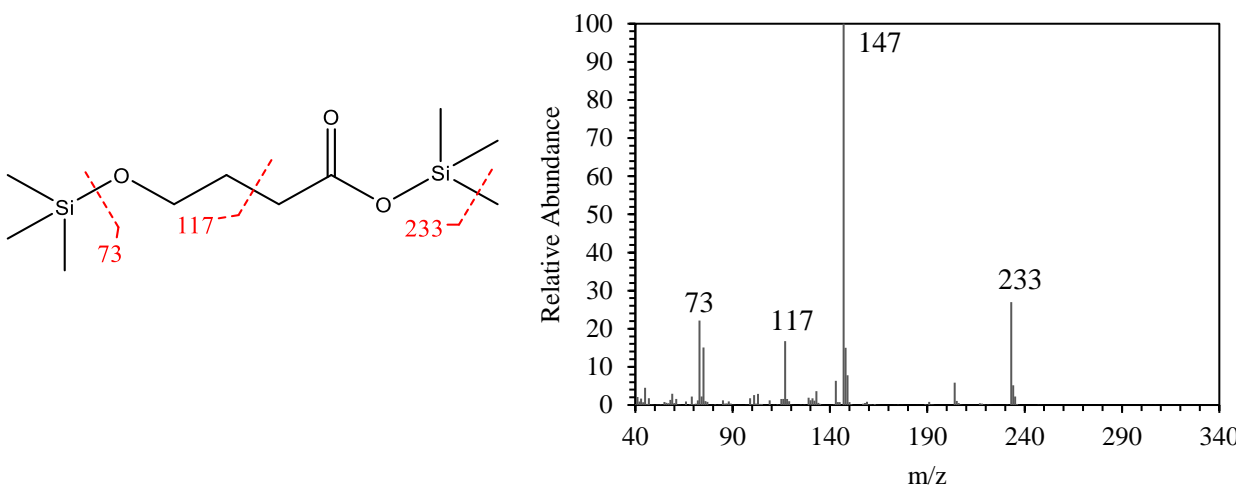


**Figure 48.** Structure and mass spectrum of GHB di-TMS. MW = 248

### *Gabapentin*

In the liquid injection method, underivatized gabapentin produced a single chromatographic peak with a mass spectrum that was identified with a NIST mass spectral library

search. The same was true of underivatized gabapentin using the TV-SPME method with an extraction temperature of 120°C. The peak exhibits fronting, which indicates that the column was overloaded with sample. The Langmuir adsorption model treats the stationary phase as a single solid layer with a finite number of active sites. When a sample introduction overloads the column and all of the sites at the head of the column are filled with analyte molecules, the remaining analyte molecules must remain completely in the mobile phase until they move farther down the column where active sites are available. This decreases the retention time for that portion of the analyte molecules, resulting in peak fronting. If a smaller amount of sample was introduced or if a larger split ratio was employed, the peak should become more symmetric. The fragmentation of gabapentin and the interpretation of its mass spectrum was discussed in chapter 1. On-fiber derivatization was unsuccessful for gabapentin with both BSTFA + 1% TMCS and DMF-DMA. No chromatographic peak for the TMS derivative was formed, and while the DMAM derivative was formed, the derivatization was incomplete.

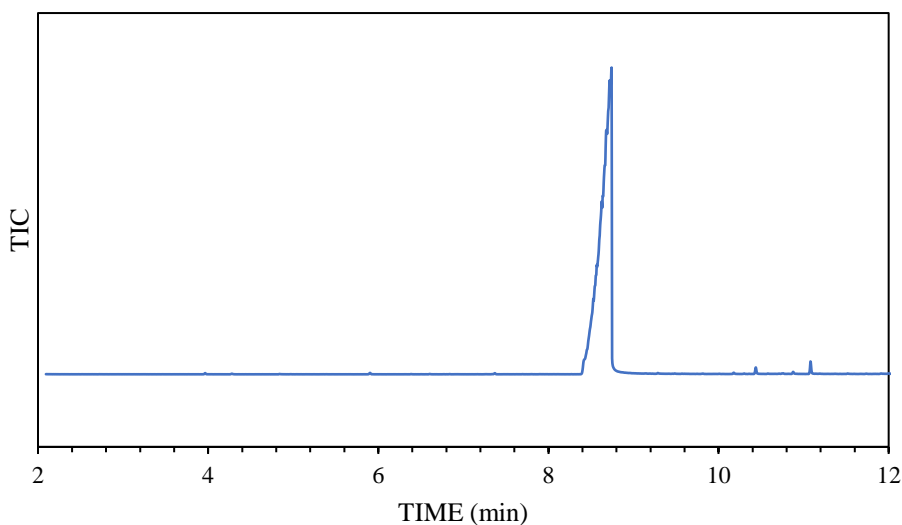


**Figure 49.** TIC of 14.4 µg of gabapentin in 24 µL of methanol.

### *Lorazepam*

Underivatized lorazepam produced a single chromatographic peak in TV-SPME, as it did in liquid injection, that was identified with a NIST mass spectral library search. The optimum extraction temperature was 150°C. The fragmentation of lorazepam and the interpretation of its mass spectrum was discussed in chapter 1. On-fiber derivatization was unsuccessful for gabapentin with both BSTFA + 1% TMCS and DMF-DMA. No chromatographic peaks were formed for either lorazepam derivative.

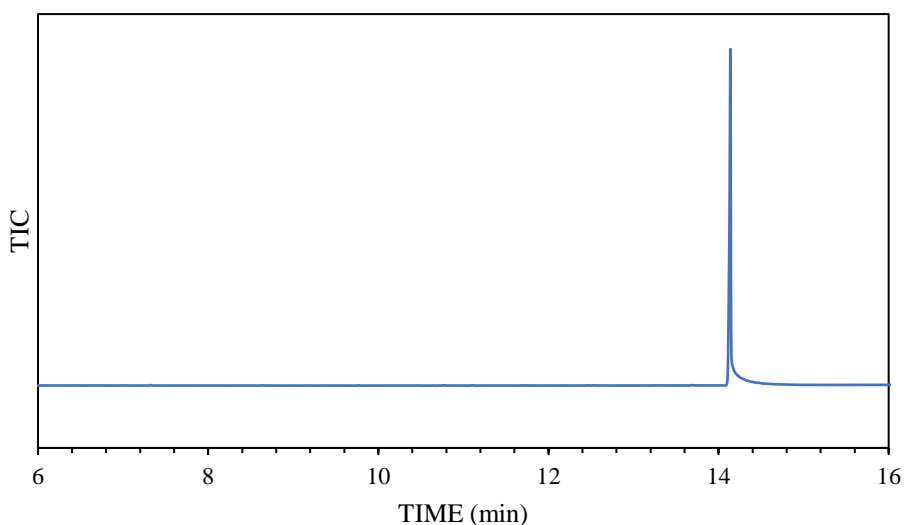


**Figure 50.** TIC of 24  $\mu\text{g}$  of lorazepam in 24  $\mu\text{L}$  of methanol.

### *Vigabatrin*

Only the dehydration product of vigabatrin was detected by TV-SPME without derivatization. No derivatives were detected with BSTFA + 1% TMCS or DMF-DMA.

### *Pregabalin*

Pregabalin was detected in the underivatized form by TV-SPME. Pregabalin was not successfully derivatized with BSTFA + 1% TMCS or DMF-DMA on-fiber.

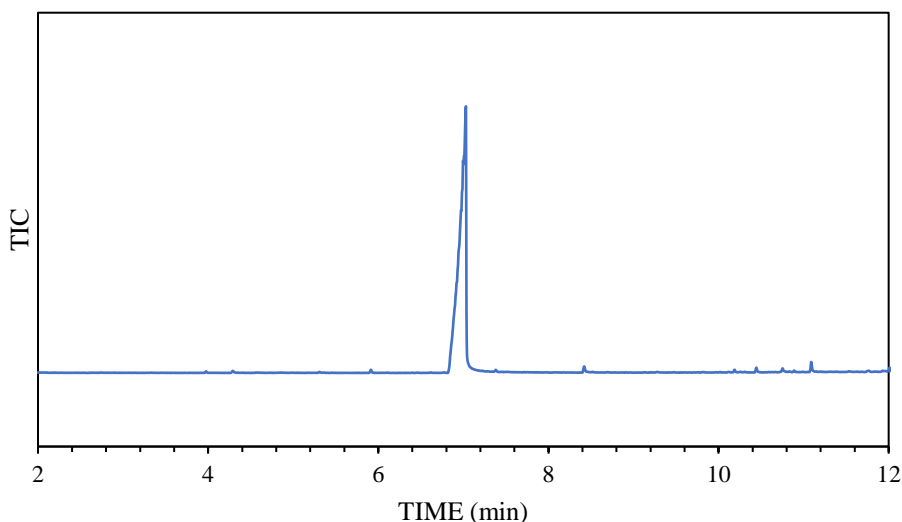


**Figure 51.** TIC of 24 µg of pregabalin in 24 µL of methanol.

### *Clorazepate*

Clorazepate was not detected by TV-SPME in either the underivatized or derivatized forms, with BSTFA + 1% TMCS or DMF-DMA.

As shown in tables 6-8, derivatization generally improved chromatographic performance. For example, though the peak symmetry for amphetamine worsened by 129% due to column overloading with TFAA derivatization, separation efficiency increased by 156% and sensitivity increased by 1%. The peak symmetry for methamphetamine improved by 10% with TFAA derivatization while separation efficiency increased by 5,552% and sensitivity increased by 16%. The peak symmetry for 2C-I improved by 9% with TFAA derivatization separation efficiency increased by 45% and sensitivity decreased by 3%. The peak symmetry for 25I-NBOMe worsened

by 9% with TFAA derivatization while separation efficiency increased by 62% and sensitivity increased by 36%. The peak symmetry for 25I-NBOH improved by 57% with TFAA derivatization while separation efficiency increased by 5,944% and sensitivity increased by 16%. The peak symmetry for psilocin improved by 73% with BSTFA + 1% TMCS derivatization while separation efficiency increased by 200% and sensitivity increased by 31%.

**Table 6.** Comparing asymmetry factors for underivatized drugs and their derivatives

Drug	Underivatized	Derivatized
Amphetamine	1.28	0.46
Methamphetamine	0.60	0.64
2C-I	0.26	0.33
25I-NBOMe	0.31	0.25
25I-NBOH	1.14	0.94
Psilocin	2.58	0.58

**Table 7.** Comparing separation efficiency (number of theoretical plates) for underivatized drugs and their derivatives

Drug	Underivatized (/10 <sup>6</sup> )	Derivatized (/10 <sup>6</sup> )
Amphetamine	0.25	0.64
Methamphetamine	0.046	2.6
2C-I	2.2	3.2
25I-NBOMe	2.1	3.4
25I-NBOH	0.091	5.5
Psilocin	1.7	5.1

**Table 8.** Comparing sensitivity (peak area) for underivatized drugs and their derivative

Drug	Underivatized (/10 <sup>7</sup> )	Derivatized (/10 <sup>7</sup> )
Amphetamine	7.7	7.8
Methamphetamine	2.5	2.9
2C-I	65	63
25I-NBOMe	110	150
25I-NBOH	1.4	16
Psilocin	16	21

## Conclusion

TV-SPME proved to be an effective technique for analyzing controlled substances both with and without on-fiber derivatization. Amphetamine, 2C-I, 25I-NBOMe, psilocin, gabapentin, lorazepam, and pregabalin were all identified by TV-SPME without derivatization.

methamphetamine and 25I-NBOH were also identified without derivatization, but chromatographic performance was unsatisfactory. To our knowledge, this is the first report of identification of 25I-NBOH by GC-MS.

Derivatization with TFAA was chosen for the amine and hydroxylamine drugs. TFAA derivatization was effective for amphetamine, methamphetamine, 2C-I, and 25I-NBOMe, and successful but incomplete for 25I-NBOH. On-fiber derivatization with TFAA proved ineffective for psilocin and psilocybin, producing no derivatives for either.

Derivatization with BSTFA + 1% TMCS was chosen for the zwitterionic drugs as well as GHB, psilocin, and psilocybin. DMF-DMA derivatization was attempted for the zwitterionic drugs. On-fiber derivatization was unsuccessful for all the zwitterionic drugs chosen, with either BSTFA + 1% TMCS or DMF-DMA. On-fiber derivatization of gabapentin with DMF-DMA was incomplete, with most of the drug remaining in the underivatized state. The other zwitterions produced no derivative with either derivatization agent.

Psilocybin produced no derivative using on-fiber derivatization with BSTFA + 1% TMCS. On-fiber derivatization of psilocin produced a psilocin-TMS derivative which dominated the chromatogram despite a small chromatographic peak for underivatized psilocin still present. GHB proved an excellent candidate for on-fiber derivatization with BSTFA + 1% TMCS. As expected, GHB could not be detected by GC-MS in the underivatized form. On-fiber derivatization, however, produced a single chromatographic peak for GHB di-TMS with strong signal.



**Table 9.** Summary of results for liquid injection and TV-SPME methods. + indicates the formation of a single chromatographic peak which could be unambiguously identified. 0 indicates that multiple peaks formed, and – indicates that no peak formed.

<b>Drug</b>	<b>Liquid Injection</b>	<b>TV-SPME</b>
Amphetamine	+	+
Amphetamine + TFAA	+	+
Methamphetamine	+	+
Methamphetamine + TFAA	+	+
Ephedrine	+	+
Ephedrine + TFAA	+	0
2C-I	+	+
2C-I + TFAA	+	+
25I-NBOMe	+	+
25I-NBOMe + TFAA	+	+
25I-NBOH	-	0
25I-NBOH + TFAA	-	0
Psilocin	+	+
Psilocin + BSTFA + 1% TMCS	+	+
Psilocybin	+	-
Psilocybin + BSTFA + 1% TMCS	-	-
GHB	-	-
GHB + BSTFA + 1% TMCS	+	+
Gabapentin	+	+
Gabapentin + BSTFA + 1% TMCS	-	-
Gabapentin + DMF-DMA	+	0
Lorazepam	+	+
Lorazepam + BSTFA + 1% TMCS	+	-
Lorazepam + DMF-DMA	-	-
Vigabatrin	-	-
Vigabatrin + BSTFA + 1% TMCS	+	-
Vigabatrin + DMF-DMA	+	-
Pregabalin	-	+
Pregabalin + BSTFA + 1% TMCS	0	-
Pregabalin + DMF-DMA	0	-
Clorazepate	-	-
Clorazepate + BSTFA + 1% TMCS	+	-
Clorazepate + DMF-DMA	-	-

While not ideal for all analytes, TV-SPME with on-fiber derivatization could be a powerful technique for amine and hydroxylamine controlled substances as well as GHB. The technique could increase analyst efficiency by reducing sample preparation time for these types of analytes. The method is particularly well-suited to the analysis of GHB since the drug cannot be analyzed by GC-MS in its native state. The technique has been tested on “realistic” seized drug samples, including GHB samples, the results of which are presented in chapter 3. The potential exists to remove sample preparation entirely by analyzing drugs of abuse in their native state (e.g. white powder) using on-fiber derivatization. This possibility is explored in chapter 4.

## CHAPTER 3. REALISTIC SAMPLES AND SOLID DRUG DERIVATIZATION

### Introduction

As discussed in Chapter 2, on-fiber derivatization has proven effective for many drugs as standards in aprotic solvents. Suspected controlled substances submitted to a laboratory, however, are often impure. The ability of the on-fiber derivatization method to handle realistic samples needed to be tested. To that end, four different kinds of realistic samples were designed – “street meth”, GHB-spiked beverages, hallucinogenic mushrooms, and solid drug powders.

The first realistic sample - referred to as “street meth” and containing methamphetamine, ephedrine, and caffeine - was meant to simulate an impure methamphetamine sample manufactured in a clandestine laboratory and adulterated. In a methamphetamine seizure, identification of cutting agents, precursors, and synthetic pathways employed can be of investigative and potentially legislative interest. There are two prominent synthetic pathways that use ephedrine or pseudoephedrine as a precursor. The Emde method, which is a two-step reduction of ephedrine to methamphetamine via chloroephedrine (figure 52), is very common in Asia<sup>35-37</sup>. Direct reduction of ephedrine or pseudoephedrine to methamphetamine via the Nagai (“red P”) method using hydriodic acid and red phosphorus (figure 53)<sup>36-38</sup> or via the “Nazi/Birch” method using lithium metal and ammonia (figure 54)<sup>39</sup> is much more common in the United States. Impurities in the final product, including unreacted starting materials, intermediates, and byproducts or the ratios of these impurities have been used to determine the synthetic route utilized in the manufacture of methamphetamine samples<sup>36-37, 40</sup>.

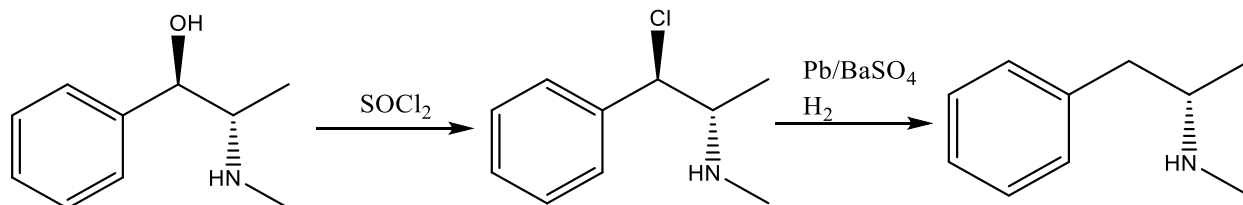


**Figure 52.** The synthetic pathway from ephedrine to methamphetamine via the Emde method<sup>35</sup>.

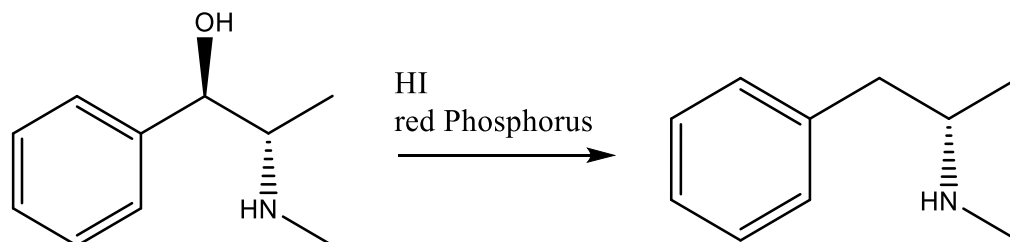


**Figure 53.** The synthetic pathway from ephedrine to methamphetamine via the Nagai method<sup>38</sup>.

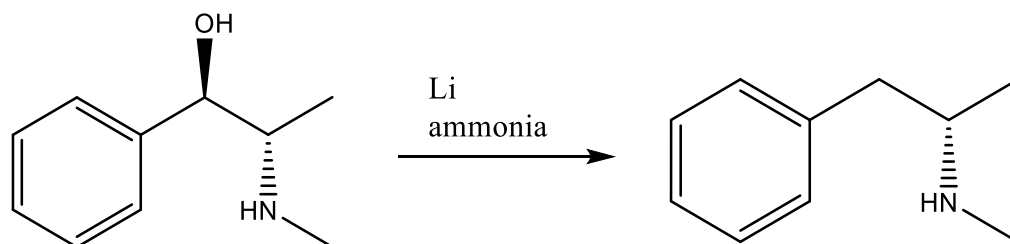


**Figure 54.** The synthetic pathway from ephedrine to methamphetamine via the "Nazi/Birch" method<sup>39</sup>.

The second type of realistic sample was beverages spiked with gamma-hydroxybutyric acid (GHB). GHB is used in drug-facilitated sexual assaults (DFSA) because it incapacitates victims, induces memory loss, and does not persist in the human body<sup>41</sup>. The drug can be surreptitiously administered to a victim's drink, in which case a forensic scientist may receive a beverage suspected of containing GHB. This drug is impossible to analyze "as is" by GC-MS due to its acidity ( $\text{pK}_a$  4.7), high polarity, low volatility, and high solubility in aqueous solution. GHB and gamma-butyrolactone (GBL) interconvert in aqueous solutions<sup>42-43</sup>. Additionally, GHB can be converted to GBL in the high heat of the GC inlet, further complicating its analysis<sup>28</sup>.

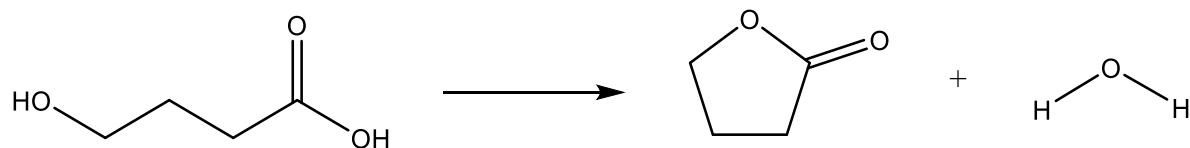


**Figure 55.** The conversion of GHB to GBL via dehydration ( $\Delta H_o = 4.5 \pm 0.2$  kJ/mol)<sup>44</sup>.

Though the most common instrumental techniques for detecting GHB are GC-MS<sup>28, 45-51</sup> and liquid chromatography-mass spectrometry<sup>52</sup>, GHB has also been identified using Raman spectroscopy<sup>53-54</sup>, infrared spectroscopy<sup>55</sup>, and nuclear magnetic resonance spectroscopy<sup>56-57</sup>. All routine GC-MS methods and many LC-MS methods for identifying GHB require derivatization following an involved extraction procedure. This makes beverages spiked with GHB ideal as realistic samples with which to test the on-fiber derivatization method.

Hallucinogenic mushrooms were the third type of realistic sample chosen. Mushrooms of the genus *Psilocybe* have been used as parts of religious rituals and ceremonies for centuries, but Wasson was the first to publish on their hallucinogenic effects in 1957<sup>58</sup>. In 1958, Hoffman et al. identified and extracted the two main psychotropic alkaloids, psilocybin and psilocin<sup>59</sup>. Both compounds are now schedule I controlled substances in the United States. In some jurisdictions the two are treated the same under the law while in others there is a distinction, in which case an analyst must have a method that can distinguish between the two alkaloids. This can prove difficult as psilocybin readily dephosphorylates to psilocin in the heated inlet of a gas chromatograph. Derivatization in the solution phase with BSTFA + 1% TMCS is routinely employed to prevent this dephosphorylation but has so far proven unsuccessful for on-fiber derivatization, as discussed in chapter 2. Even so, on-fiber derivatization with BSTFA + 1% TMCS was tested on hallucinogenic mushroom samples donated by the Indiana State Police. The dried mushrooms were analyzed without any extraction procedures.

The final type of realistic sample tested was solid drug powders. As discussed in Chapter 2, on-fiber derivatization performed in aprotic solvents has proven effective in decreasing sample preparation time for problematic drugs of abuse. We also explored the possibility of analyzing solid powders directly with on-fiber derivatization, which would eliminate the use of any solvent. To test this possibility, one drug from each class explored in this thesis was analyzed as a powder. Methamphetamine was chosen to represent secondary amines, 2C-I was chosen to represent primary amines, gabapentin was selected to represent zwitterions, GHB was selected to represent hydroxycarboxylic acids, and ephedrine was selected to represent hydroxy phenylethylamines.

## **Experimental**

### *Materials*

Methamphetamine HCl, ephedrine HCl, and dimethyl formamide dimethyl acetal (DMF-DMA) were purchased from Sigma-Aldrich (St. Louis, Missouri). 4-iodo-2,5-dimethoxy- $\beta$ -phenethylamine (2C-I) hydrochloride, gamma-hydroxybutyric acid (GHB), and gabapentin were purchased from Cayman Chemical (Ann Arbor, Michigan). HPLC grade methanol, Optima acetonitrile, trifluoroacetic anhydride (TFAA), and N,O-bis(trimethylsilyl)trifluoroacetamide with 1% trimethylchlorosilane (BSTFA + 1% TMCS) were purchased from Thermo Fisher Scientific (Waltham, Massachusetts). Polydimethyl siloxane solid phase microextraction fibers, 100  $\mu$ m film thickness, were purchased from Supelco (Bellefonte, Pennsylvania). Coke<sup>®</sup> and rum were purchased from a local supermarket.

### *Simulated “Street Meth”*

To create a simulated “street meth” sample, 11 mg of methamphetamine, 2 mg of ephedrine, and 28 mg of caffeine were mixed together. This mixture was dissolved in 28 mL of methanol to create a solution with the following concentrations for each drug: 0.39 mg/mL methamphetamine, 0.07 mg/mL ephedrine, and 1.0 mg/mL caffeine. An aliquot of 240  $\mu$ L of this solution was placed into a 20-mL headspace vial. The methanol was evaporated to dryness and reconstituted in 18  $\mu$ L of acetonitrile for analysis. On-fiber derivatization was accomplished by exposing the SPME fiber to the headspace of a vial containing TFAA for five minutes before moving it to the sample, which was vaporized by heating at 90°C. After an extraction time of 10 minutes, the fiber was moved to the inlet of the GC for desorption at 250°C.

### *GHB-Spiked Beverages*

According to the United States Drug Enforcement Agency, the average dose of GHB is between 1 and 5 grams<sup>41</sup>. The drug users’ forum Erowid lists the range for a “strong dose” of GHB as 2-4 g<sup>60</sup>. A typical mixed drink is 7 fluid ounces or 207 mL. Therefore, if the smallest “strong dose” of GHB, 2 mg, were dissolved in a typical mixed drink with a volume of 207 mL, the resulting solution would have a GHB concentration of 9.7 mg/mL. Erring on the conservative side, spiked beverage samples were created by adding 250  $\mu$ L of beverage to 2 mg of solid GHB and allowing to dissolve, creating an 8 mg/mL solution. 2.5  $\mu$ L of the resulting solution was then added to a 20 mL headspace vial for analysis. Due to its success derivatizing GHB in solutions of acetonitrile and dichloromethane, as seen in chapter 2, BSTFA + 1% TMCS was chosen for use in beverage samples as well. Because BSTFA reacts with water, it was necessary to saturate the fiber with the derivatization agent so that it could react with the water and leave enough BSTFA free to

react with the GHB. This was accomplished by increasing the time that the fiber spent in the headspace of the derivatization vial. Times of 10, 20, 30, 40, 50, and 60 were tested. After the fiber was saturated with derivatization agent, it was moved to the sample vial, where the sample was vaporized by heating to 60°C. After an extraction time of 10 minutes, the fiber was moved to the inlet of the GC for desorption at 250°C.

#### *Hallucinogenic Mushrooms*

A few dried stems and a dried cap from the mushrooms were placed in a 20-mL headspace vial for analysis. A fresh vial of BSTFA + 1% TMCS was prepared by placing several drops of the derivatization agent in the bottom of a 20-mL headspace vial. For analysis, a PDMS SPME fiber was exposed to the headspace of the derivatization vial for 50 minutes then moved to the headspace of the sample vial, which was heated at 120°C. After 10 minutes extraction time, the fiber was moved to the inlet of the GC, heated at 250°C, for desorption.

#### *Solid Drug Samples*

One milligram of powder was placed in a 20-mL headspace vial for analysis. A fresh vial of derivatization agent was prepared daily by placing several drops of derivatization agent in the bottom of a 20-mL headspace vial. For analysis, a PDMS SPME fiber was exposed to the headspace of the derivatization vial for 5 minutes, then moved to the headspace of the sample vial, which was heated at 60°C for GHB, 90°C for methamphetamine and ephedrine, or 120°C for 2C-I and gabapentin. After 10 minutes extraction time, the fiber was moved to the inlet of the GC, heated at 250°C, for desorption.



### *GC-MS Parameters*

An Agilent 6890N GC coupled to an Agilent 5975 inert Mass Selective Detector with an attached Gerstel PAL RTC MultiPurpose Sampler (MPS) was used for all experiments. The GC column was an Agilent Technologies DB-5MS column with a length of 30 m, a 0.250 mm inner diameter, and a 0.25  $\mu\text{m}$  film thickness. Straight inlet liners of 1.2 mm inner diameter from SGE Analytical Science were used.

The inlet temperature was set to 250°C and operated in split mode with a 15:1 split ratio. The initial oven temperature of 60°C was held for one minute, then the temperature was ramped at 15°C/min to 280°C where it was held for three minutes. A constant flow of 2.5 mL/min of hydrogen was maintained. The source was kept at 230°C and the quadrupoles were kept at 150°C. A scan range of  $m/z$  40-  $m/z$  550 was used, with a solvent delay of 2 minutes.

## **Results**

### *Simulated "Street Meth"*

Using the method parameters outlined in chapter 2, the concentration of ephedrine in the sample was too low. The sample volume was therefore increased from 24  $\mu\text{L}$  to 240  $\mu\text{L}$  of the methanol solution. With this larger sample size, the ephedrine derivative, the methamphetamine derivative, and caffeine were all detected. However, the signal for the ephedrine derivative was weaker than that of two unidentified peaks in the chromatogram. Though this is not ideal, the ephedrine was detected, so investigative leads about the precursor and synthetic pathway could still be obtained.

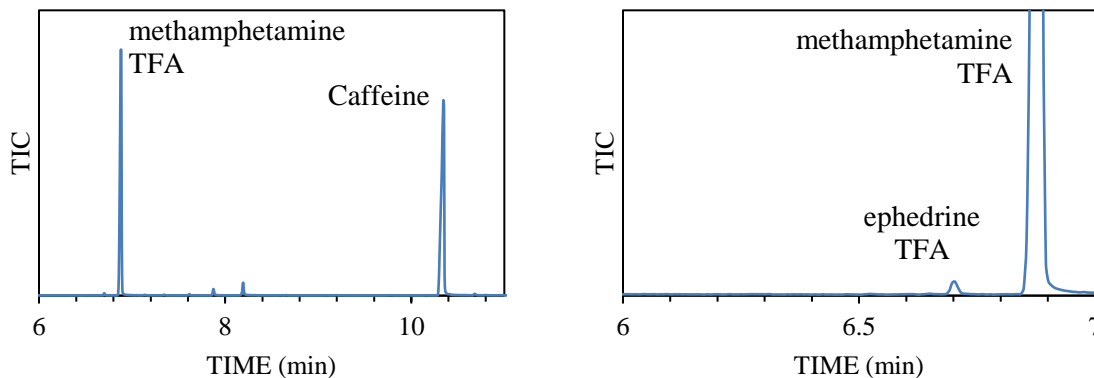


**Figure 56.** “street meth” chromatogram showing the methamphetamine derivative and caffeine (left) and zoomed in to show the ephedrine derivative (right).

#### *GHB-Spiked Beverages*

The time that the SPME fiber was exposed to the headspace of the BSTFA vial was tested from 10 minutes to 60 minutes to determine the shortest time necessary to saturate the fiber enough to produce a clear chromatographic peak for the derivative. The sample for the tests was 2.5  $\mu\text{L}$  of water spiked with GHB. Though the highest signal was obtained for 60 minutes, it was determined that 50 minutes was adequate time to produce a clear peak. It would be ideal to achieve this increased signal while simultaneously decreasing analysis time by dosing the fiber with derivatization agent more quickly. Possible solutions to achieve this will be discussed in chapter 4.

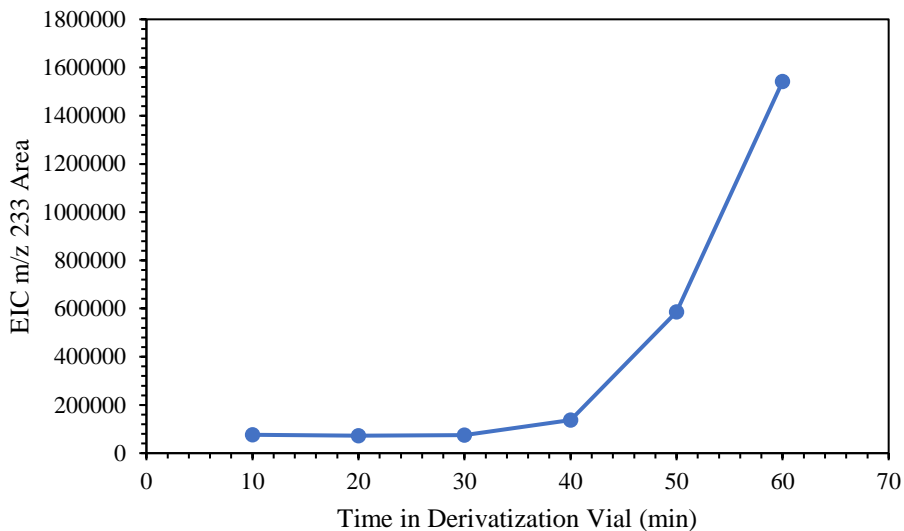


**Figure 57.** Plot of the GHB signal (measured by the area under the curve for EIC m/z 233) vs the time spent by the SPME fiber in headspace of the derivatization vial.

Once the fiber saturation time was determined, the method was used to analyze 3 different beverages spiked with GHB: Coke<sup>®</sup>, rum, and a rum & Coke<sup>®</sup> mixed drink. Each beverage sample was first analyzed without derivatization to illustrate that the GHB could not be detected this way, then with on-fiber derivatization using BSTFA + 1% TMCS to assess the utility of the method. Blank samples of the beverage that had not been spiked with GHB were also tested, both with and without derivatization, to ensure that GHB was not detected from the beverages themselves. GHB was not detected in unspiked beverages, nor in spiked beverages without derivatization. GHB was clearly identified in all three spiked beverages using on-fiber derivatization.

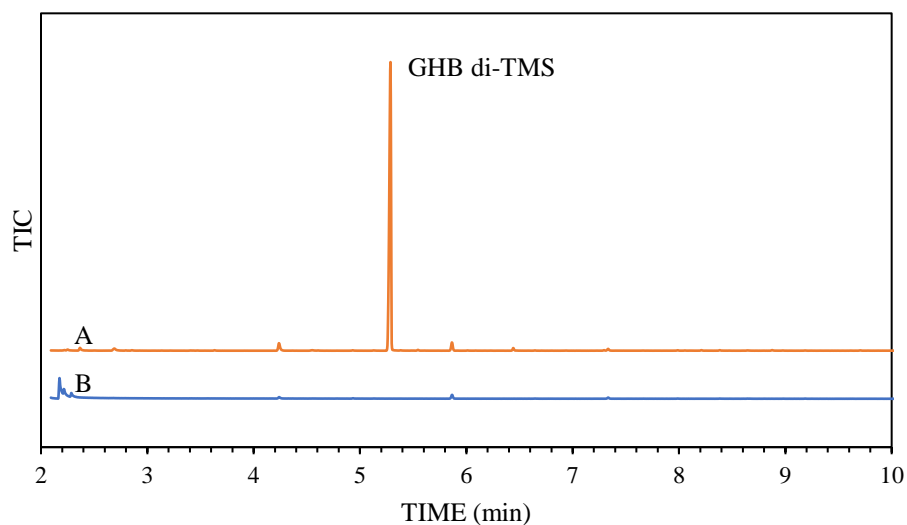


**Figure 58.** Stacked chromatograms for Coke® spiked with 8 mg/mL GHB, analyzed without derivatization (B) and with on-fiber derivatization using BSTFA + 1% TMCS (A)

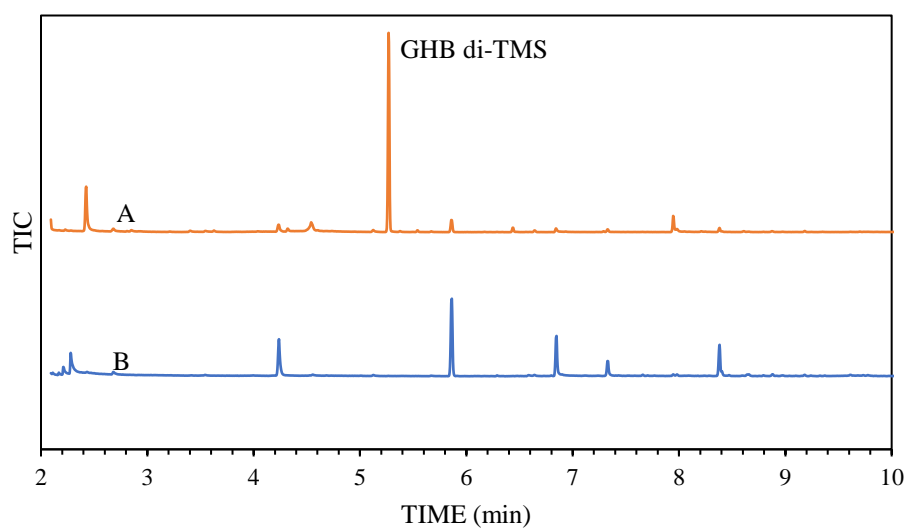


**Figure 59.** Stacked chromatograms for rum spiked with 0.8 mg/mL GHB, analyzed without derivatization (B) and with on-fiber derivatization using BSTFA + 1% TMCS (A)

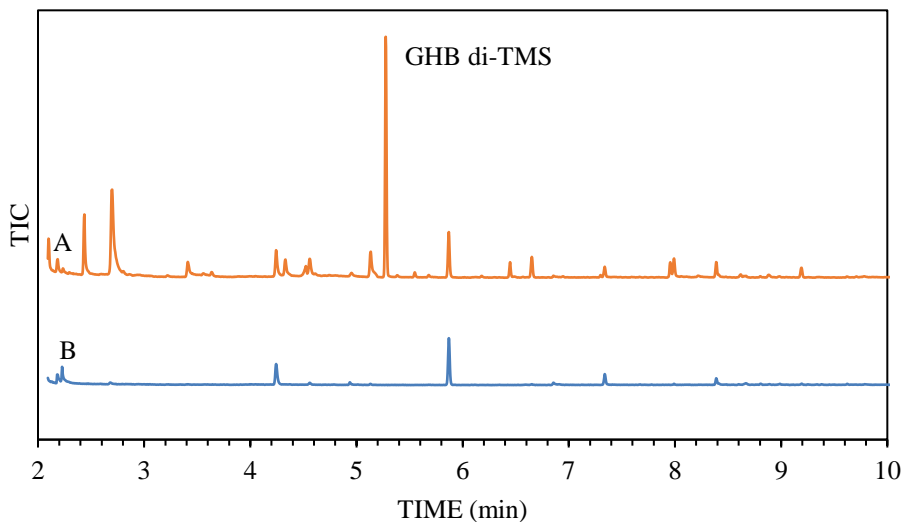


**Figure 60.** Stacked chromatograms for rum spiked with 8 mg/mL GHB, analyzed without derivatization (B) and with on-fiber derivatization using BSTFA + 1% TMCS (A)

### *Hallucinogenic Mushrooms*

The dried mushroom caps and stems were not subjected to any extraction before analysis. No psilocybin, psilocin, or derivative of either was detected. These results indicate that on-fiber derivatization is not suitable for mushroom samples. Because previous work with pure psilocybin on-fiber derivatization has also yielded negative results, it is possible that this drug is incompatible with this method. Changes to the method must be made to accommodate psilocybin, such as different fiber chemistry, an even longer derivatization time, or a different derivatization agent.

### *Solid Drugs*

Methamphetamine, GHB, and ephedrine produced single chromatographic peaks for their derivatives when analyzed as solid powders. Derivatization of gabapentin was incomplete, with the presence of a large chromatographic peak split into two peaks corresponding to underivatized gabapentin. The derivatization of 2C-I was complete, suggesting that TFSA could be used as an

effective derivatization agent for analysis of primary amines as solid powders. However, the chromatogram showed not only 2C-I TFA, but also a species corresponding to 2C-I TFA that had lost the iodine atom. Attempts to stop this effect by manipulating extraction temperature were unsuccessful.

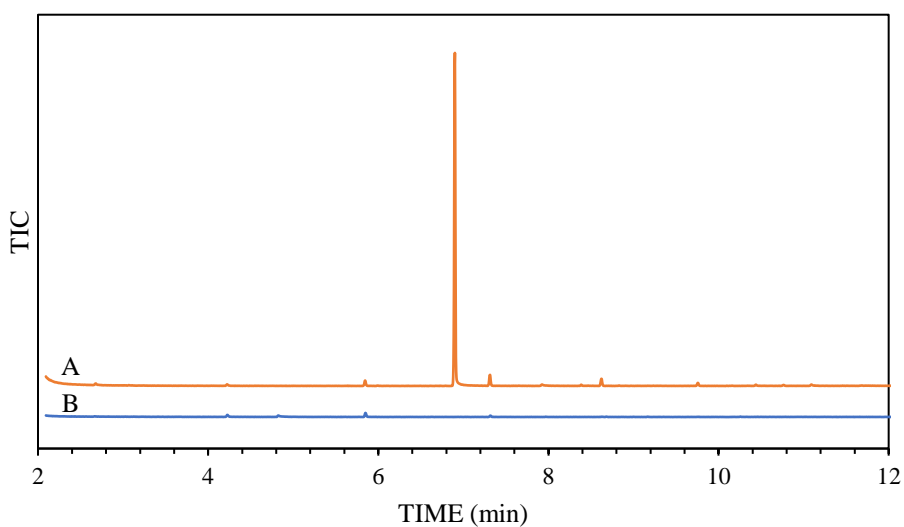


**Figure 61.** Chromatograms for A: methamphetamine TFA and B: methamphetamine underivatized

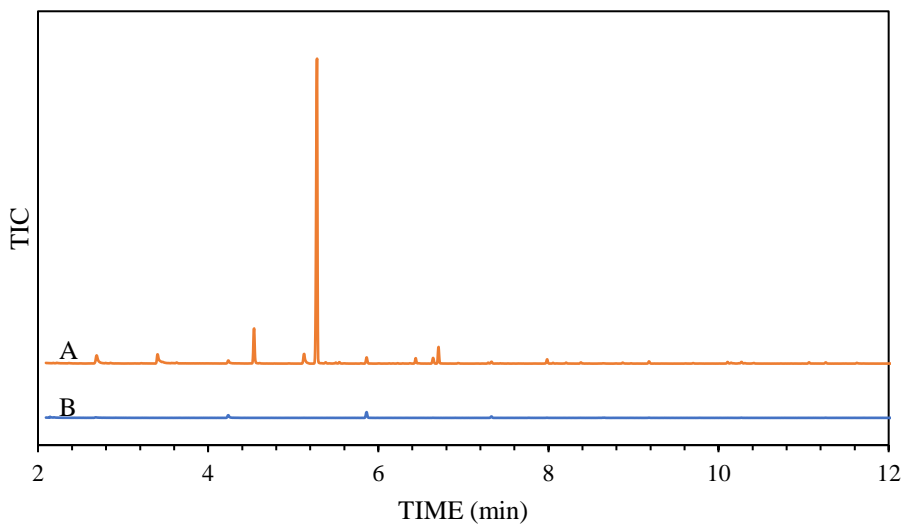


**Figure 62.** Chromatograms for A: GHB di-TMS and B: GHB underivatized

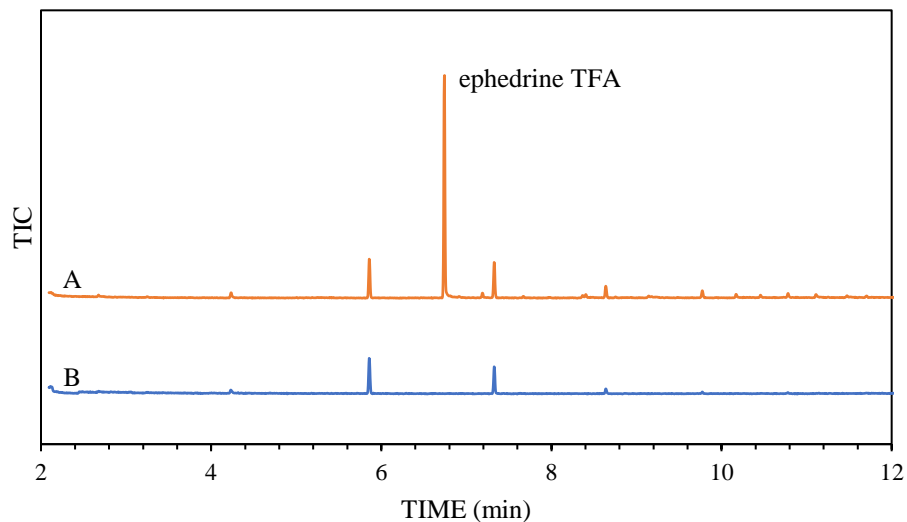


**Figure 63.** Chromatograms of A: ephedrine TFA and B: ephedrine underivatized

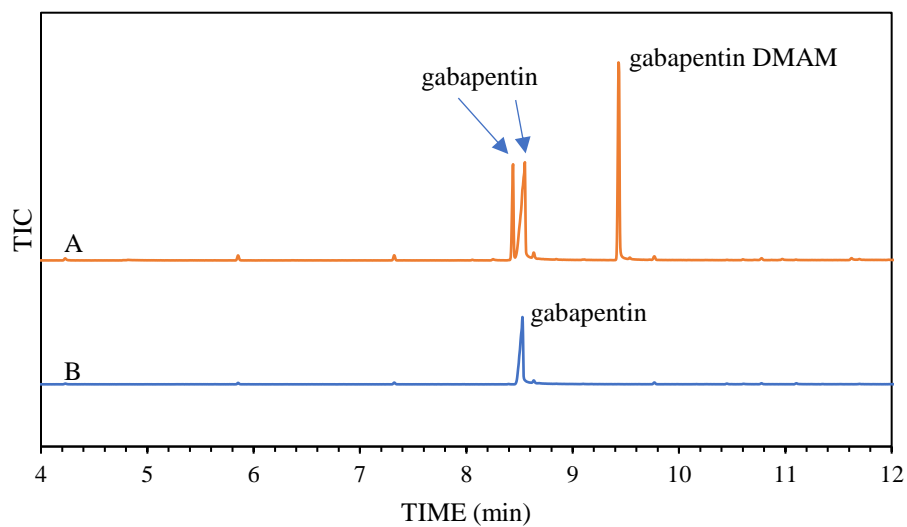


**Figure 64.** Chromatograms of A: gabapentin DMAM and B: gabapentin underivatized

## Conclusion

On-fiber derivatization has been proven to be an effective and useful tool for analysis of realistic seized drug samples, particularly for amines and GHB. On-fiber derivatization was unsuccessful for hallucinogenic mushrooms in this study, however, and requires further research.

TV-SPME with on-fiber derivatization using TFSA was able to identify all three components of a simulated impure sample of methamphetamine, detecting methamphetamine and ephedrine as the TFA derivatives and caffeine underivatized. This method was applied to the identification of GHB in mixed drinks, where it excelled. Despite the presence of protic solvents, on-fiber derivatization with BSTFA + 1% TMCS resulted in unambiguous identification of GHB in samples of water, Coke<sup>®</sup>, rum, and a 2:1 mixture of rum and Coke<sup>®</sup>. Powdered controlled substances were also analyzed with on-fiber derivatization, in their solid forms. The results were promising for all drug classes that were analyzed successfully by on-fiber derivatization as solutions. This discovery greatly improves the utility of the technique, as controlled substances are most often encountered in their solid forms in forensic science laboratories. The application of this technique to beverage samples and solid drug powders is of most interest, as these applications represent a significant decrease in sample preparation.



## CHAPTER 4. FUTURE WORK

### Toxicology

The work presented in this thesis makes up the bulk of a large project on the derivatization of controlled substances by GC-MS focused on developing TV-SPME on-fiber derivatization techniques. The next and final phase of the project is the demonstration of the technique's utility for toxicological samples. The technique has already been proven effective for GHB as well as phenethylamine and phenethylamine-derived drugs in aprotic solvents and as solid powders. In the case of GHB, the technique has also been demonstrated to be remarkably effective in aqueous and alcoholic solutions. Adaptation of the technique to urine samples therefore should be straightforward. The challenges will be in assessing the technique's flexibility, or its ability to derivatize and identify the many metabolites of drugs of interest, and its sensitivity when working with the much lower concentrations of drugs and metabolites in toxicological samples as compared to seized drug samples.

Methamphetamine represents a best-case-scenario drug for adaptation from seized drug to toxicological samples because methamphetamine itself is excreted in urine, and its primary metabolite is amphetamine<sup>3, 21</sup>, both of which yielded strongly positive results for on-fiber derivatization. The zwitterionic drugs will present a much greater challenge. Gabapentin, vigabatrin, and pregabalin are largely excreted in urine with little metabolism<sup>61-63</sup> while clorazepate is metabolized to nordiazepam<sup>64</sup> and lorazepam is metabolized primarily to its glucuronide and several minor metabolites<sup>65</sup>, though clorazepate and lorazepam are both excreted in urine as well. In general, the need to detect and identify metabolites as well as parent drugs will complicate the toxicological adaptation of the method, though many of the metabolites should also

be amenable to derivatization. It is not advisable to attempt toxicological testing with the zwitterions, however, until a satisfactory method for their detection in organic solutions with on-fiber derivatization is developed.

The conditions for the identification of GHB in mixed drinks are the most closely analogous to toxicological samples that are presented in this thesis. Toxicological samples are generally aqueous solutions just as the mixed drink samples were. Therefore, the same saturation of the fiber with derivatization agent will be necessary. This method has already proven effective for GHB analysis and provides a great starting point for toxicological analyses. GHB presents additional obstacles in toxicological analyses, however. Firstly, greater than 95% of GHB taken orally is metabolized to carbon dioxide and water and the rest is rapidly eliminated, becoming undetectable in blood and urine after 12 hours<sup>66-67</sup>. GHB is a naturally-occurring neurotransmitter and a metabolite of the neurotransmitter gamma-aminobutyric acid (GABA)<sup>68</sup> and is therefore present in the human body at low levels even without consumption of GHB. This is evidenced by preliminary data collected by Kymeri Davis in our laboratory which highlights yet another application of on-fiber derivatization. Kymeri placed a human hair in a headspace vial, analyzed it via on-fiber derivatization with BSTFA + 1% TMCS, and detected endogenous GHB. Her data is shown in figures 65 and 66, below. As one would expect, the signal for the GHB di-TMS derivative in the hair sample was much lower than that for spiked beverages. The chromatographic peak for GHB di-TMS is not visible in the TIC (figure 65), but can be seen in the extracted ion chromatogram for  $m/z$  233 (figure 66).

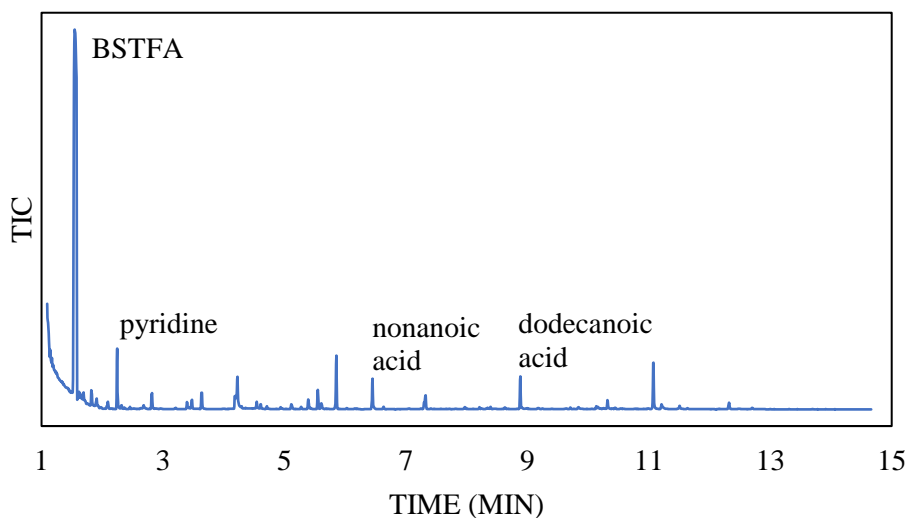


**Figure 65.** TIC of human hair derivatized with BSTFA + 1% TMCS (Data courtesy of Kymeri Davis).

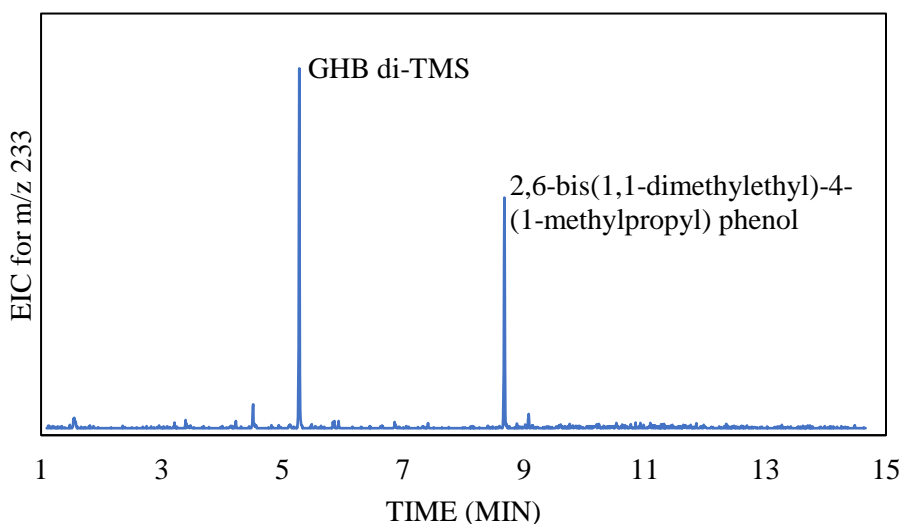


**Figure 66.** EIC for m/z 233 of human hair derivatized with BSTFA + 1% TMCS (Data courtesy of Kymeri Davis)

A study to determine the concentration of GHB naturally present in biological fluids found that GHB was present in 670 urine samples in the range of 34-575  $\mu\text{g/dL}$  and in 240 blood samples in the range of 17-151  $\mu\text{g/dL}$ <sup>51</sup>. The same study suggests endogenous GHB cutoff levels of 1000  $\mu\text{g/dL}$  in urine and 500  $\mu\text{g/dL}$  in blood. Any toxicological methods require quantitation, and this

is especially true of GHB analyses because of its natural presence in biological fluids. The on-fiber derivatization method for GHB detection presented in this thesis could be easily adapted to a quantitative technique by creating calibrants of varying concentrations and adding an internal standard to each of them and to the sample of unknown concentration. Deuterated GHB (GHB-D6) is recommended for the internal standard.

### **Beverage Samples**

A quantitative technique is necessary for GHB not only in toxicological samples but in drinks as well. This is because GHB is naturally occurring at low levels in some beverages. A study from 2005 reported that of 50 alcoholic beverages tested in the UK, GHB was only detected in those beverages which were made from fermenting grapes. It was detected in red wine vermouth at 8.2 mg/L, Sherry at 9.7 mg/L, red wine at 4.1-21.4 mg/L, and white wine at “<3-9.6 mg/L”<sup>69</sup>. A study published in 2017, however, detected GHB in beverages unrelated to the fermentation of grapes. This study tested both alcoholic and non-alcoholic beverages and found GHB in tonic water at 130-180 ng/mL, in rum at 100-150 ng/mL, in vodka at 160-190 ng/mL, in tequila at 210-270 ng/mL, in fruit juice from 300-500 ng/mL, in beer at 330-430 ng/mL, in red wine at 9300-12000 ng/mL, and in white wine at 2500-3200 ng/mL<sup>70</sup>. Luckily, these concentrations are well below pharmacologically active doses. Even so, this highlights the importance of using quantitative methods for the analysis of GHB not just in biological fluids but in beverages as well.

### **Method Improvement**

Though the on-fiber derivatization with TV-SPME method presented in this thesis showed great promise and utility, several drug derivatizations which were amenable to liquid injection

methods were not amenable or were unsatisfactory for SPME methods. Most notable of these were the zwitterionic anti-epileptics (gabapentin, vigabatrin, lorazepam, pregabalin, and clorazepate) and psilocybin, for which derivatization was incomplete or no derivative was detected at all. The incomplete derivatization of gabapentin suggests that there is hope for complete derivatization at least for gabapentin and potentially for the rest of the zwitterions as well. Additional experimentation should be done to attempt to obtain complete derivatization for as many of these drugs as possible. For example, longer time in the headspace of the derivatization vial could be tested, introducing more derivatization agent to the sample. Additional extraction time could also be explored, allowing the reaction more time to take place. It is also possible that DMF-DMA is not volatile enough at room temperature for a sufficient amount of the agent to volatilize and adsorb to the fiber. Derivatizations using this agent could potentially be improved by heating the agent when exposing the fiber, if this is the case. Furthermore, as discussed in chapter 1, larger silylation reagents such as MTBSTFA are slower to form but more stable, and therefore may be more successful in derivatizing these difficult analytes. Though the ephedrine TFA derivative was detected as a single chromatographic peak, the sensitivity achieved was far less than ideal in TV-SPME, so this reaction could also be improved.

It is desirable to shorten sample analysis time as much as possible. This is particularly true of the beverage sample method, which takes nearly an hour and a half per sample due to the 50 minutes necessary to saturate the fiber with derivatization agent. As discussed in chapter 3, significantly better sensitivity could be attained by allowing the fiber to stay in the derivatization agent vial even longer, but this is not desirable. Therefore, methods to saturate the fiber more quickly should be explored. One potential solution is to heat the derivatization vial, thereby increasing the amount of the agent in the headspace. Unfortunately, this method was initially

attempted and proven disadvantageous for TFAA derivatization, as the heated TFAA rapidly deteriorated the septum of the vial cap, which coupled with the increased pressure within the vial caused the septum to rupture. Heating may be compatible with vials of BSTFA + 1% TMCS or DMF-DMA, however. An interesting idea is to immerse the fiber in a solution of derivatization agent in an aprotic solvent for a short time. The concentration of derivatization agent, the solvent chosen, and the immersion time would all need to be investigated, but this change could have the potential to drastically reduce analysis time.

A few clarifications are also of interest. For instance, the electron ionization (EI) spectrum of 25I-NBOH is relatively unknown, as this drug is not typically detected by GC-MS. The spectrum shows an  $[M-2]^+$  ion, the origin of which was hypothesized in chapter 2. It is hypothesized that perhaps the amine and hydroxyl hydrogens, being close together, leave the molecule as  $H_2$ . This hypothesis could be tested using deuterium labeling. Deuterium (D) is a stable isotope of hydrogen which has one neutron in addition to the one proton of normal hydrogen (protium). Therefore, deuterium is one mass unit heavier than hydrogen. If the hydroxyl and amine hydrogens of 25I-NBOH were replaced with deuterium, the molecular weight would be increased from 413 to 415. If our hypothesis about these two hydrogens leaving together was true, we would expect to see an  $[M-4]^+$  ion in place of the  $[M-2]^+$ , which would still be at  $m/z$  411. We would also expect to see a  $m/z$  108 fragment rather than an  $m/z$  107 and all other fragments in the mass spectrum would remain at the same  $m/z$  value.

Throughout this thesis and in other works utilizing a similar technique, the technique has been referred to as “on-fiber” derivatization, implying that the derivatization reaction takes place directly on the fiber substrate. However, it is unclear whether the reaction indeed takes place directly on the fiber or if it really takes place in the headspace surrounding the fiber. Testing this

may prove difficult. One could dose one fiber with derivatization agent and expose the dosed fiber and a second clean fiber to the headspace of an analyte vial and test the fibers for the presence of the derivative. The issue with this approach is that some of the derivatization agent itself could leave the dosed fiber and adsorb to the second fiber, confounding the results. While this distinction is of academic interest and certainly worth exploring, it does not affect the effectiveness of the method.

## REFERENCES

1. Ash, J. R. Design and implementation of Gas Chromatography/Mass Spectrometry (GC/MS) methodologies for the analysis of thermally labile drugs and explosives. Purdue University, 2016.
2. Smith, F.; Siegel, J. A., *Handbook of Forensic Drug Analysis*. 1 ed.; Elsevier Science: Burlington, MA, 2004.
3. Jurado, C.; Gimenez, M.; Soriano, T.; Menendez, M.; Repetto, M., Rapid analysis of amphetamine, methamphetamine, MDA, and MDMA in urine using solid-phase microextraction, direct on-fiber derivatization, and analysis by GC-MS. *Journal of analytical toxicology* **2000**, 24 (1), 11-16.
4. Hulshoff, A.; Lingeman, H., Derivatization reactions in the gas—liquid chromatographic analysis of drugs in biological fluids. *Journal of pharmaceutical and biomedical analysis* **1984**, 2 (3-4), 337-380.
5. Brettell, T. A., Analysis of N-mono-trifluoroacetyl derivatives of amphetamine analogues by gas chromatography and mass spectrometry. *Journal of Chromatography A* **1983**, 257, 45-52.
6. Schummer, C.; Delhomme, O.; Appenzeller, B. M.; Wennig, R.; Millet, M., Comparison of MTBSTFA and BSTFA in derivatization reactions of polar compounds prior to GC/MS analysis. *Talanta* **2009**, 77 (4), 1473-1482.
7. Orata, F., Derivatization reactions and reagents for gas chromatography analysis. In *Advanced Gas Chromatography-Progress in Agricultural, Biomedical and Industrial Applications*, InTech: 2012.
8. Thenot, J.-P.; Horning, E.; Stafford, M.; Horning, M., Fatty acid esterification with N, N-dimethylformamide dialkyl acetals for GC analysis. *Analytical Letters* **1972**, 5 (4), 217-223.
9. Thenot, J.; Horning, E., Amino acid N-dimethylaminomethylene alkyl esters. New derivatives for GC and GC-MS studies. *Analytical Letters* **1972**, 5 (8), 519-529.
10. Grubb, M. F.; Callery, P. S., Derivatization of N-methyl and cyclic amino acids with dimethylformamide dimethyl acetal. *Journal of Chromatography A* **1989**, 469, 191-196.
11. Kataoka, H.; Kijima, K., Analysis of heterocyclic amines as their N-dimethylaminomethylene derivatives by gas chromatography with nitrogen-phosphorus selective detection. *Journal of Chromatography A* **1997**, 767 (1-2), 187-194.
12. Mudiam, M. K. R.; Chauhan, A.; Jain, R.; Ch, R.; Fatima, G.; Malhotra, E.; Murthy, R., Development, validation and comparison of two microextraction techniques for the rapid and sensitive determination of pregabalin in urine and pharmaceutical formulations after ethyl chloroformate derivatization followed by gas chromatography–mass spectrometric analysis. *Journal of pharmaceutical and biomedical analysis* **2012**, 70, 310-319.
13. Sowjanya, K.; Thejaswini, J.; Gurupadaya, B.; Raja, P., Quantitative Determination of Pregabalin by Gas Chromatography using Ethyl Chloroformate as a Derivatizing Reagent in Pure and Pharmaceutical Preparation. *Ind. Drugs* **2011**, 48 (3), 43-47.
14. Hlozek, T.; Bursova, M.; Coufal, P.; Cabala, R., Gabapentin, pregabalin and vigabatrin quantification in human serum by GC-MS after hexyl chloroformate derivatization. *J. Anal. Toxicol.* **2016**, 40 (9), 749-753.



15. Kostic, N.; Dotsikas, Y.; Malenovic, A., Critical review on the analytical methods for the determination of zwitterionic antiepileptic drugs-vigabatrin, pregabalin, and gabapentin-in bulk and formulations. *Instrum. Sci. Technol.* **2014**, 42 (4), 486-512.
16. Theobald, D. S.; Pütz, M.; Schneider, E.; Maurer, H. H., New designer drug 4-iodo-2, 5-dimethoxy- $\beta$ -phenethylamine (2C-I): studies on its metabolism and toxicological detection in rat urine using gas chromatographic/mass spectrometric and capillary electrophoretic/mass spectrometric techniques. *Journal of mass spectrometry* **2006**, 41 (7), 872-886.
17. Van Lente, F.; Gatautis, V., Cost-efficient use of gas chromatography–mass spectrometry: a “piggyback” method for analysis of gabapentin. *Clinical chemistry* **1998**, 44 (9), 2044-2045.
18. Centini, F.; Masti, A.; Comparini, I. B., Quantitative and qualitative analysis of MDMA, MDEA, MA and amphetamine in urine by head-space/solid phase micro-extraction (SPME) and GC/MS. *Forensic science international* **1996**, 83 (3), 161-166.
19. Blachut, D.; Bykas-Strekowska, M.; Taracha, E.; Szukalski, B., Application of gas chromatography/mass spectrometry (GC/MS) to the analysis of benzodiazepines. *Z Zagadnien Nauk Sadowych* **2004**, 59, 5-37.
20. Nakahara, Y.; Takahashi, K.; Shimamine, M.; Takeda, Y., Hair analysis for drug abuse: I. Determination of methamphetamine and amphetamine in hair by stable isotope dilution gas chromatography/mass spectrometry method. *Journal of Forensic Science* **1991**, 36 (1), 70-78.
21. Lin, H. R.; Lua, A. C., Simultaneous determination of amphetamines and ketamines in urine by gas chromatography/mass spectrometry. *Rapid communications in mass spectrometry* **2006**, 20 (11), 1724-1730.
22. Kushnir, M.; Crossett, J.; Brown, P.; Urry, F., Analysis of gabapentin in serum and plasma by solid-phase extraction and gas chromatography-mass spectrometry for therapeutic drug monitoring. *Journal of analytical toxicology* **1999**, 23 (1), 1-6.
23. Roman, P. E.; Knapp, J. A.; Horn, C. K.; Stillman, S. L.; Evans, J. E.; Arfsten, D. P., Comparison of LC-MS-MS and GC-MS analysis of benzodiazepine compounds included in the drug demand reduction urinalysis program. *J. Anal. Toxicol.* **2016**, 40 (3), 201-207.
24. de Baires, A. V.; de Almeida, R. M.; Pantaleão, L.; Barcellos, T.; Silva, S. M. e.; Yonamine, M., Determination of low levels of benzodiazepines and their metabolites in urine by hollow-fiber liquid-phase microextraction (LPME) and gas chromatography–mass spectrometry (GC–MS). *Journal of Chromatography B* **2015**, 975 (Supplement C), 24-33.
25. McLafferty, F. W., *Interpretation of Mass Spectra*. Fourth ed.; University Science Books: Sausalito, California, 1993.
26. Rainey, C. L.; Bors, D. E.; Goodpaster, J. V., Design and optimization of a total vaporization technique coupled to solid-phase microextraction. *Analytical chemistry* **2014**, 86 (22), 11319-11325.
27. Bors, D.; Goodpaster, J., Mapping explosive residues on galvanized pipe bomb fragments using total vaporization solid phase microextraction (TV-SPME). *Analytical Methods* **2015**, 7 (23), 9756-9762.
28. Meyers, J. E.; Almirall, J. R., Analysis of gamma-hydroxybutyric acid (GHB) in spiked water and beverage samples using solid phase microextraction (SPME) on fiber derivatization/gas chromatography-mass spectrometry (GC/MS). *Journal of Forensic Science* **2005**, 50 (1), JFS2003280-6.

29. Krogh, M.; Pedersen-Bjergaard, S.; Rasmussen, K., Propyl chloroformate derivatisation and SPME-GC for screening of amines in urine. *Applications of solid phase microextraction* **1999**, *1*, 461-469.
30. Pawliszyn, J.; Snow, N. H., On-fiber derivatization for analysis of steroids by SPME and GC-MS. In *Applications of Solid Phase Microextraction*, 1999; pp 486-496.
31. Namera, A.; Yashiki, M.; Liu, J.; Okajima, K.; Hara, K.; Imamura, T.; Kojima, T., Simple and simultaneous analysis of fenfluramine, amphetamine and methamphetamine in whole blood by gas chromatography-mass spectrometry after headspace-solid phase microextraction and derivatization. *Forensic science international* **2000**, *109* (3), 215-223.
32. bin Abdullah, L.; Ahmad, F.; Miskelly, G. M., Formation of Trifluoroacetylated Ephedrine During the Analysis of a Pseudoephedrine-Formaldehyde Adduct by TFAA Derivatization Followed by GC-MS. *Journal of forensic sciences* **2009**, *54* (2), 365-369.
33. Khaled, M. M.; Abdulsallam, B., Comparison of 3 Derivatization Methods for the Analysis of Amphetamine-Related Drugs in Oral Fluid by Gas Chromatography-Mass Spectrometry. *Analytical Chemistry Insights* **2017**, *12*, 1177390117727533.
34. Nakahara, Y.; Kikura, R., Hair analysis for drugs of abuse XIX. Determination of ephedrine and its homologs in rat hair and human hair. *Journal of Chromatography B: Biomedical Sciences and Applications* **1997**, *700* (1), 83-91.
35. Emde, H., Über Diastereomerie I. Konfiguration des Ephedrins. *Helvetica Chimica Acta* **1929**, *12* (1), 365-376.
36. Ko, B. J.; Suh, S.; Suh, Y. J.; In, M. K.; Kim, S.-H., The impurity characteristics of methamphetamine synthesized by Emde and Nagai method. *Forensic Science International* **2007**, *170* (2), 142-147.
37. Lee, J. S.; Han, E. Y.; Lee, S. Y.; Kim, E. M.; Park, Y. H.; Lim, M. A.; Chung, H. S.; Park, J. H., Analysis of the impurities in the methamphetamine synthesized by three different methods from ephedrine and pseudoephedrine. *Forensic science international* **2006**, *161* (2-3), 209-215.
38. Skinner, H. F., Methamphetamine synthesis via hydriodic acid/red phosphorus reduction of ephedrine. *Forensic Science International* **1990**, *48* (2), 123-134.
39. Person, E. C.; Meyer, J. A.; Vyvyan, J. R., Structural determination of the principal byproduct of the lithium-ammonia reduction method of methamphetamine manufacture. *Journal of Forensic Science* **2005**, *50* (1), JFS2004204-9.
40. Kunalan, V.; Nic Daéid, N.; Kerr, W. J.; Buchanan, H. A.; McPherson, A. R., Characterization of route specific impurities found in methamphetamine synthesized by the Leuckart and reductive amination methods. *Analytical chemistry* **2009**, *81* (17), 7342-7348.
41. D.E.A., Drug Fact Sheet - GHB.
42. Ciolino, L. A.; Mesmer, M. Z.; Satzger, R. D.; Machal, A. C.; McCauley, H. A.; Mohrhaus, A. S., The chemical interconversion of GHB and GBL: forensic issues and implications. *Journal of Forensic Science* **2001**, *46* (6), 1315-1323.
43. Hennessy, S. A.; Moane, S. M.; McDermott, S. D., The reactivity of gamma-hydroxybutyric acid (GHB) and gamma-butyrolactone (GBL) in alcoholic solutions. *Journal of Forensic Science* **2004**, *49* (6), JFS2003340-10.
44. Wiberg, K. B.; Waldron, R. F., Lactones. 2. Enthalpies of hydrolysis, reduction, and formation of the C4-C13 monocyclic lactones. Strain energies and conformations. *Journal of the American Chemical Society* **1991**, *113* (20), 7697-7705.

45. Blair, S.; Song, M.; Hall, B.; Brodbelt, J., Determination of gamma-hydroxybutyrate in water and human urine by solid phase microextraction-gas chromatography/quadrupole ion trap spectrometry. *Journal of Forensic Science* **2001**, *46* (3), 688-693.
46. Couper, F. J.; Logan, B. K., Determination of  $\gamma$ -hydroxybutyrate (GHB) in biological specimens by gas chromatography-mass spectrometry. *Journal of analytical toxicology* **2000**, *24* (1), 1-7.
47. Elian, A. A., GC-MS determination of gamma-hydroxybutyric acid (GHB) in blood. *Forensic science international* **2001**, *122* (1), 43-47.
48. LeBeau, M. A.; Montgomery, M. A.; Miller, M. L.; Burmeister, S. G., Analysis of biofluids for gamma-hydroxybutyrate (GHB) and gamma-butyrolactone (GBL) by headspace GC-FID and GC-MS. *Journal of analytical toxicology* **2000**, *24* (6), 421-428.
49. Paul, R.; Tsanaclis, L.; Kingston, R.; Berry, A.; Guwy, A., Simultaneous determination of GHB and EtG in hair using GCMS/MS. *Drug testing and analysis* **2011**, *3* (4), 201-205.
50. Elian, A. A., A novel method for GHB detection in urine and its application in drug-facilitated sexual assaults. *Forensic science international* **2000**, *109* (3), 183-187.
51. Elian, A. A., Determination of endogenous gamma-hydroxybutyric acid (GHB) levels in antemortem urine and blood. *Forensic science international* **2002**, *128* (3), 120-122.
52. Kaufmann, E.; Alt, A., Determination of GHB in urine and serum by LC/MS using a simple one-step derivative. *Forensic science international* **2007**, *168* (2-3), 133-137.
53. Brewster, V.; Edwards, H. G.; Hargreaves, M. D.; Munshi, T., Identification of the date-rape drug GHB and its precursor GBL by Raman spectroscopy. *Drug testing and analysis* **2009**, *1* (1), 25-31.
54. Munshi, T.; Brewster, V.; Edwards, H. G.; Hargreaves, M. D.; Jilani, S.; Scowen, I. J., Monitoring of the interconversion of gamma-butyrolactone (GBL) to gamma hydroxybutyric acid (GHB) by Raman spectroscopy. *Drug testing and analysis* **2013**, *5* (8), 678-682.
55. Chappell, J. S.; Meyn, A. W.; Ngim, K. K., The extraction and infrared identification of gamma-hydroxybutyric acid (GHB) from aqueous solutions. *Journal of Forensic Science* **2003**, *49* (1), 1-8.
56. Palomino-Schätzlein, M.; Wang, Y.; Brailsford, A. D.; Parella, T.; Cowan, D. A.; Legido-Quigley, C.; Pérez-Trujillo, M., Direct Monitoring of Exogenous  $\gamma$ -Hydroxybutyric Acid in Body Fluids by NMR Spectroscopy. *Analytical Chemistry* **2017**, *89* (16).
57. Lesar, C. T.; Decatur, J.; Lukasiewicz, E.; Champeil, E., Report on the analysis of common beverages spiked with gamma-hydroxybutyric acid (GHB) and gamma-butyrolactone (GBL) using NMR and the PURGE solvent-suppression technique. *Forensic science international* **2011**, *212* (1), e40-e45.
58. Wasson, R. G., Seeking the magic mushroom. *Life* **1957**, *42* (19), 100-120.
59. Hofmann, A.; Frey, A.; Ott, H.; Petrzilka, T.; Troxler, F., Konstitutionsaufklärung und synthese von psilocybin. *Experientia* **1958**, *14* (11), 397-399.
60. Erowid GHB Dosage. [https://erowid.org/chemicals/ghb/ghb\\_dose.shtml](https://erowid.org/chemicals/ghb/ghb_dose.shtml) (accessed June 15).
61. Hengy, H.; Kölle, E.-U., Determination of gabapentin in plasma and urine by high-performance liquid chromatography and pre-column labelling for ultraviolet detection. *Journal of Chromatography B: Biomedical Sciences and Applications* **1985**, *341*, 473-478.

62. Ratnaraj, N.; Patsalos, P. N., A high-performance liquid chromatography micromethod for the simultaneous determination of vigabatrin and gabapentin in serum. *Therapeutic drug monitoring* **1998**, *20* (4), 430-434.
63. Rodríguez, J.; Castaneda, G.; Muñoz, L., Direct determination of pregabalin in human urine by nonaqueous CE-TOF-MS. *Electrophoresis* **2013**, *34* (9-10), 1429-1436.
64. Rey, E.; Giraux, P.; d'Athis, P.; Turquais, J.; Chavinie, J.; Olive, G., Pharmacokinetics of the placental transfer and distribution of clorazepate and its metabolite nordiazepam in the feto-placental unit and in the neonate. *European journal of clinical pharmacology* **1979**, *15* (3), 181-185.
65. Elliott, H., Metabolism of lorazepam. *British journal of anaesthesia* **1976**, *48* (10), 1017-1023.
66. Ferrara, S. D.; Tedeschi, L.; Frison, G.; Castagna, F.; Gallimberti, L.; Giorgetti, R.; Gessa, G. L.; Palatini, P., Therapeutic gamma-hydroxybutyric acid monitoring in plasma and urine by gas chromatography—mass spectrometry. *Journal of Pharmaceutical and Biomedical Analysis* **1993**, *11* (6), 483-487.
67. Dyer, J. E.,  $\gamma$ -Hydroxybutyrate: A health-food product producing coma and seizurelike activity. *The American Journal of Emergency Medicine* **1991**, *9* (4), 321-324.
68. Vayer, P.; Mandel, P.; Maitre, M., Gamma-hydroxybutyrate, a possible neurotransmitter. *Life Sciences* **1987**, *41* (13), 1547-1557.
69. Elliott, S.; Burgess, V., The presence of gamma-hydroxybutyric acid (GHB) and gamma-butyrolactone (GBL) in alcoholic and non-alcoholic beverages. *Forensic Science International* **2005**, *151* (2), 289-292.
70. Tucci, M.; Stocchero, G.; Pertile, R.; Favretto, D., Detection of GHB at low levels in non-spiked beverages using solid phase extraction and gas chromatography—mass spectrometry. *Toxicologie Analytique et Clinique* **2017**, *29* (2), 225-233.